Bone Marrow Lesions in Progression of Knee Osteoarthritis

A Thesis submitted to The University of Adelaide in fulfilment of the requirements for the degree of Doctor of Philosophy

By

Dzenita Muratovic, BHSc (Hons)

Discipline of Orthopaedics and Trauma

Adelaide Medical School

Faculty of Health and Medical Sciences

The University of Adelaide

South Australia

Adelaide

January 2018

رَّبِّ زِدْنِي عِلْمًا

Rabbi zidnee ‘ilman

“O my Lord, increase me in knowledge!”

Surah Ash-Shu’ara (Chapter 26), verses: 83-85.

Table of contents

Thesis abstract

Bone marrow lesions (BMLs) are magnetic resonance imaging (MRI)-identified pathological changes in subchondral bone, closely associated with joint pain and osteo-chondral structural degeneration in knee osteoarthritis (KOA). Despite the usefulness of BMLs as diagnostic and prognostic markers in KOA, what they represent at the tissue level remains unclear. Thus, the thesis aim was to perform a comprehensive investigation of BMLs at the tissue level and their relationship with the structural changes in KOA. We hypothesised that BML imaged using MRI reflect changes in subchondral tissue of proximal tibia that related to OA disease severity and/or progression.

The first study provided comprehensive tissue characterization of BMLs detected using two [proton density fat saturated (PDFS) and T1)] specific MRI sequences. Multi-modal tissue level analyses of the whole depth of the tibial osteochondral unit were performed. The results from tissue level analyses showed that BMLs detected by specific MRI sequences associate strongly with the degree of structural change in the osteochondral unit in KOA. Specifically, BMLs detected by the combination of PDFS and T1 weighted MR-sequences represent an advanced structural stage of OA disease, while BMLs detected only by PDFS weighted sequence represent less severe OA, and potentially have the ability to resolve.

In the second study, potential causal factors (mechanical loading and vascular pathology) of BML formation were investigated by assessing the accumulation of microdamage, and the qualitative and quantitative aspects of blood vessels in BML and non-BML tissue. Increased microdamage density and increased

arteriolar density, with altered characteristics of vascular walls, were found in the zones of BML tissue, supporting the notion that both excessive and biomechanically unfavourable loading and vascular pathology contribute to the occurrence of BMLs in tibial subchondral bone tissue.

In the third study, a potential role for components of the metabolic syndrome in BML development and its potential influences on the progression of KOA was investigated. Results from this study suggested that a combination of specific metabolic factors such as central obesity with BMI 30 or greater, dyslipidaemia, high blood pressure and high fasting glucose levels might promote the occurrence of BMLs in tibial subchondral bone tissue and that metabolic factors might contribute to the progressive osteochondral degeneration in KOA.

The fourth study described microarchitectural changes in whole tibial plateaus (TP), based on the presence/absence of a BML. Tissue from healthy/control knees was also used to compare with that from OA with no BML and OA with BML, to better understand the course of OA disease and BML involvement in disease progression. In comparison with non-OA (control) subjects, the bone microstructure of the subchondral plate and trabeculae varies significantly between subregions of the TP in KOA. Secondly, in KOA subjects, two types of structural changes were identified, which were dependent on the presence or absence of a BML in the TP, and which related to the extent of cartilage degradation. Thirdly, the presence of a BML had implications for the microstructure of regions of the TP beyond the zone of the BML.

In conclusion, this series of related studies demonstrates that BMLs as a feature of subchondral bone strongly associate with the progressive state of OA disease and therefore play a significant role in KOA pathogenesis. This demonstrated that

BMLs are valuable imaging biomarkers of KOA and that BMLs might provide attractive targets for therapeutic intervention in OA.

Declaration

I, Dzenita Muratovic certify that this work contains no material which has been accepted for the award of any other degree or diploma in my name, in any university or other tertiary institution and, to the best of my knowledge and belief, contains no material previously published or written by another person, except where due reference has been made in the text. In addition, I certify that no part of this work will, in the future, be used in a submission in my name, for any other degree or diploma in any university or other tertiary institution without the prior approval of the University of Adelaide and where applicable, any partner institution responsible for the joint-award of this degree.

I acknowledge that copyright of published works contained within this thesis resides with the copyright holder(s) of those works.

I also give permission for the digital version of my thesis to be made available on the web, via the University's digital research repository, the Library Search and also through web search engines, unless permission has been granted by the University to restrict access for a period of time.

I acknowledge the support I have received for my research through the provision of an Australian Government Research Training Program Scholarship.

Dzenita Muratovic

Date 22/1/2018

Acknowledgements

Firstly, I would like to express my special appreciation and thanks to my supervisors, Dr Julia Kuliwaba and Professor David Findlay, who provided me an opportunity to join their team. I could not wish for a better advisors and mentors for my PhD study. Julia, you have been tremendous mentor for me. I would like to thank you for encouraging my research and for allowing me to grow as a research scientist. Your advice on both research as well as on my career have been invaluable. David, your continuous support, patience, motivation, and immense knowledge helped me to develop great enthusiasm for research and the desire to one day be a great mentor- just like you.

I would also like to express my gratitude toward Professor Flavia Cicuttini and Associate Professor Anita Wluka, for being supportive and full of understanding when I ask all sorts of clinical questions.

In addition, a very special gratitude goes to Ms. Olivia (Yea Rin) Lee for her unfailing support and assistance, always when I needed it most and to Dr Agatha Labrinidis and Ms Ruth Williams from Adelaide Microscopy at the University of Adelaide for help and support with Micro CT data.

Last but not least, I would like to thank my family and friends: A special thanks to my beloved husband Muradif, for ultimate support and all of the sacrifices that you’ve made on my behalf. To my beloved sons Imran and Harun, for being such good boys and always cheering me up, to my mother Senada and my sisters Mahira and Nermina for supporting me and encouraging me throughout this experience, despite being 15 000 kilometres away. My sincere thanks also go to my very best friend, Dr Sabina Gredelj for being a big support, encouragement,

motivation and especially for organising all those lovely little trips for our families when we all needed a break and refreshment. I am grateful to my other family members and friends who have supported me along this journey.

Dzenita Muratovic

December 2017

Published abstracts (reviewed)

D. Muratovic, F.M. Cicuttini, A.E. Wluka, Y. Wang, D.M. Findlay, S. Otto, D.J. Taylor, S. Collings, J.M. Humphries, Y.R. Lee, G. Mercer, J.S. Kuliwaba (2015) Bone Marrow Lesions Detected by Different Magnetic Resonance Sequences as Potential Biomarkers for Knee Osteoarthritis: Comprehensive Tissue Level Analysis. Osteoarthritis and Cartilage 04/2015; 23: A303-A305.

D. Muratovic, F.M. Cicuttini, A.E. Wluka, Y. Wang, D.M. Findlay, S. Otto, D.J. Taylor, S. Collings, J.M. Humphries, Y.R. Lee, G. Mercer, J.S. Kuliwaba. Bone Marrow Lesions Detected by Two MRI Sequences Associate with Severity detected Osteoarthritis, Internal Medicine Journal © 2015 Royal Australasian College of Physicians Volume 45, Issue Supplement S2, pages 1–46, May 2015

D. Muratovic, F.M. Cicuttini, A.E. Wluka, Y. Wang, D.M. Findlay, S. Otto, D.J. Taylor, S. Collings, J.M. Humphries, Y.R. Lee, G. Mercer, J.S. Kuliwaba Knee Osteoarthritis; Metabolic Syndrome in Patients with Tibial Bone Marrow Lesions. Internal Medicine Journal © 2015 Royal Australasian College of Physicians Volume 45, Issue Supplement S2, pages 1–46, May 2015

Scientific communications

<u>D. Muratovic</u>, F.M. Cicuttini, A.E. Wluka, Y. Wang, D.M. Findlay, S. Otto, D.J. Taylor, S. Collings, J.M. Humphries, Y.R. Lee, J.S. Kuliwaba. **Knee Osteoarthritis: Bone Marrow Lesions Detected by Specific MRI Sequences Associate with Severity of Osteochondral Degeneration**. *22nd Annual Australian & New Zealand Orthopaedic Research Society (ANZORS) Conference, Melbourne, Australia, October 13-15, 2016, (oral presentation).*

<u>D. Muratovic</u>, F.M. Cicuttini, A.E. Wluka, Y. Wang, D.M. Findlay, S. Otto, D.J. Taylor, S. Collings, J.M. Humphries, Y.R. Lee, G. Mercer, J.S. Kuliwaba. **Multiple Drivers of Bone Marrow Lesion Development in Osteoarthritis: Microdamage, Vascularity and the Metabolic Syndrome.** *Florey International Postgraduate Research Conference 2016, Adelaide, Australia, September 26, 2016, (poster presentation).*

<u>D. Muratovic</u>, F.M. Cicuttini, A.E. Wluka, Y. Wang, D.M. Findlay, S. Otto, D.J. Taylor, S. Collings, J.M. Humphries, Y.R. Lee, J.S. G. Mercer, J.S. Kuliwaba. **Knee Osteoarthritis: Comprehensive Histological Characterization of Bone Marrow Lesions Identified on MRI.** *9th International Workshop on Osteoarthritis Imaging, Oulu, Finland, June 15-18, 2016, (oral presentation).*

<u>D. Muratovic</u>, F.M. Cicuttini, A.E. Wluka, Y. Wang, D.M. Findlay, S. Otto, D.J. Taylor, S. Collings, J.M. Humphries, Y.R. Lee, G. Mercer, J.S. Kuliwaba. **Bone Marrow Lesions: Development and Roles in the Progression of Knee Osteoarthritis**. *Annual scientific meeting of the Australian Society for Medical*

Research SA Scientific Meeting (ASMR) (South Australian Division). Adelaide, Australia, June 6, 2016, (oral presentation).

D. Muratovic, F.M. Cicuttini, A.E. Wluka, Y. Wang, D.M. Findlay, S. Otto, D.J. Taylor, S. Collings, J.M. Humphries, Y.R. Lee, G. Mercer, J.S. Kuliwaba. **Knee Osteoarthritis: Bone Marrow Lesions Detected by Specific MRI Sequences Associate with Severity of Osteochondral Degeneration***. American Academy of Orthopedic Surgeons/Orthopaedic Research Society (AAOS/ORS) Tackling Joint Disease by Understanding Crosstalk between Cartilage and Bone Research Symposium Chicago, USA, April 28-30, 2016, (oral presentation).*

D. Muratovic, F.M. Cicuttini, A.E. Wluka, Y. Wang, D.M. Findlay, S. Otto, D.J. Taylor, S. Collings, J.M. Humphries, Y.R. Lee, G. Mercer, J.S. Kuliwaba. **Bone Marrow Lesions: A Localized Tissue Repair Response to Mechanical Injury?** *9th Clare Valley Bone Meeting, Clare, Australia, April 1-4, 2016, (oral presentation).*

D. Muratovic, F.M. Cicuttini, A.E. Wluka, Y. Wang, D.M. Findlay, S. Otto, D.J. Taylor, S. Collings, J.M. Humphries, Y.R. Lee, G. Mercer, J.S. Kuliwaba. **Are Bone Marrow Lesions Potential MRI biomarkers for knee Osteoarthritis.** *Postgraduate Conference 2015, Centre for Orthopaedic and Trauma Research, Adelaide, Australia, December 9, 2015, (oral presentation).*

D. Muratovic, F.M. Cicuttini, A.E. Wluka, Y. Wang, D.M. Findlay, S. Otto, D.J. Taylor, S. Collings, J.M. Humphries, Y.R. Lee, G. Mercer, J.S. Kuliwaba. **Knee Osteoarthritis: Bone Marrow Lesions Detected by Specific MRI Sequences**

Associate with Severity of Osteochondral Degeneration. *Annual Scientific Meeting 2015, Australian New Zealand Bone & Mineral Society (ANZBMS), Hobart, Australia, November 1-4, 2015, (poster presentation).*

D. Muratovic, F.M. Cicuttini, A.E. Wluka, Y. Wang, D.M. Findlay, S. Otto, D.J. Taylor, S. Collings, J.M. Humphries, Y.R. Lee, G G. Mercer, J.S. Kuliwaba. **Bone Marrow Lesions Detected by Two MRI Sequences Associate with Severity of Knee Osteoarthritis.** *2015 Annual Scientific and General Meeting of the Australian Rheumatology Association (ARA), (South Australian Branch). Adelaide, Australia, October 23, 2015, (oral presentation).*

D. Muratovic, F.M. Cicuttini, A.E. Wluka, Y. Wang, D.M. Findlay, S. Otto, D.J. Taylor, S. Collings, J.M. Humphries, Y.R. Lee, G. Mercer, J.S. Kuliwaba. **Knee Osteoarthritis: Bone Marrow Lesions Detected by Specific MRI Sequences Associate with Severity of Osteochondral Degeneration.** *Florey International Postgraduate Research Conference 2015, Adelaide, Australia, September 26, 2015, (poster presentation).*

D. Muratovic, F.M. Cicuttini, A.E. Wluka, Y. Wang, D.M. Findlay, S. Otto, D.J. Taylor, S. Collings, J.M. Humphries, Y.R. Lee, G. Mercer, J.S. Kuliwaba. **Knee Osteoarthritis: Incidence of Metabolic Syndrome in Patients with Tibial Bone Marrow Lesions.** *Annual scientific meeting of the Australian Society for Medical Research SA Scientific Meeting (ASMR) (South Australian Division). Adelaide, Australia, June 3, 2015, (poster presentation).*

D. Muratovic, F.M. Cicuttini, A.E. Wluka, Y. Wang, D.M. Findlay, S. Otto, D.J.

Taylor, S. Collings, J.M. Humphries, Y.R. Lee, G. Mercer, J.S. Kuliwaba. **Are Bone Marrow Lesions Potential MRI biomarkers for knee Osteoarthritis.** *Australian Society for Medical Research SA Scientific Meeting (ASMR) (South Australian Division). Adelaide, Australia, June 3, 2015, (poster presentation).*

D. Muratovic, F.M. Cicuttini, A.E. Wluka, Y. Wang, D.M. Findlay, S. Otto, D.J. Taylor, S. Collings, J.M. Humphries, Y.R. Lee, G. Mercer, J.S. Kuliwaba. **Knee Osteoarthritis; Metabolic Syndrome in Patients with Tibial Bone Marrow Lesions.** *The Australian Rheumatology Association (ARA), 56th Annual Scientific Meeting Adelaide, Australia, May 23-26, 2015, (poster presentation).*

D. Muratovic, F.M. Cicuttini, A.E. Wluka, Y. Wang, D.M. Findlay, S. Otto, D.J. Taylor, S. Collings, J.M. Humphries, Y.R. Lee, G. Mercer, J.S. Kuliwaba Bone **Marrow Lesions Detected by Two MRI Sequences Associate with Severity detected Osteoarthritis**. *The Australian Rheumatology Association (ARA), 56th Annual Scientific Meeting Adelaide, Australia, May 23-26, 2015, (oral presentation).*

D. Muratovic, F.M. Cicuttini, A.E. Wluka, Y. Wang, D.M. Findlay, S. Otto, D.J. Taylor, S. Collings, J.M. Humphries, Y.R. Lee, G. Mercer, J.S. Kuliwaba (2015) **Bone Marrow Lesions Detected by Different Magnetic Resonance Sequences as Potential Biomarkers for Knee Osteoarthritis: Comprehensive Tissue Level Analysis.** *Osteoarthritis Research Society International (OARSI), Seattle, Washington USA, April 30-May 3, 2015, (poster presentation).*

D. Muratovic, F.M. Cicuttini, A.E. Wluka, Y. Wang, D.M. Findlay, S. Otto, D.J. Taylor, S. Collings, J.M. Humphries, Y.R. Lee, G. Mercer, J.S. Kuliwaba. **Bone Marrow Lesions Detected by Two MRI Sequences Associate with Severity of Knee Osteoarthritis**. *Australian Orthopaedic Association (AOA) Queen Elizabeth Hospital Adelaide, Australia, April 10, 2015, (oral presentation).*

D. Muratovic, F.M. Cicuttini, A.E. Wluka, Y. Wang, D.M. Findlay, S. Otto, D.J. Taylor, S. Collings, J.M. Humphries, Y.R. Lee, G. Mercer, J.S. Kuliwaba. **Bone Marrow Lesions Detected by Two MRI Sequences Associate with Severity of Knee Osteoarthritis.** *General Scientific Meeting, Australian Orthopaedic Association (AOA) Adelaide, Australia, November 10, 2015, (oral presentation).*

D. Muratovic, F.M. Cicuttini, A.E. Wluka, Y. Wang, D.M. Findlay, S. Otto, D.J. Taylor, S. Collings, J.M. Humphries, Y.R. Lee, G. Mercer, J.S. Kuliwaba. **Knee Osteoarthritis Bone Marrow Lesions Detected by Two Different Magnetic Resonance Sequences are Characterised by Different Morphological and Microstructural Changes in Osteochondral unit.** *2014 Annual Scientific and General Meeting of the Australian Rheumatology Association (ARA), (South Australian Branch). Adelaide, Australia, October 31, 2014, (oral presentation).*

D. Muratovic, F.M. Cicuttini, A.E. Wluka, Y. Wang, D.M. Findlay, S. Otto, D.J. Taylor, S. Collings, J.M. Humphries, Y.R. Lee, G. Mercer, J.S. Kuliwaba. **Bone Marrow Lesions in Progression of Knee Osteoarthritis.** *Florey International Postgraduate Research Conference 2015, Adelaide, Australia, September 25, 2014, (poster presentation).*

D. Muratovic, F.M. Cicuttini, A.E. Wluka, Y. Wang, D.M. Findlay, S. Otto, D.J. Taylor, S. Collings, J.M. Humphries, Y.R. Lee, G. Mercer, J.S. Kuliwaba**. Bone Marrow Lesions Detected by Two Different Sequences are Characterized by Different Morphological and Structural Characteristics.** *21st Annual Australian & New Zealand Orthopaedic Research Society (ANZORS) Conference, Adelaide, Australia, September 23, 2014, (oral presentation).*

D. Muratovic, F.M. Cicuttini, A.E. Wluka, Y. Wang, D.M. Findlay, S. Otto, D.J. Taylor, S. Collings, J.M. Humphries, Y.R. Lee, G. Mercer, J.S. Kuliwaba**. Bone Marrow Lesions in Progression of Knee Osteoarthritis.** ***2014*** *Annual Scientific Meeting of the Australian Society for Medical Research SA Scientific Meeting (ASMR) (South Australian Division). Adelaide, Australia, June 3, 2014, (oral presentation).*

D. Muratovic, F.M. Cicuttini, A.E. Wluka, Y. Wang, D.M. Findlay, S. Otto, D.J. Taylor, S. Collings, J.M. Humphries, Y.R. Lee, G. Mercer, J.S. Kuliwaba. **Bone Marrow Lesions in Knee Osteoarthritis**. *8th Clare Valley Bone Meeting, Clare Valley, Australia, March 28-31, 2014 (poster presentation).*

D. Muratovic, F.M. Cicuttini, A.E. Wluka, Y. Wang, D.M. Findlay, S. Otto, D.J. Taylor, S. Collings, J.M. Humphries, Y.R. Lee, G. Mercer, J.S. Kuliwaba. **Bone Marrow Lesions in Progression of Knee Osteoarthritis.** *General and Scientific Meeting, Australian Orthopaedic Association (AOA), November 11, 2013, (oral presentation).*

D. Muratovic, F.M. Cicuttini, A.E. Wluka, Y. Wang, D.M. Findlay, S. Otto, D.J. Taylor, S. Collings, J.M. Humphries, Y.R. Lee, G. Mercer, J.S. Kuliwaba. **Bone Marrow Lesions in Progression of Knee Osteoarthritis**. *2013 Annual Scientific and General Meeting of the Australian Rheumatology Association (ARA), (South Australian Branch). Adelaide, Australia, October 18, 2013, (oral presentation).*

Awards and achievements

The following awards were received for original work in this thesis:

ANZORS Travel Award to attend 22nd Annual Australian & New Zealand Orthopaedic Research Society (ANZORS) Conference, Melbourne, Australia, 2016.

Yung Investigator Award for the highest-ranking abstract at 9th International Workshop on Osteoarthritis Imaging, Oulu, Finland, 2016.

School of Medicine Travel Award, (round 1) to attend 9th International Workshop on Osteoarthritis Imaging, Oulu, Finland, 2016.

Finalist for Ross Wishart Memorial Award at Australian Society for Medical Research SA Scientific Meeting (ASMR), Adelaide, Australia 2016.

Young Investigator Award for the most outstanding abstract at AAOS/ORS Tackling Joint Disease by Understanding Crosstalk between Cartilage and Bone, Research Symposium, Rosemont, IL, 2016.

New Investigator Travel Award to attend and participate at the AAOS/ORS Tackling Joint Disease by Understanding Crosstalk between Cartilage and Bone, Research Symposium, Rosemont, IL, 2016.

Christopher & Margie Nordin Young Investigator Poster Award at the Australian and New Zealand Bone & Mineral Society Annual Scientific Meeting, Hobart, Australia, 2015.

ANZBMS Travel Award to attend the Australian and New Zealand Bone and Mineral Society Annual Scientific Meeting, Hobart, Australia, 2015.

Best Clinical Science Free Paper for 2015 at The Australian Rheumatology Association, 56th Annual Scientific Meeting, Adelaide, Australia 2015.

Florey Medical Research Foundation Prize at the Florey International Postgraduate Research Conference, Adelaide, Australia 2014.

School of Medicine Prize at the Florey International Postgraduate Research Conference Adelaide, Australia, 2014.

Abbreviations

ANOVA	Analysis of variance
BMI	Body mass index
BML	Bone marrow lesions
BML1	BMLs detected by PDFS weighted sequence only; in the same area signal on T1 weighted sequence is absent.
BML2	BMLs detected by both PDFS and T1 sequences
BLOKS	Boston Leeds Osteoarthritis Knee Score
BV	Bone volume
BV/TV	Bone volume fraction
COMP	Cartilage oligomeric matrix protein
Cr.Dn	Linear microcrack density
Cr.Le	Average linear microcrack length
Cr.S.Dn	Linear microcrack surface density
DA	Degree of anisotropy
DESS	Dual-echo steady state
DD.Ar	Diffuse damage density area
DD.Dn	Diffuse damage density
EL.Dn	Empty lacunar density
EL/TL	Percent of empty lacunae
ES.Dn	Eroded density
ES.Le	Average eroded surface length
ES.S.Dn	Eroded surface density
FLASH	Fast low-angle shot
H&E	Hematoxylin and eosin
IGF	Insulin-like growth factor

K&L	Kellgren and Lawrence
KOA	Knee osteoarthritis
KOSS	Knee Osteoarthritis Scoring System
MetS	Metabolic syndrome
Micro-CT	Micro computed tomography
MOAKS	MRI Osteoarthritis Knee Score
MRI	Magnetic resonance imaging
OA	Osteoarthritis
OARSI	Osteoarthritis Research Society International
OCU	Osteochondral unit
PDFS	Proton density fat suppressed weighted sequences
Ot.Dn	Osteocyte density
OPG	Osteoprotegerin
Pl.Po	Plate porosity
Pl.Th	Plate thickness
PTHrP	Parathyroid hormone related protein
RANK-L	Receptor activator of nuclear factor kappa B ligand
ROI	Region of interest
SMAD3	Mothers against decapentaplegic homolog 3
SPGR	Spoiled-gradient-recalled
Tb.N	Trabecular number
Tb.Pf	Trabecular bone pattern factor
Tb.Sp	Trabecular separation
Tb.Th	Trabecular thickness
TKR	Total knee replacement
TL.Dn	Total lacunar density

TP	Tibial plateau
TGFβ	Transforming growth factor beta
TWIST1	Transcription factor Twist-related protein 1
WHO	World Health Organization
WORMS	Whole Organ Magnetic Resonance Imaging Score

List of Figures

List of Tables

Chapter 1

Literature review and project aims

1.1 Introduction

Osteoarthritis (OA) is a multifactorial slow-progressive disease of the whole joint. According to the Australian Bureau of Statistics and the Australian Institute of Health and Welfare, approximately 2.1 million Australians (9% of the population) suffered from OA in 2014–15, based on self-reported data [1]. The prevalence of OA is higher among females and the older population. Approximately 10% of females have OA compared to 6% of males. Also, it is estimated that 52% of people aged 75 and over suffer from this condition, compared with only 1% of people aged less than 25 years. The World Health Organization (WHO) estimates that 10% of the world's population over 60 years of age suffers from OA, and that 80% of people with OA experience limitation of movement and 25% cannot perform activities of daily living [2].

While OA can affect all joints in the human body, it is most common in the knee. The knee is the largest synovial joint in the body and it is composed of 3 bones (femur, tibia and patella) and 2 joints; tibio-femoral joint, which itself is comprised of a medial and a lateral compartment, and the patello-femoral joint (**Figure 1-1**) [3]. The proximal part of the tibia, known as the tibial plateau, is the most affected side of the tibio-femoral joint and suffers the most severe structural changes in joint disease. The current treatment options for knee OA are largely to help relieve the clinical symptoms. The main options are; lifestyle measures such as weight loss and exercises, pharmacological pain management and when those are not sufficient, joint replacement surgery to repair or replace damaged joints may also be considered. Surgical procedures restore joint function, help relieve pain and in general improve quality of life of OA sufferers [4].

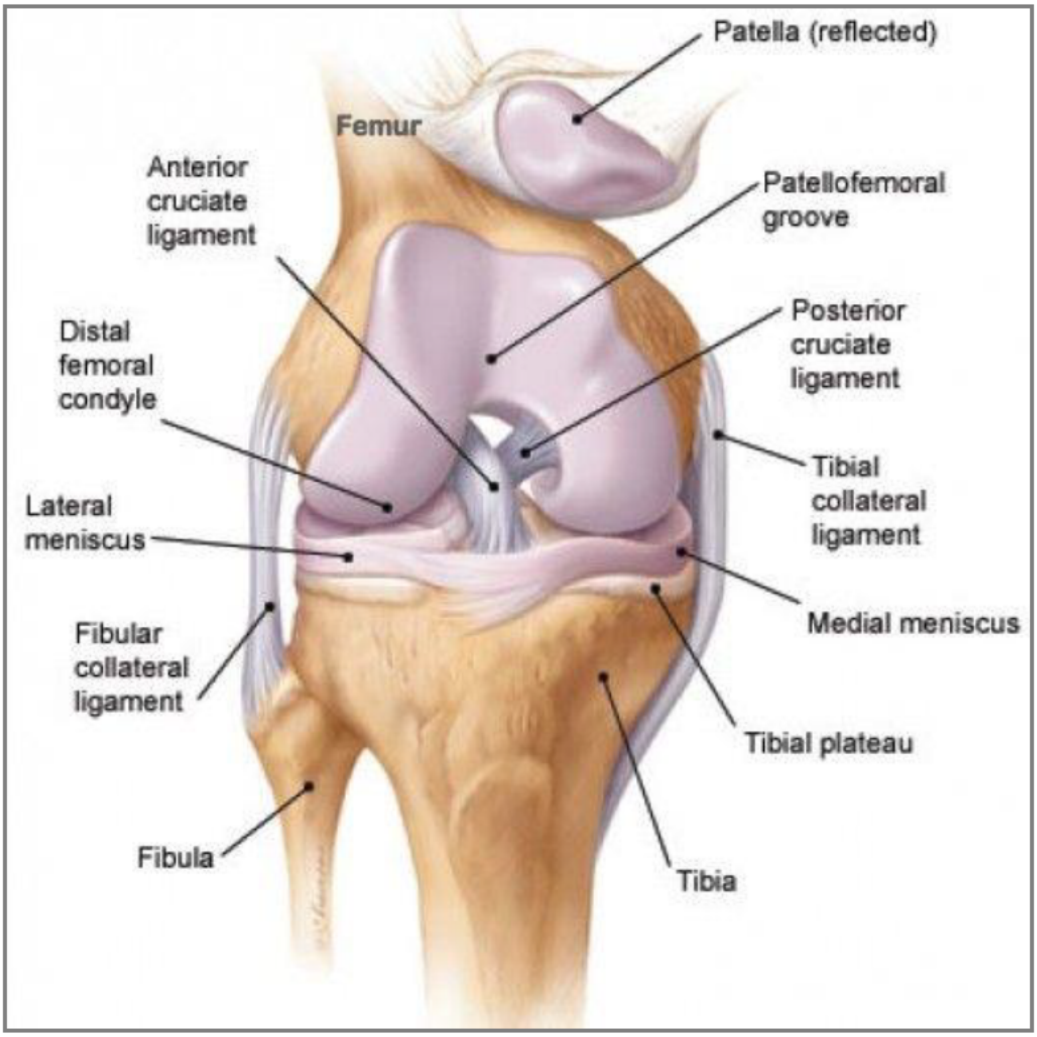

Figure 1-1:The frontal view of the right knee joint showing tibia, femur, fibula, ligaments, and meniscus. Image reproduced from https://flexcin.com/dealing-with-treating-knee-pain-from-an-mcl-injury.

Unfortunately, surgical treatment involves certain risks of complications such as; postoperative infection, development of blood clots, nerve damage and, in very rare circumstances, death [5].

In Australia, the number of total knee replacements (TKR) is continually increasing (**Figure 1-2**) [1]. According to the Australian Institute of Health and Welfare and the Australian Joint Replacement registry, the number of TKRs between 2000–01 and 2007–08 increased from 16,089 to 26,712, or 67% over 7 years. In their last published report in 2014-15, 47,087 TKRs were performed, an increase of 75% over 7 years [1, 6]. There are no consensus criteria to determine for which patients TKR is an appropriate method of treatment. Thus, it has been noted that the proportion of younger patients (<65 years of age) receiving TKR is also increasing [7]. In order to improve the current clinical management of KOA, there is an urgent need to understand disease aetiology, with a clear definition of early and late stage disease. This would then contribute to the development of more optimised approaches to OA treatment and disease management.

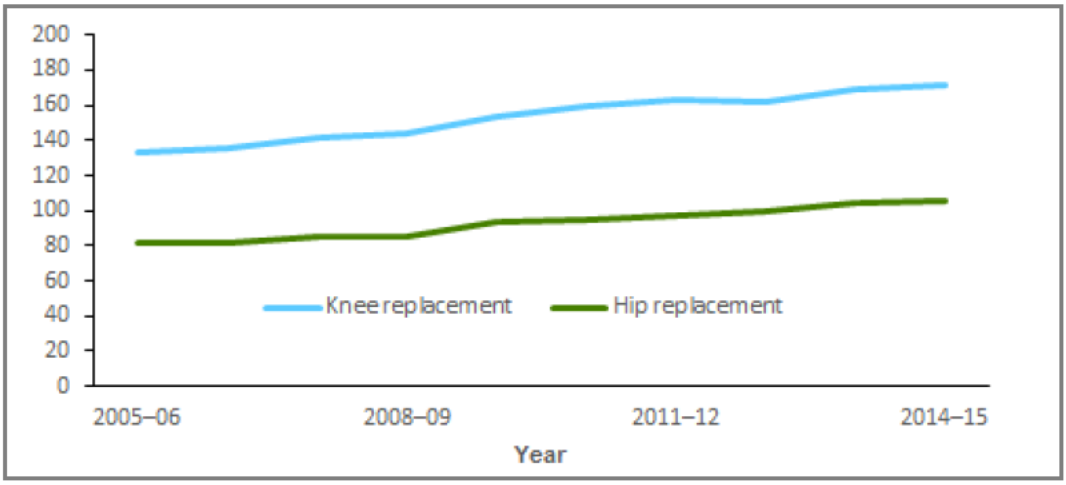

Figure 1-2: The number of knee and hip replacements in the Australian population for period 2005/6-2014/15. Image reproduced from https://www.aihw.gov.au/reports/arthritis-other-musculoskeletal-conditions).

1.2 Definition of knee osteoarthritis

The current definition of KOA is that it is a disease of the whole joint. Specifically, its pathogenesis involves changes in the cartilage, subchondral bone, synovial ligaments and menisci. However, it is well accepted that in the course of the disease the most severe progressive and degenerative structural changes occur at the bone and cartilage interface, also known as the osteochondral unit (OCU) (**Figure 1-3**).

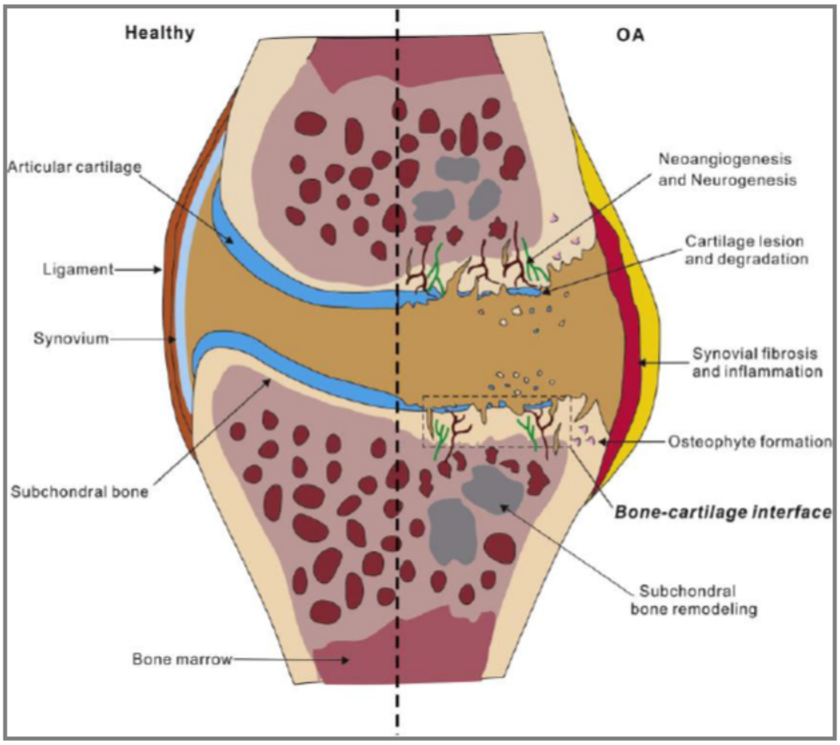

Figure 1-3: Difference between the healthy and osteoarthritic (OA) joint. Image reproduced and adapted from "Bone-cartilage interface crosstalk in osteoarthritis: potential pathways and future therapeutic strategies" Yuan *et al.*, 2014.

Structural changes in the OCU include loss of articular cartilage, and modifications of the subchondral bone, such as new bone formation, leading to sclerosis of subchondral bone and formation of osteophytes, the presence of bone marrow lesions (BML) and subchondral cysts. These changes lead to debilitating clinical symptoms, primarily severe pain, joint stiffness and immobility, which may eventually lead to TKR surgery [8-12]. To investigate the structural changes indicative of OA, different imaging modalities can be used.

1.3 Imaging modalities in KOA

1.3.1 Plain radiography

Plain radiographs (x-rays) are the most commonly used to assess structural changes associated with KOA (Figure 1-4). Radiographs demonstrate and evaluate narrowing of the distance between bones, defined as 'joint space narrowing', which indirectly provides an estimate of cartilage thickness. Radiological grading schemes, such as the Kellgren-Lawrence grading system and Osteoarthritis Research Society International (OARSI) classification score have been developed to assist assessment of OA progression by radiographic imaging [13-15]. However, these methods are limited, as they only indicate changes defined as joint space loss, which does not change linearly over the course of OA disease [13]. In general, radiographs have been criticized as not being sensitive to early changes, not able to demonstrate all components of the joint and often prone to measurement error due to change of patient positioning [16].

Figure 1-4: X-Ray of the knee with normal joint space (left) and OA knee with reduced joint space, osteophyte and sclerotic subchondral bone. Image reproduced from http://www.docjoints.com/knee-arthritis.

1.3.2 Magnetic resonance imaging (MRI)

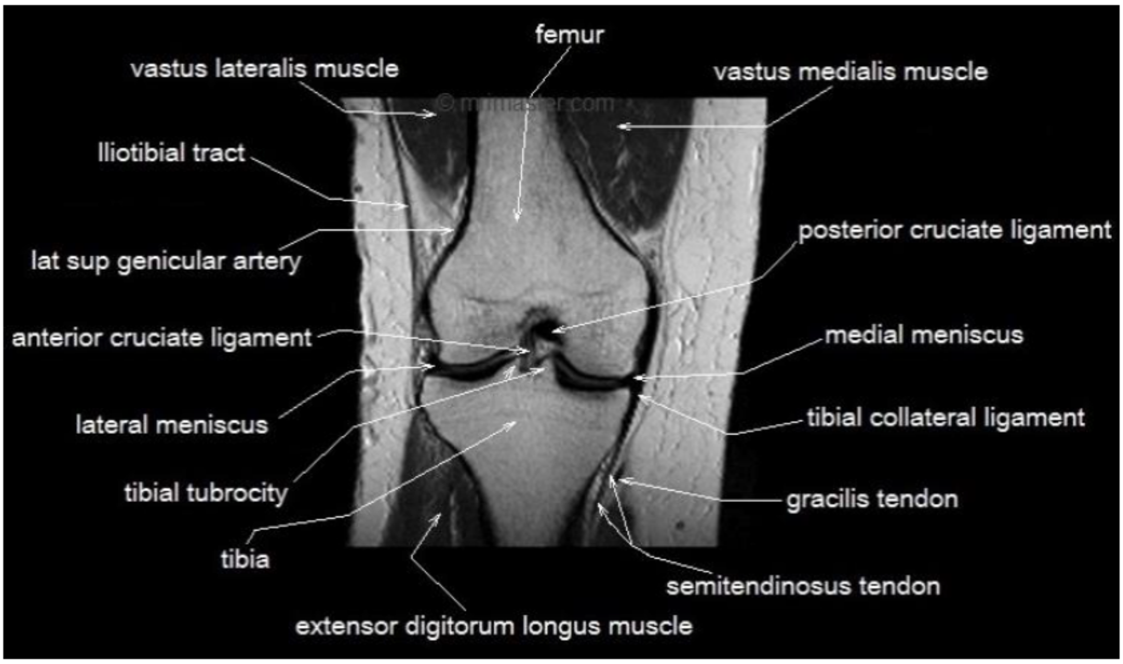

Figure 1-5: Components of the knee joint visualised by MRI.Image adapted from http://www.docjoints.com/knee-arthritis.

The development of magnetic resonance imaging (MRI) using powerful magnetic fields instead of x-rays allows detailed visualization of all components of the knee joint (**Figure 1-5**) and enables examination of the structural changes across disease progression in OA [17, 18]. Importantly, specific pathology of the OCU, such as changes in cartilage volume, bone marrow lesions (BMLs), subchondral cysts, bone attrition and osteophytes can all be assessed by MRI at an early stage and followed through the progression of the disease. Also, it has been shown that MRI is more powerful than radiographic assessment of patients with more advanced OA disease [17-19]. Several semi-quantitative morphologic whole-organ scoring systems have been proposed to help to understand the associations between MRI detected OCU pathologies, the progression of knee structural damage and clinical manifestation of symptoms, especially pain (**Table 1-1**). One of the first published scoring systems was the Whole Organ Magnetic Resonance Imaging Score (WORMS), [20]. Since then, the Knee Osteoarthritis Scoring System (KOSS) [21], the Boston Leeds Osteoarthritis Knee Score (BLOKS) [22], and the MRI Osteoarthritis Knee Score (MOAKS) [23] have been developed. The reproducibility and sensitivity of these semi-quantitative systems have been tested in several studies [21, 22, 24]. In comparison to previous systems, the MOAKS exhibited very good reliability for the majority of features assessed, and to date it is the most recommended tool for semi-quantitative MRI assessment of KOA [23].

Table 1-1. Most commonly used whole-organ scoring systems for knee OA

Scoring system	Scored features and grades
WORMS (Whole Organ Magnetic Resonance Imaging Score) [20]	Cartilage (0–6); BMLs size (0–3); subchondral cysts (0–3); bone attrition (0–3); effusion and synovitis (0–3); periarticular cysts (0–3); bursitides (0–3); loose bodies (0–3); osteophytes (0–7); meniscal tear (0-4); cruciate and collateral ligaments (0–1)
KOSS (The Knee Osteoarthritis Scoring System) [21]	Cartilage size and depth (0–3); BMLs size (0–3); subchondral cysts (0–3); osteophytes (0–3); effusion (0–3); meniscal tear (0–3); meniscal extrusion (0–3); popliteal cysts (0–3); synovial thickening (0–1)
BLOKS (Boston Leeds Osteoarthritis Knee Score) [22]	Cartilage size and depth (0–3, plus extent of any cartilage loss); BMLs size (0–3, for each lesion); osteophytes (0–3); effusion (0–3); meniscal extrusion (0–3); synovitis (in Hoffa's fat pad 0–3 and at 5 additional sites 0–1); meniscal status (0–1 for intrameniscal signal, tears, maceration, meniscal cyst, each scored individually); ligaments (0–1); periarticular cysts/bursitis (0–1); loose bodies (0–1).
MOAKS (MRI Osteoarthritis Knee Score) [23]	Cartilage size and depth (0–3); BMLs size (0–3, for each lesion); osteophytes (0–3); effusion-synovitis (0–3); Hoffa synovitis (0–3); meniscal extrusion (0–3); meniscal status (0–1, for intrameniscal signal, tears, maceration, meniscal cyst, hypertrophy; scored individually); ligaments (0–1); periarticular cysts/bursitides (0–1, scored individually); loose bodies (0–1)

Table 1 Adapted from "MRI based semi-quantitative scoring of joint pathology in osteoarthritis" Nature Reviews, Rheumatology, 2013 [25].

1.4 Osteochondral unit as the functional unit of the knee joint

The osteochondral unit consists of three morphologically and physiologically distinct units; articular cartilage, subchondral bone (subchondral plate and subchondral trabeculae) and fatty bone marrow located between the trabeculae (**Figure 1-6**). While those units represent different anatomical compartments, it is important to stress that they are in close relationship and function as one unit. Therefore, it is believed that a pathological change in one will adversely affect the others [26-28].

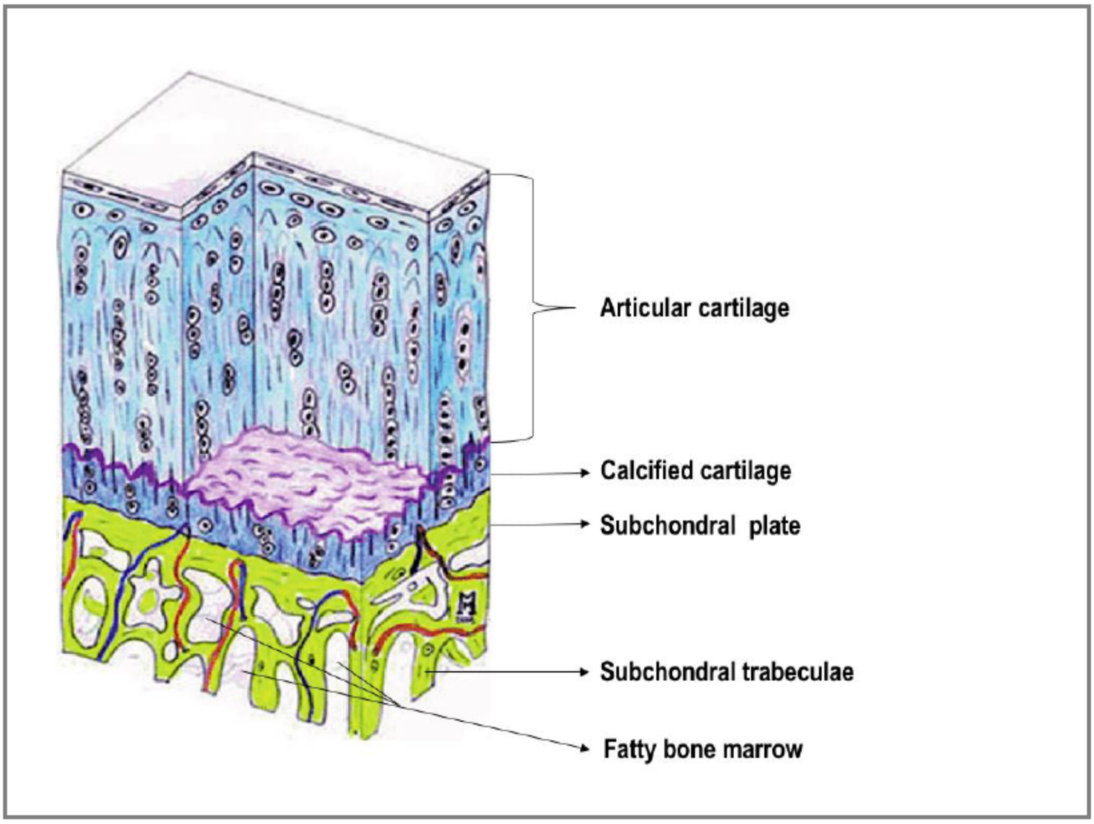

Figure 1-6 : Diagram of the osteochondral unit and its components. Image adapted from Imhof, H., et al., Subchondral bone and cartilage disease: a rediscovered functional unit. Invest Radiology, 2000) [27].

1.4.1 Articular cartilage

The articular cartilage is a 2 to 4 mm thick layer of specialised connective tissue covering the ends of bones that form articulating joints. The main function of the cartilage is to allow friction-free movements inside the joint and to spread the transmission of mechanical loading onto the underlying bone. Articular cartilage is composed mainly of water, collagen, proteoglycans, and small amounts of non-collagenous proteins and glycoprotein [29]. Based on the orientation of the cartilage fibrils and the morphology of the cartilage cells, the chondrocytes, cartilage can be divided into four zones or layers; superficial layer, transitional or reserve (resting) layer, proliferation or deep layer and hypertrophy zone or calcified layer (**Figure 1-7**) [29].

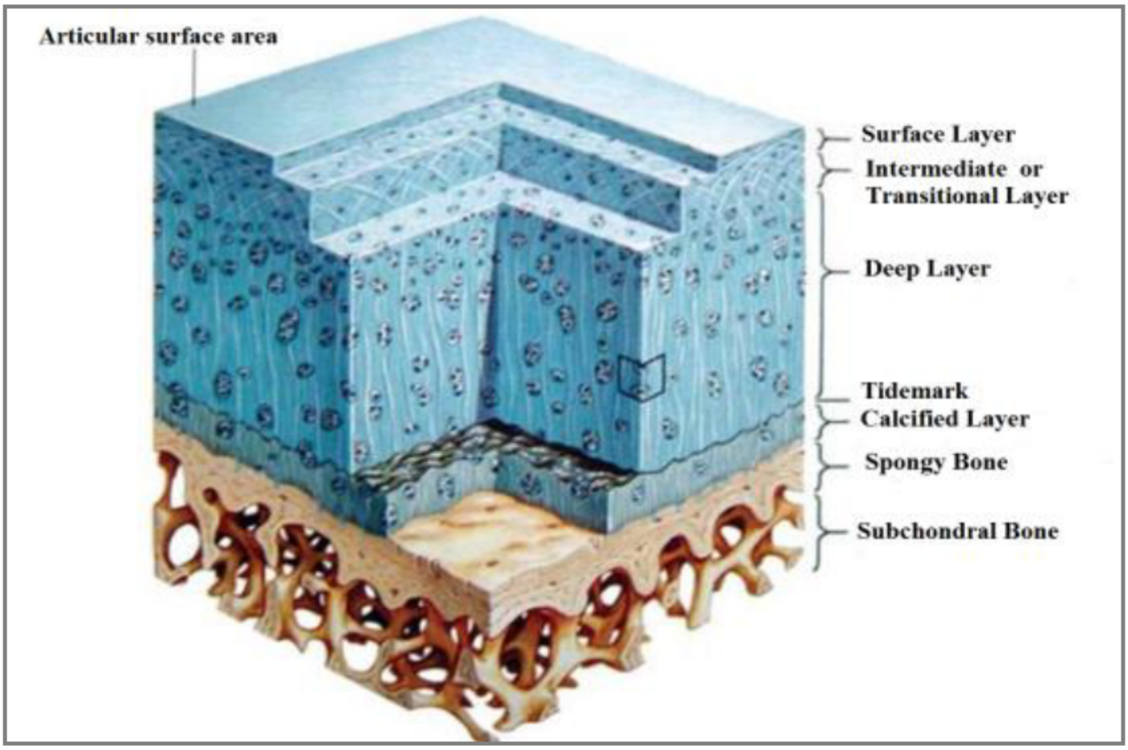

Figure 1-7: A cross sectional view of the cartilage and its zones. Image adapted from https://www.jplrc.com/cartilage-defects.html.

The superficial zone occupies about 10% to 20% of the articular cartilage thickness. Inside this zone chondrocytes are arranged parallel to the articular surface. The reserve or transitional zone, represents 40% to 60% of the cartilage. In this zone collagen fibrils are arranged diagonally and the chondrocytes are spherical to the articular surface. The deep zone represents approximately 30% of articular cartilage and it is responsible for providing resistance to compressive forces. Collagen fibrils in this zone are arranged perpendicular to the articular surface and chondrocytes have a parallel orientation to the collagen. The zone of the calcified layer represents approximately 5% of the cartilage, and it acts as a transition zone from the cartilage to the bone. In this zone chondrocytes are hypertrophic. Healthy articular cartilage is avascular and without nerves or lymphatics supply.

1.4.2 Subchondral bone

Subchondral bone has been defined as the thin layer of calcified tissue, located immediately below the articular cartilage. It consists of two distinctive structural formations; the subchondral plate and subchondral trabeculae (**Figure 1-8**) [26, 28, 30]. The subchondral plate is a plate-like structure located between the calcified cartilage at one end and subchondral trabeculae and fatty marrow between trabeculae at the other end [28]. Also, it has been noted by Lyons *et al.* that fingers of uncalcified cartilage, delineated by the tidemark, dip through the calcified cartilage into the subchondral bone and marrow spaces [31]. Thus, the cartilage and subchondral bone show both mechanical linkage and physical contact to allow the exchange of nutrients and bioactive molecules.

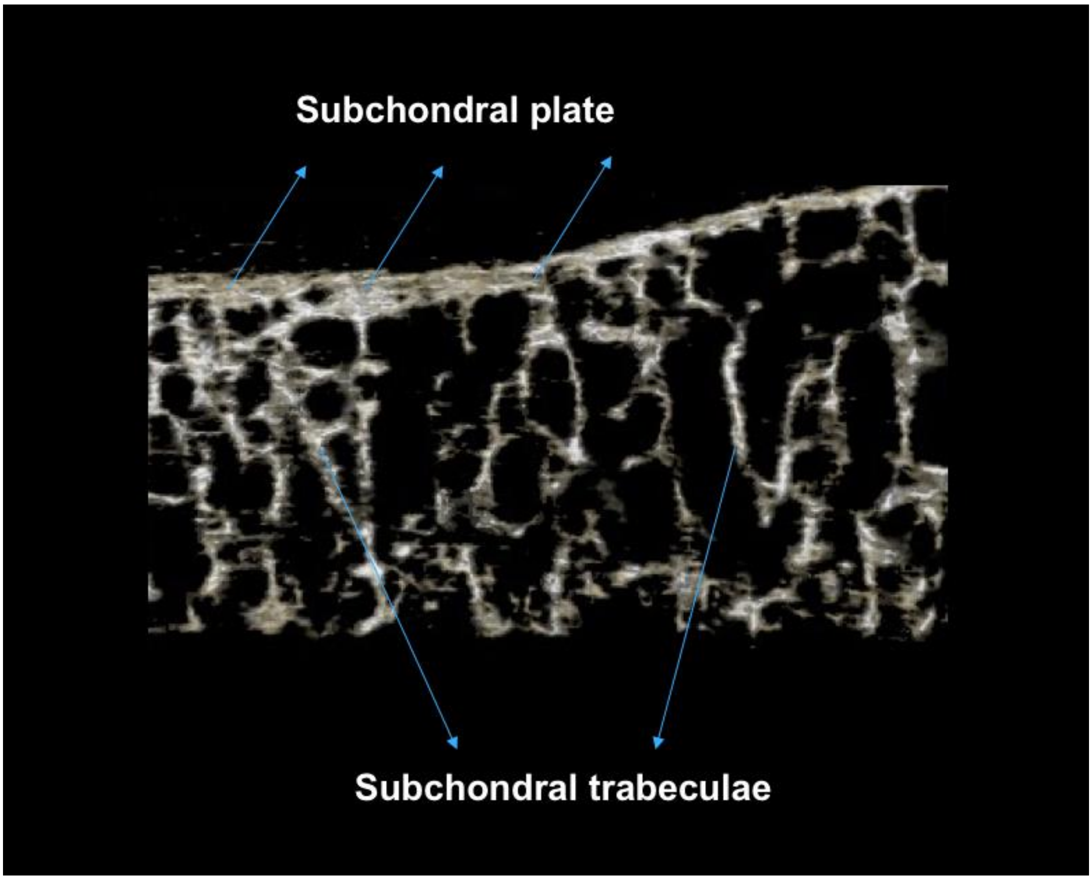

Figure 1-8 Micro computed tomography image (sagittal plane) of human proximal tibial subchondral bone indicating two distinctive structural formations; subchondral plate and subchondral trabeculae.

The thickness of the subchondral plate varies between different joints, between males and females, and between different age groups, and it has been found that heavily loaded areas have greater thickness [26, 32]. From the subchondral plate arise the subchondral trabeculae, consisting of interconnected rods and plates. The extent of trabecular bone below the subchondral plate considered as part of the OCU (in the human proximal tibia) is 6-10 mm [33]. The subchondral plate and subchondral trabeculae are architecturally, physiologically and mechanically different and respond differently during OA pathogenesis [28, 34]. They undergo significant changes and modifications during the development and progression of OA, resulting in the appearance of subchondral bone sclerosis, cysts, bone marrow lesions (BMLs) and/or osteophytes [34].

Much of the research focus in KOA has been on investigating the loss of cartilage cellular and structural integrity. However, a substantial amount of evidence has been collected showing that changes in subchondral bone have an important impact on the progression of KOA disease [26, 28, 35]. Animal models suggest that changes in the subchondral bone may even precede cartilage changes [36-40]. Understanding changes in the subchondral bone that may alter the bone quality and may contribute to the joint pathogenesis of OA is essential for better understanding of OA aetiology and also might be important information for the development of effective treatments for KOA.

1.5 Subchondral bone quality and osteoarthritis

Bone quality represents the sum of all characteristics of bone that together describe the composition and structure that contribute to bone strength, and also may be independent of bone mineral density [41, 42]. Bone might be qualitatively different in strength despite similar bone density. For example, in young adults, bone is stronger across all levels of bone density compared to bone in older adults. So, the concept of bone strength includes a number of characteristics of bone besides bone density that collectively are termed “bone quality” [43]. Thus, it includes; bone turnover, microarchitecture, mineralisation, microdamage and composition of the bone matrix and mineral [44]. These components are interdependent, so often changes in one result in changes to the others. In particular, changes in bone turnover affect other components of bone quality (such as the degree of mineralisation) and hence its measurement in clinical practice is of key importance [44].

1.5.1 Bone turnover

The rate of bone remodelling is an important determinant of bone quality. It refers to the total volume of bone that is both resorbed and formed over a period of time [45]. Under ideal circumstances the amount of bone resorbed equals the amount reformed. Bone remodelling can be estimated in clinical practice by measuring circulating and excreted biochemical markers of resorption and formation [44, 46]. In a naturally occurring OA guinea-pig model, markers of bone formation and resorption are reported to be higher before visible cartilage degeneration [37], indicating that one of the earliest changes in OA is a change in bone remodelling. Bone remodelling is a harmonised process of cellular activity responsible for bone renewal and repair. Understanding the cell biology of this process is essential, since abnormalities of bone remodelling may have involvement in metabolic bone diseases [47]. The bone remodelling cycle (**Figure 1-9**) begins with an *activation phase* that involves recruitment of osteoclast precursors to the skeletal site that is to be remodelled [47]. Next is the *phase of bone resorption,* during which osteoclasts remove bone and then undergo programmed cell death (apoptosis). In the final stage, *bone formation* takes place to replace the removed bone. It begins with recruitment of osteoblast precursors to the remodelling site. These cells then differentiate into mature osteoblasts and start to form a new bone matrix (osteoid), which subsequently becomes calcified to form mature mineralised bone [47].

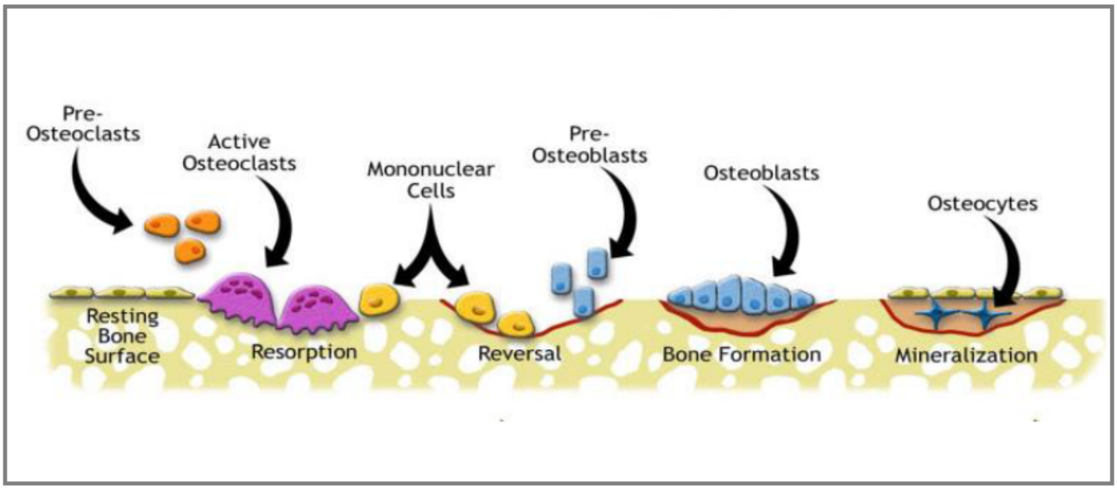

Figure 1-9: Bone remodelling is a coordinated process of three major types of cells: osteoclasts- bone resorbing cells, osteoblasts- bone forming cells and osteocytes- bone matrix cells. Image reproduced from http://www.orthopaedicsone.com.

It was long believed that during the pathogenesis of OA, subchondral bone underwent only appositional new bone formation, which resulted in sclerotic bone. However, at least in animal models, bone attrition and bone loss are characteristic of early stage OA [38, 48]. Also, in an early experimental OA mouse model, gene microarray analysis of subchondral bone showed increased expression of catabolic factors before any signs of cartilage degeneration [49]. In OA patients with progressive KOA, evidence of increased bone resorption are seen; whereas, in general, non-progressing OA patients do not show evidence of altered resorption [50]. Based on current published data from human studies it is very hard to distinguish if changes in bone turnover are causative of human OA or a consequence of the disease process.

1.5.2 Cellular components

There are four main cell types in bone tissue; osteoprogenitor cells of the osteoblast lineage, osteoblasts, osteocytes, and osteoclasts (osteoclast progenitors are recruited to bone *via* the circulation), (**Figures 1-9 & 1-10**).

Osteoprogenitor cells are primitive cells derived from the mesenchyme (Figure 10a). They form in the inner layer of the periosteum and also line the marrow cavity, as well as Haversian and Volkmann's canals of compact bone. During the period of growth and remodelling, these cells are stimulated to differentiate into osteoblasts that lay down new bone. They can also differentiate into other cell types such as fibroblasts, chondroblasts and adipose cells [51].

Osteoblasts are large cells with abundant basophilic cytoplasm, which originate from primitive mesenchymal cells. Their main function is to lay down new bone in the form of osteoid, which consists mainly of collagen that is essential for later mineralisation in the form of hydroxyapatite [52]. Deposition of mineral makes the bone matrix stiff, and capable of bearing loads [51].

In the course of OA, it has been noted that osteoblasts display biological and morphological differences [53, 54]. Also, it has been noted that OA osteoblasts have altered expression of important bone factors (RANK-L: receptor activator of nuclear factor kappa B ligand, OPG: osteoprotegerin, IGF: insulin-like growth factor, PTHrP: parathyroid hormone related protein) [54]. Further, gene expression analysis of osteoblasts derived from hip OA showed that dysregulated expression of the transcription factor Twist-related protein 1 (TWIST1), transforming growth factor-beta (TGFβ1) and Mothers against decapentaplegic homolog 3 (SMAD3) was present in OA osteoblasts, both *in vivo* and *ex vivo*, suggesting that altered intrinsic properties of osteoblasts might have a role in OA aetiology [55, 56].

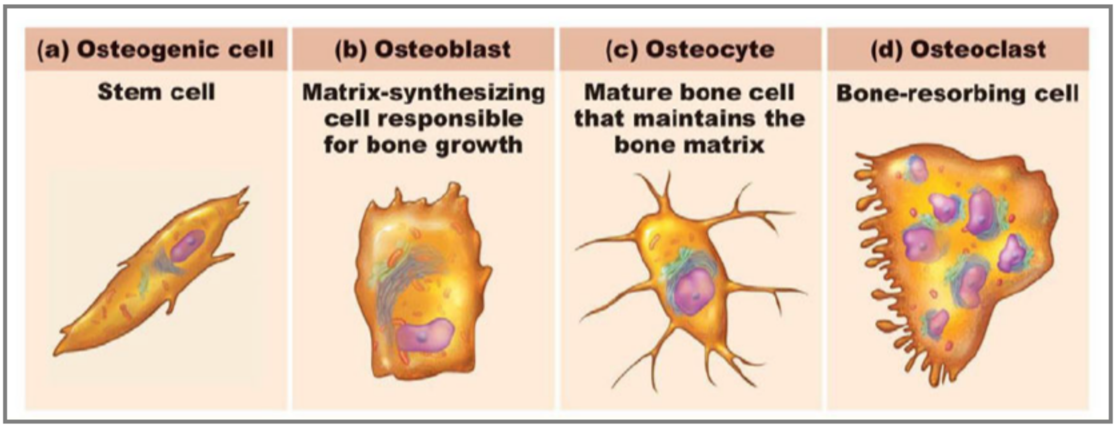

Figure 1-10: Cell types in bone tissue; osteoprogenitor cell, osteoblast- bone forming cell, osteocyte, and osteoclast- bone resorbing cell. Image reproduced from https://infograph.venngage.com/p/185921/bone-project).

Osteoclasts are large multinucleated cells derived from the monocyte/macrophage cell lineage [57]. They can be found attached to the bone surface at sites of active bone resorption [58]. Osteoclasts have a short lifespan of several weeks and their role is the resorption of the mineral and organic components of bone tissue [59]. Osteoclasts are important for maintenance of bone quality as they actively participate in shaping bones, and removing damage and/or non-vital bone [60]. Osteoclastic formation and activity are regulated by RANKL [61]. The relative excess of RANKL has been shown to play a role in focal bone loss pathologies [62, 63]. Osteoclasts have been found to have an important role in joint disease, with the majority of evidence of their involvement in the progression of joint disease coming from rheumatoid arthritis studies, where osteoclasts play an active role in bone erosion [60, 62, 64, 65]. The role of osteoclasts in OA pathogenesis is less clear, particularly in human disease. Evidence from animal studies suggested that use of antiresorptive therapy (bisphosphonate) decreased OA progression, suppressing subchondral bone resorption, reducing osteophyte size, and preventing cartilage degradation [66] [67]. This effect of bisphosphonates is believed to act by a direct inhibitory effect on osteoclasts and bone turnover [66]. However, data from human studies has not demonstrated a clear benefit of antiresorptive therapy in human OA [68, 69]. Osteocytes reside within the bone matrix, connected to each other *via* long cell extensions, which run through canaliculi (Figure 10c) [70]. Osteocytes are present in the bone at high density, although the number, size and position of osteocytes vary according to the type of bone and skeletal sites they inhabit [59, 71]. Recently, Buenzli and Sims estimated that the total number of osteocytes within the average human skeleton is ~42 billion and the total number of osteocyte dendrites are ~3.7 trillion [72]. Furthermore, based on the average time of the remodelling cycle in the adult, this study estimated that 9.1 million osteocytes are restored on a daily basis in the skeleton, signifying the intriguing and dynamic nature of the osteocyte network [72]. Also, it is believed that osteocyte viability may play a significant role in the maintenance and integrity of bone quality, since it has been shown that osteocyte apoptosis has essential roles in the repair of microdamage in bone [73]. Osteocytes appear to have a number of important roles in bone [74, 75]. They possess the ability to reabsorb (and reform) bone mineral, in a process termed osteocytic remodelling [74]. Osteocytes thereby maintain the structural integrity of the mineralised matrix and may mediate short term release of calcium for the purpose of systemic calcium homeostasis in the body. Verborgt *et al*. described a central role for osteocytes in bone matrix repair [76], and more recent studies have shown that osteocytes direct focal modelling and remodelling by detecting strain in bone [77-80]. Because of this, bone with a reduced number of osteocytes, such as has been reported in the bone of patients with a fragility fracture, may have an impaired ability to repair microdamage [81]. In OA pathogenesis, altered morphology and viability of osteocytes have been reported in sclerotic regions of the subchondral bone in OA [82]. However, osteocyte number and viability, in relation to the progression of OA, has not been investigated.

In addition, it is important to mention bone tissue resident macrophages, named osteomacs, that are found to reside at the bone remodelling site [83]. Osteomacs are closely related to osteoclasts by sharing a dependence on the lineage-specific growth factor CSF-1 [83]. However, osteomacs express the epidermal growth factor seven transmembrane (EGF-TM7) protein EMR1/F4/80 which clearly distinguishes them from osteoclasts. *In vivo*, osteomacs are found at the sites of bone modeling forming a distinctive canopy structure over mature osteoblasts, whereas *in vitro* they enhanced osteoblast mineralisation suggesting that osteomacs are likely to have a role in anabolic bone modelling [83, 84].

1.5.3 Mineralisation

An important aspect of the material properties of bone is the degree of mineralisation. Overly mineralised bone tissue is more frail, and less resistant during impact loading, while under mineralised bone may be too flexible for the function it must perform [85]. Bone must at the same time be stiff enough to be resistant to bending and elastic during dynamic loading so it retains the same length without damage [86]. These contradictory properties are achieved by varying the mineral content of the collagen tissue of bone [85]. The mineralisation of the bone matrix is dependent on the age of the bone; in general older bone is more mineralised because of alterations in bone remodelling rates [87]. However, in OA, decreased mineralisation of subchondral bone has been noted in both the subchondral plate and trabeculae in animal models and humans [88-90].

1.5.4 Microarchitecture

The high power, non-destructive imaging method of Micro Computer Tomography (Micro CT) has been developed to enable high resolution (5 µm-50 µm), 3-dimensional visualisation and direct quantification of bone microarchitecture [44, 91, 92]. Changes in the microarchitecture of subchondral bone is an important characteristic of OA and it is believed to result largely from high joint loading. Animal OA studies have substantially contributed to the understanding of subchondral bone changes during progression of OA, suggesting that changes in subchondral microarchitecture may occur before, during and/or after cartilage damage [37, 38]. Furthermore, it has been suggested that different types of changes in subchondral bone microarchitecture may occur at different stages of OA disease progression. Thus, all changes and modifications in SCB should be treated as significant pathophysiological events [35].

In animal OA models [39, 48] the early stage of OA is characterised by a thinner subchondral bone plate, increased plate porosity [48, 93, 94], fewer subchondral bone trabeculae that are rod-like in structure and show reduced connectivity, with an overall decrease in bone volume [50, 95-98]. In late stage OA, changes in the SCB are described as a thicker subchondral bone plate, increased trabecular bone density, trabecular thickness and trabecular number, while the separation between trabeculae is decreased and transformation of trabeculae from rod-like into plate-like is evident [99-101]. However, these findings have not been observed consistently [33, 102].

Recently, it has been suggested that according to the features of subchondral bone (sclerotic and non-sclerotic trabecular bone), two subtypes of OA exist, suggesting different mechanisms of disease progression [103]. Also, it has been noted that specific changes, such as an increase in trabecular thickness, closely correlate with increased cartilage histological grade (increased degradation) [104], while an increase in trabecular number and a decrease in separation and SMI associates with loss of cartilage volume [40, 105]. Furthermore, it was deduced from a guinea pig OA study that retention of a rod-like structure might protect cartilage from damage during impact loading [105]. It is also important to apply an optimal measure parameter for assessment of plate/rod geometry in human bone structure as it has been suggested that SMI might not be the optimal parameter [106].

1.5.5 Microdamage

Microscopic bone damage (microdamage) is an important aspect of bone quality, with biomechanical relevance. Microdamage may occur in one or more of the constituents of bone’s material composition, and at nano-, micro-or macro structural levels (**Figure 1-11**) [86]. The accumulation of microdamage in bone tissue contributes to reduced bone strength, stiffness and resistance to mechanical loading [51], factors that may subsequently contribute to the progression of OA [107]. Microdamage in bone tissue may be present in the form of microfractures, linear microcracks [107] and diffuse damage [108] that each has different mechanical and biological consequences [86, 109-111].

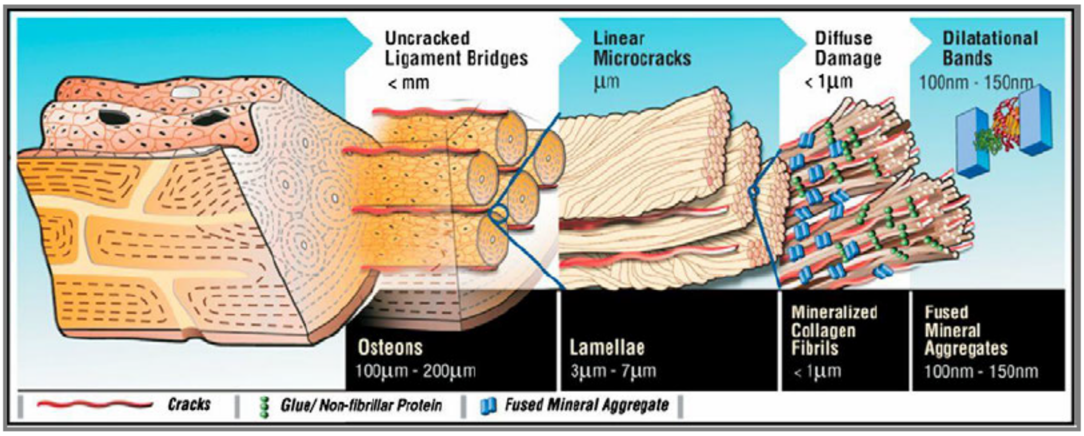

Figure 1-11: Microdamage manifests in multiple forms across the scales of hierarchy in bone. Image adapted from Poundarik and Vashishth, Multiscale imaging of bone microdamage, Connect Tissue Res. 2015) [111]

Microfracture is a type of damage that extends horizontally and completely across trabeculae. It measures about 500 microns (µm) in diameter and can be visualised when the fracture is surrounded by microcallus, indicating a healing process (**Figure 1-12**) [112]. It is believed that this type of damage is the result of normal physical activity and that its accumulation increases with age [112, 113].

Linear microcracks and diffuse damage are identified at a smaller scale. Linear microcracks are characterised by their linear shape and relative size of an average 100 µm in length [114]. Formation and accumulation of microdamage depends on the microstructure of the bone, the type and amount of stress imposed, and the age of the bone [86]. Accumulation of linear microcracks has been associated with compressive loading, which reduces the toughness (ability to resist further damage) in the plate, and reduces the strength and stiffness in trabeculae [109, 110, 115]. The formation and accumulation of diffuse damage, defined as many small cracks (<10µm length), depends on the bone quality and the amount and type of imposed load. Accumulation of diffuse damage has been associated with tensile loading [110, 115].

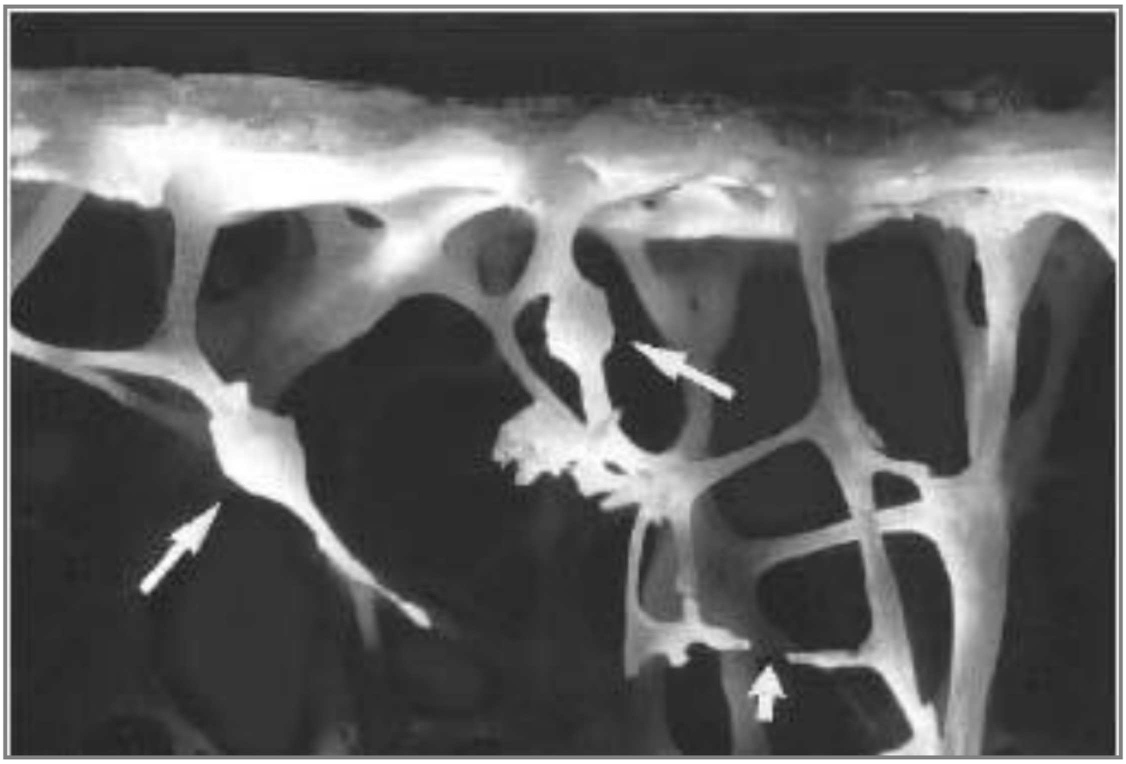

Figure 1-12: Healing microfracture with callus (white arrow) identified by the scanning electron micrograph. Image reproduced from Frost HM. The Utah Paradigm of Skeletal Physiology Vol 1. 2004; 4:208-219).

There is an opinion that the accumulation of diffuse damage is an early form of fatigue, which, if not repaired might transform into linear cracks [116, 117]. Others have proposed that diffuse damage might represent a different form of microdamage but that it shares some characteristics with linear microcracks [118]. There are several theories as to how microdamage can be induced in bone tissue; extensive and repetitive loading, increased vascular porosity, or a change in blood perfusion [119]. It has been shown that repair of microdamage is initiated by osteocytes and that osteocyte apoptosis is essential for initiation of the repair process [120]. Frost was the first to suggest that remodelling targets microdamage in the bone to maintain the skeletal integrity [121]. Later on this hypothesis was proven experimentally when fatigue processes exceed the rate of bone repair, microdamage accumulates in the tissue and ultimately affects bone quality and may have implications in musculoskeletal diseases such as OA [107].

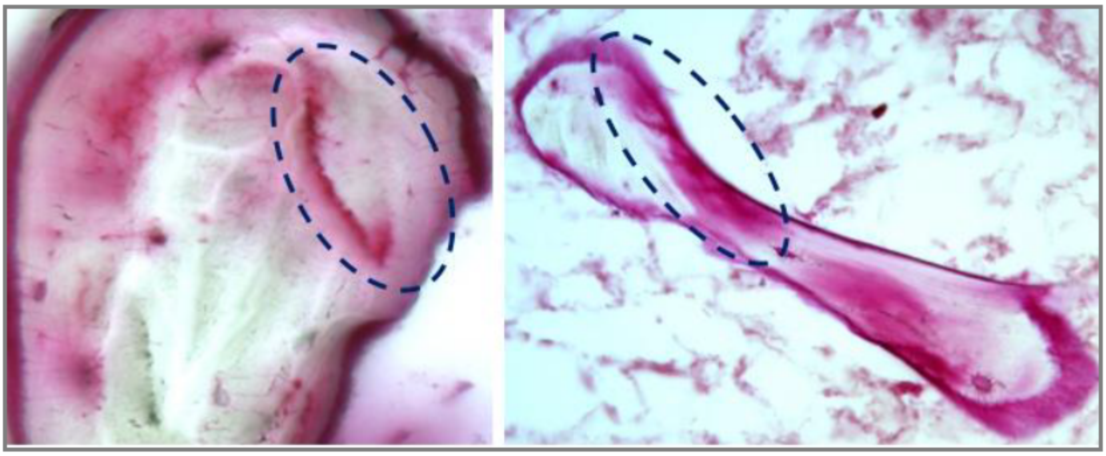

Figure 1-13: Representative images of linear microcrack (left) and diffuse damage (right) in human proximal tibial subchondral trabecular bone identified in a 70 μm thick resin section stained by basic fuchsin.

1.5.6 Vascularization of OCU

While cartilage is completely avascular, subchondral bone is highly vascularized (**Figure 1-14**). The high density of blood vessels is essential for proper levels of oxygenation, nutrition and elimination of waste in bone [122]. It has also been proposed that subchondral bone acts as a zone of nutrient exchange between bone and cartilage. It is estimated that about 50% of the nutrition (glucose, oxygen and water) requirements for cartilage is provided by vasculature in subchondral bone [27, 123].

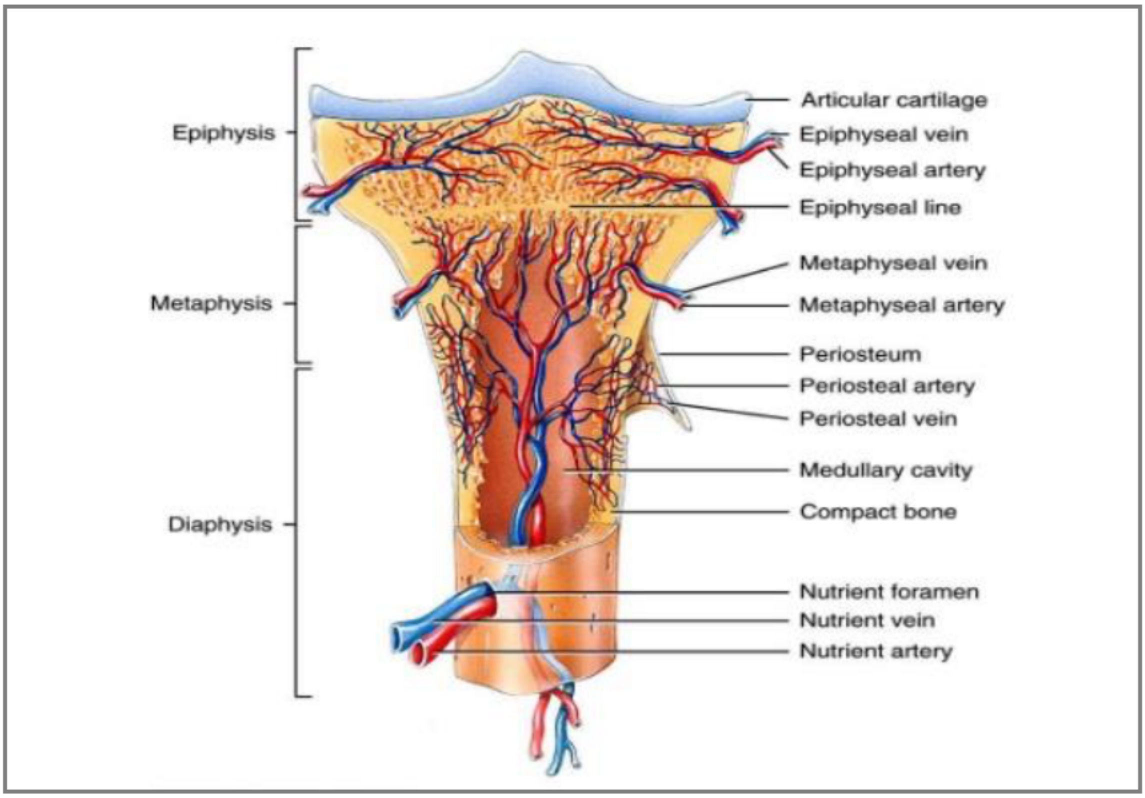

Figure 1-14: Vascularisation of proximal end of tibia. Image reproduced from http://keywordsuggest.org/gallery/.html.

In weight bearing joints such as the knee, regions of increased focal stress have a greater density of vessels compared to zones of low impact [28]. This suggests that regions of increased stress may have high requirements for nutrients [124]. Hence, a decrease of blood supply in subchondral bone may have critical consequences for the whole OCU. Animal studies have shown that disruption in the vascular network of subchondral bone indirectly caused degeneration of cartilage [125]. In OA, vascular pathology may play an important role in the progression of disease [124]. Vascular changes also cause increased intraosseous pressure and capillary permeability, associated with loss of cartilage volume and increased bone remodelling [122, 126]. Although it seems that vascular pathology may be important in OA, only a few human studies have investigated a direct role for the vasculature in the pathogenesis of OA. There have been no studies that have investigated the quantity and quality of blood vessels in OA subchondral bone. Thus, the relationship between blood vessels and changes in the subchondral bone due to OA are not fully understood. Understanding the role of vascularisation in subchondral bone could provide benefits for the development of appropriate therapies [2].

1.6 Subchondral bone imaging features in KOA

1.6.1 Osteophytes

Osteophyte formation is one of the most commonly seen radiographic features in OA. In the knee, osteophytes are usually found at the margins of the joint and their presence is an important criterion for the diagnosis of KOA (**Figure 1-15**). It has been found that the presence of osteophytes has significant clinical impact in KOA, where they associate with pain, loss of joint function and decreased mobility. However, it is important to state that two large longitudinal studies reported that there is no significant positive association between osteophytes and pain [127, 128]. Growth factors such as TGF-beta appear to play a major role in both chondrogenesis and osteophyte formation [129, 130]. Osteophytes can be seen early in the development of OA and prior to joint space narrowing [131]. It has also been suggested that the presence of osteophytes in the knee might have a protective role, as they often develop in the posterior and anterior aspect of the joint after tears of the anterior cruciate ligament, stabilizing the joint in the sagittal plane [131]. In addition, removal of medial and/or lateral osteophytes increases varus-valgus motion [132]. However, large longitudinal KOA studies have reported that the presence of large osteophytes in the knee is associated with an increased risk of joint space narrowing and cartilage loss [133, 134]. The relationship of osteophytes to the progression of OA is complex and it was suggested by Felson *et al.* that osteophytes represent a sign of the presence of OA, rather than affecting the progression of the disease [135].

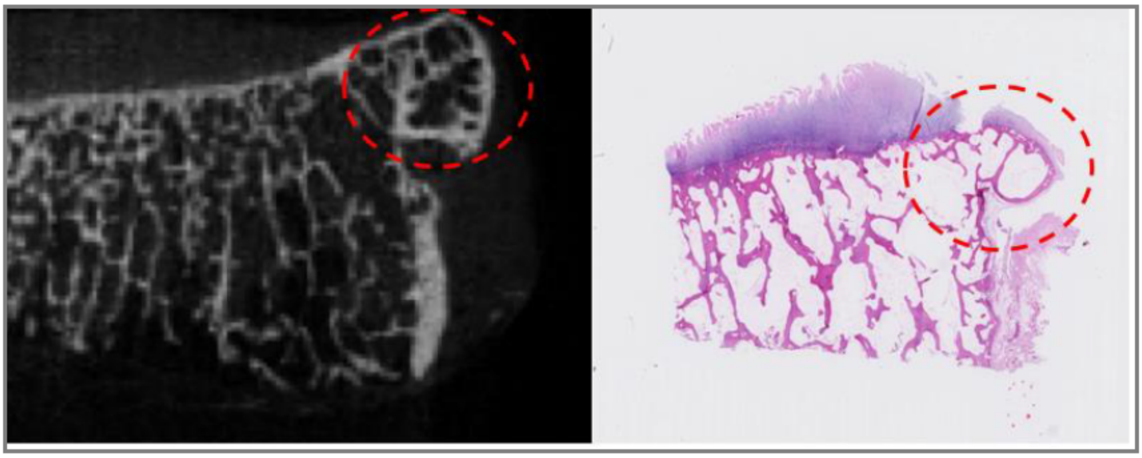

Figure 1-15: Representative images of an osteophyte on the edge of a human tibial plateau detected in a 76-year-old female KOA patient, left- Micro CT (sagittal view), right- corresponding histological section (Haematoxylin & Eosin).

1.6.2 Subchondral bone cysts

Subchondral bone cysts are a common imaging feature of OA, in particular when the disease is at an advanced stage. Subchondral bone cysts represent areas of increased bone resorption in areas of high intra-articular pressure (Figure 16). Cysts are visible by radiography, computed tomography (CT) and MRI. On MRI, cysts are defined as areas of well-defined hyper-signal [136]. MRI is the most sensitive technique for detection of subchondral cysts as it is able to detect smaller sized cysts than radiographic imaging.

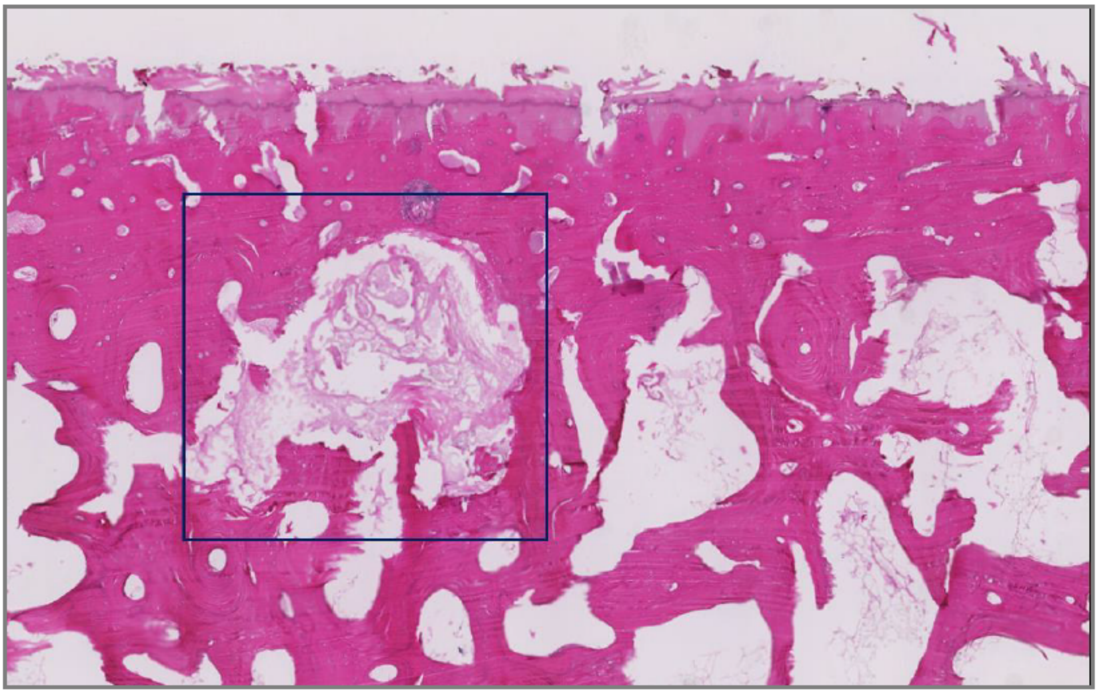

Figure 1-16: Subchondral bone cyst identified in a histological section of proximal tibial subchondral bone in a 72-year-old male KOA patient (Haematoxylin & Eosin).

There are several theories as to how subchondral cysts arise in the tissue. One of the theories is that they initiate due to elevated intra-articular pressure and/or synovial fluid leak through the damaged cartilage into subchondral bone [137]. However, in a recent large study, Crema *et al*. used MRI to identify subchondral cysts, indicated as well-defined rounded areas of fluid-like signal intensity on unenhanced images, and found that 46.5% of identified cysts were present in subregions with no full thickness cartilage loss [137]. They suggested that a more acceptable theory is one of bone contusion, a possible consequence of traumatic bone necrosis after the impact of two opposing articular surfaces [137].

Studies that examined the relationship between subchondral bone cysts and clinical symptoms such as knee pain found conflicting evidence [128, 138]. However, the relationship between subchondral bone cysts and structuralchanges in the knee has been demonstrated in several studies [9]. In individuals with OA, over a 24-month period, the development of new cysts and the progression of existing cysts were positively associated with cartilage volume loss [139]. Also, a positive correlation was found between mean cyst size change (mm) and cartilage loss in the medial femoral condyle [139]. In a separate study, subjects with cysts had lower mean tibial cartilage volume at baseline, and greater loss of medial tibial cartilage volume over a 2-year period, as well as an increased risk of knee-joint replacement over a 4-year period. These findings suggest that the presence of a subchondral bone cyst is in association with severe structural changes and poor clinical outcomes [9].

1.6.3 Bone marrow lesions

One of the most interesting subchondral bone pathologies in KOA imaged by MRI is the bone marrow lesion (BML), (**Figure 1-17**). Its significance in KOA pathophysiology is reflected by a close relationship with both clinical symptoms and structural degradation. From a large number of clinical studies, it has been suggested that BMLs may be valuable imaging biomarkers, offering information regarding initiation, progression and potential outcome in KOA. Furthermore, BMLs are identified in subchondral bone in both symptomatic and asymptomatic patients and it has been shown that BMLs are dynamic, with the ability to appear and disappear over time [140-143]. This suggests that BMLs might be modifiable features and as such might be potential targets or outcome measures for OA treatments.

Figure 1-17: MRI of the tibial plateau (sagittal view) of a 62-year-old female KOA patient taken *ex-vivo* (post knee replacement surgery). In PDFS-weighted sequences, BMLs (purple oval shape) are visualised as an ill-defined area of hyper-intense signal. In T1-weighted sequences, BMLs appear as a hypo-intense signal.

1.7 BML in the progression of KOA

A BML is defined as an ill-defined area of hyper-intense signal on fluid sensitive sequences (T2-weighted, PD-proton density weighted, PDFS-proton density fat suppressed, FSE-fast spin echo and STIR-short tau inversion recovery) or as a hypo-intense signal on fat sensitive sequences (T1-weighted), compared to normal subchondral bone appearance (**Figure 1-17**), [142, 144]. A BML is a specific signal detected only by MRI and cannot be visualised by x-ray, ultrasound or CT [142, 145].

Wilson *et al.* were the first to describe this subchondral bone pathology and referred to it as “Oedema-like Lesions” or “Bone Marrow Oedema” [146]. Later, this term was replaced, based on histology findings, with the more appropriate and currently used term by the OA research community “Bone Marrow Lesion” or “BML” [25]. A similar MRI signal in bone is observed in several other pathologies, such as rheumatoid arthritis, trauma, stress fracture, and vertebral Modic changes in the spine [142]. However, when a BML is present in conjunction with clinical symptoms, it is indicative of specific OA pathology. This review will specifically describe BMLs related to OA. While the majority of the OA research has described BMLs in the knee joint, it is important to state that BMLs are seen in other joints, including the hip [147-149], hand [150] shoulder [151], foot and ankle [152, 153]. BMLs have also been observed in animal OA models [154, 155]. The choice of the appropriate MR sequence in the assessment of BMLs is of critical importance. Fluid sensitive sequences such as T2-weighted, PD-weighted or PDFS-weighted are among those that are the most appropriate and recommended for use to delineate the maximum extent of a BML [24, 156]. Several studies have indicated that sequences such as gradient-echo sequences (eg. dual-echo steady state [DESS], fast low-angle shot [FLASH], or spoiled-gradient-recalled [SPGR] acquisition in steady state) are less sensitive for BML detection and therefore not appropriate for BML assessment [8, 10, 157-160].

1.7.1 Characteristics of OA BMLs

The prevalence of BMLs is much higher in established OA (painful with radiographic evidence of loss of joint space), where it has been reported to vary between 50-80% [11, 12, 161], compared to asymptomatic joints, where it is around 15% [141]. There are conflicting data regarding the presence of BMLs and gender. Davies-Tuck *et al.* found that there is no association between the presence, development or persistence of BML and gender [141]. However, it was also reported that males were more likely to have BMLs than females, and that BMLs in males are larger and more likely to increase in size over time [12, 162].

The size of BMLs is measured quantitatively as BML volume (expressed in mm^3) or as the largest diameter (expressed in mm) of the lesion on MRI [128, 163], and semi-quantitatively by using whole organ scoring systems; WORMS, KOSS, BLOKS and MOAKS [25]. While it is more practical to use whole organ scoring systems, as they have a 4-point grading score (0 as no lesion, 1=BML occupy up to 25% of the region, 2=25%-50% of region and 3=BML occupy more than 50% of the region), quantitative methods are more sensitive and more reliable for following up changes longitudinally [22]. The average diameter of BMLs in KOA is reported to be from <0.5 to >2 cm [128, 163].

Importantly, BMLs have the ability to change in size. Over time, BMLs may enlarge, regress or completely disappear [140, 143, 163] [164]. However, the existence of BMLs is quite variable. In healthy and asymptomatic populations, two studies reported that a high proportion of BMLs (46%) completely resolved over 2 years [140, 141]. However, in KOA populations observations are much more diverse. Hunter *et al.* assessed 217 KOA patients and performed MRI at baseline, 15 months and 30 months follow-up and found that over time BMLs often become larger and that less than 1% of the cohort showed a reduction in size or resolution [164]. Roemer *et al.* assessed 395 KOA patients over 30 months and found that more than 60% of BMLs changed in size, with almost 50% showing reduction in size or complete resolution [140, 143]. Similarly, Phan *et al.*

reported both a decrease and an increase in BML score over 2 years [163]. Furthermore, Garnero *et al.* and Felson *et al.* reported that BML size can fluctuate in a matter of weeks [165, 166]. Finally, Foong *et al.* observed 198 subjects over eight years and found that the proportion of BMLs increasing and decreasing in size is very similar (24% and 21%, respectively) while the majority (55%) remained stable [162].

1.7.2 Histopathology of BML

Zanetti *et al.* were one of the first to investigate and describe the histology of BMLs [167]. Surprisingly, they found that oedema is minimally present and suggested that an adequate term for these features would be “Bone Marrow Lesion” [167]. Since then only a few histological studies have been performed that explore BML at the tissue level. Those studies mainly indicated the presence of non-specific pathologies and a mixture of abnormalities such as necrosis, fibrosis, oedema, fibro-vascular ingrowth in the bone marrow, and abnormal trabeculae with evidence of microfractures [147, 148, 154, 167-169]. Similarly, BML histopathology findings have been reported in animal models of OA [154]. Results from those studies were unable to find a specific histopathology of BML or to explain the MR signal [148, 155, 170]. Also, none of the histological studies explored whether BMLs seen using water sensitive and/or fat sensitive MR sequences are different at the tissue level.

1.7.3 BML and clinical symptoms

BMLs are closely associated with OA related symptoms such as pain. Felson *et al.* was the first to report an association between painful knees and BMLs [11]. Since then, several other studies have confirmed this association [138, 171-174]. It has been hypothesized that fibro-vascular replacement of fatty bone marrow within BML areas might be a potential source of the pain in OA [175]. However, the exact source of the pain is still unknown. Larger BMLs and/or increased BML size are associated with increased knee pain in OA patients [176-178]. Also, a decrease in size and/or resolution of BML resulted in less pain and reduced cartilage loss [176, 178].

1.7.4 BML and structural degradation

Both cross sectional and longitudinal studies indicate that there is an association between the presence of a BML, BML progression and formation of new BMLs, and cartilage damage in the same location [141, 143, 164, 179, 180]. The presence of a BML at baseline has been related to compartment specific deterioration [11, 181], and the size of a BML is considered to be the main determinant factor in association with increased cartilage loss and subchondral attrition [178, 182]. In three knee studies, micro-computed tomography was used, showing that the structure of the subchondral bone within the zone of a BML was much more variable compared to the subchondral bone without a BML [168, 183, 184]. Specifically, subchondral bone in BML zones was characterised by a focal sclerotic appearance; thick subchondral plate, increased bone volume percentage, more trabeculae, which were thicker and less separated and more plate-like [168, 183, 184]. Also, the presence of a medial BML associates with subsequently increased local bone mineral density (BMD) in the medial compartment [185]. Several more studies have confirmed that the presence of BMLs is strongly associated with increased local BMD but not with distant BMD [186, 187], higher relative medial tibial bone density, less mineralisation and variable bone microarchitecture [168, 183]. Lowitz *et al.* found increased BMD, measured precisely in areas of BML, compared to surrounding areas [188]. In addition, an association between BMLs and subchondral cyst formation has been found [137]. In longitudinal studies, the subchondral bone within BMLs was associated with the appearance of cysts over time, suggesting that BMLs might be an early cystic formation [136, 137, 189]. However, the relationship between BMLs and subchondral cysts remains unclear, as not all BMLs will give rise to cysts [136].

1.7.5 BML development in the tissue

Despite the fact that BMLs are often observed in clinical studies of KOA, their pathogenesis is poorly understood. There is evidence that the presence of BMLs in knee joints is related to greater mechanical loading [190]. It has been reported that high loads increase the risk of the presence and progression of BML [144]. Also, BMLs are related to dynamic knee loading and knee adduction moments [190, 191]. Knee malalignment is associated with both the incidence and progression of BML [156]. These findings strongly support the hypothesis that greater mechanical loading of the medial compartment plays a role in the pathogenesis of BML in KOA [190].

Another theory regarding the formation of BMLs is based on the water-like signal on MR sequences. However, the histology of BMLs indicates minimal oedema [167]. Thus, it was proposed that BMLs might represent an area of capillary leakage caused by a local change in capillary walls or by increased vascular pressure due to increased blood flow to bone marrow or decreased venous clearance in the marrow space [124, 192]. This possibility was later partially supported by histological findings of increased fibrovascular ingrowth and vascular fibrosis in areas of BML [148, 169], although BMLs persist in bone ex vivo [154, 183].

Finally, there is a theory that the presence of a BML might be in association with systemic metabolic factors. A few studies indicated that dietary factors such as saturated fatty acid intake, increased serum cholesterol and triglycerides associated with the incidence of BMLs [193-195].

The cause of the formation of BMLs in subchondral tissue is most likely multifactorial. However, more tissue-based evidence is required to understand what factors contribute to the initiation of BMLs and what factors contribute to their healing or enlargement. Given the important role of BML in OA, identifying these contributing factors may ultimately identify targets for the treatment and prevention of knee OA.

1.7.6 Possible treatments for BMLs

Currently, there are no approved drugs to modify the structural progression of OA. For patients with severe pain associated with degenerative OA changes, TKR is often recommended. However, TKR is an invasive surgery that is associated with significant cost, postoperative complications, morbidity and occasional mortality. Being that BMLs closely correlate with symptoms and structural degeneration, and have the ability to regress and can be monitored closely by MRI, they represent potential therapeutic targets.

The novel technique named “subchondroplasty” has been proposed as a method to treat areas of BML, on the basis that they are areas of non-healing bone [196-198]. The technique involves injecting a calcium phosphate paste (synthetic bone void filler) into the BML zone to promote bone healing. Only two (non-randomized controlled trial) studies have evaluated the efficacy of this method for a small number of patients. The first study of 59 patients, 25% of whom had continued pain and elected to undergo TKR, reported the remainder of the patients having pain improvement in the first 6 months [198]. The second study of only 5 patients reported an improvement in pain and functional capacity in patient follow up at 6, 12 and 24 months after surgery [197].

Other studies have proposed the use of anti-resorptive therapies, based on animal studies, in which this approach has shown efficacy to prevent or slow the progression of OA. Laslett *et al.,* in a pilot study, reported a reduction in the size of BMLs and a reduction in pain after 6 months of treatment with zoledronic acid [199]. Strontium ranelate reduced cartilage volume loss and decreased the total BML score over 36 months [200]. In both studies, better results were recorded in individuals with less structural degeneration, suggesting that early treatment might be more effective. The full benefit of these proposed therapies and treatments is poorly known. Given that BMLs detected in established OA (with pain and radiographic progression) appear to resolve less often compared to those in asymptomatic populations, individualised and early treatment may be a more appropriate solution for individuals diagnosed with BMLs. Also, there is the possibility that the difference in the appearance of BMLs on different MRI sequences may indicate different tissue processes, which might be an important indicator for the choice of treatment. Thus, there is an urgent need to investigate if and how BML monitoring can be useful as a clinical tool.

1.8 Summary and research gap

Improvement in imaging modalities has opened a new door for understanding the aetiology of OA. Hence, there is no doubt that changes in the subchondral bone are important in the initiation, development and progression of KOA. However, the pathogenesis of human OA disease is still vague. Obtaining early OA tissue samples is difficult, and because OA is a slowly progressing disease it would take a long time to follow disease progression from early stage to advanced stage. There is a need for a disease-specific biomarker. The OA research community consensus is that BMLs in the subchondral bone are of considerable interest as they have strong association with both clinical symptoms and structural changes in the OCU. Moreover, these features show the ability to reduce in size and even to completely resolve in affected tissue, resulting in pain reduction. Hence, it has been suggested that BMLs could act as potential targets or bio-indicators in the prevention and treatment of OA.

However, BMLs are complex formations and what they represent at the tissue level, or what mechanisms lead to BML development in bone tissue is not well understood. Understanding of the structural and cellular nature of BMLs is necessary for their rational use as imaging biomarkers in the future management of OA patients and/or potential targets for the development of an appropriate therapeutic treatment.

1.9 Research objectives

The research described in this thesis sought to learn more about the relationships that exist between the presence of BMLs and the progression of human KOA. Specifically, four individual studies were carried out to comprehensively investigate BMLs at the tissue level and their relationship with the structural progression of OA.

Hypothesis: BML imaged using MRI reflect changes in subchondral tissue of proximal tibia that related to OA disease severity and/or progression.

Thesis Aims:

- To investigate the histopathology of the human OCU (cartilage, subchondral bone and subchondral bone marrow) based on the presence or absence of a BML.
- To perform comprehensive tissue characterization of BMLs detected using two specific MRI sequences in human KOA.
- To explore the mechanisms, by which BMLs might develop in the tissue and which might influence the progression of human KOA.
- To evaluate subchondral bone microarchitectural changes across the whole human tibial plateau in order to understand what role the presence/absence of a BML might play locally and to surrounding regions.

Chapter 2 is a recently published study, which characterised human KOA BMLs imaged using two different MRI sequences at the tissue level. Chapter 3 describes a study, in which causal factors of BML formation were investigated. Evidence of high mechanical loading and vascular pathology were investigated by assessing the accumulation of microdamage, and the qualitative and quantitative aspects of blood vessels in BML and non-BML tissue. Chapter 4 describes a study of investigating a potential role for components of the metabolic syndrome in BML development in KOA. Chapter 5 describes a study investigating a microarchitectural changes in whole tibial plateaus, based on the presence/absence of a BML. Tissue from healthy/control knees was compared with that from OA with no BML and OA with BML, to better understand the course of OA disease and BML involvement in disease progression

1.10 References

1. Goverment A. Osteoarthritis. In: Welfare AIoHa Ed. https://www.aihw.gov.au/reports/arthritis-other-musculoskeletal-conditions/osteoarthritis/contents/who-gets-osteoarthritis2016.
2. Racine J, Aaron RK. Pathogenesis and epidemiology of osteoarthritis. R I Med J (2013) 2013; 96: 19-22.
3. Keats E, Khan ZA. Unique responses of stem cell-derived vascular endothelial and mesenchymal cells to high levels of glucose. PLoS One 2012; 7: e38752.
4. Association) AAO. Annual Report. . Adelaide: Australian Orthopaedic Association National Joint Replacement Registry 2015.
5. Mulcahy H, Chew FS. Current concepts in knee replacement: complications. AJR Am J Roentgenol 2014; 202: W76-86.
6. Registry AJR. Annual Reports 2016. 2016.
7. Losina E, Katz JN. Total knee arthroplasty on the rise in younger patients: are we sure that past performance will guarantee future success? Arthritis Rheum 2012; 64: 339-341.

8. Crema MD, Roemer FW, Hayashi D, Guermazi A. Comment on: Bone marrow lesions in people with knee osteoarthritis predict progression of disease and joint replacement: a longitudinal study. Rheumatology (Oxford) 2011; 50: 996-997; author reply 997-999.
9. Tanamas SK, Wluka AE, Pelletier JP, Martel-Pelletier J, Abram F, Wang Y, et al. The association between subchondral bone cysts and tibial cartilage volume and risk of joint replacement in people with knee osteoarthritis: a longitudinal study. Arthritis Res Ther 2010; 12: R58.
10. Tanamas SK, Wluka AE, Pelletier JP, Pelletier JM, Abram F, Berry PA, et al. Bone marrow lesions in people with knee osteoarthritis predict progression of disease and joint replacement: a longitudinal study. Rheumatology (Oxford) 2010; 49: 2413-2419.
11. Felson DT, Chaisson CE, Hill CL, Totterman SM, Gale ME, Skinner KM, et al. The association of bone marrow lesions with pain in knee osteoarthritis. Ann Intern Med 2001; 134: 541-549.
12. Dore D, Quinn S, Ding C, Winzenberg T, Zhai G, Cicuttini F, et al. Natural history and clinical significance of MRI-detected bone marrow lesions at the knee: a prospective study in community dwelling older adults. Arthritis Res Ther 2010; 12: R223.
13. Felson DT, Niu J, Guermazi A, Sack B, Aliabadi P. Defining radiographic incidence and progression of knee osteoarthritis: suggested modifications of the Kellgren and Lawrence scale. Ann Rheum Dis 2011; 70: 1884-1886.
14. Kraus VB. Waiting for action on the osteoarthritis front. Curr Drug Targets 2010; 11: 518-520.
15. Altman RD, Gold GE. Atlas of individual radiographic features in osteoarthritis, revised. Osteoarthritis Cartilage 2007; 15 Suppl A: A1-56.

16. Guermazi A, Roemer FW, Burstein D, Hayashi D. Why radiography should no longer be considered a surrogate outcome measure for longitudinal assessment of cartilage in knee osteoarthritis. Arthritis Res Ther 2011; 13: 247.

17. Ding C, Zhang Y, Hunter D. Use of imaging techniques to predict progression in osteoarthritis. Curr Opin Rheumatol 2013; 25: 127-135.

18. Sharma L, Chmiel JS, Almagor O, Dunlop D, Guermazi A, Bathon JM, et al. Significance of preradiographic magnetic resonance imaging lesions in persons at increased risk of knee osteoarthritis. Arthritis Rheumatol 2014; 66: 1811-1819.

19. Galea A, Giuffre B, Dimmick S, Coolican MR, Parker DA. The accuracy of magnetic resonance imaging scanning and its influence on management decisions in knee surgery. Arthroscopy 2009; 25: 473-480.

20. Peterfy CG, Guermazi A, Zaim S, Tirman PF, Miaux Y, White D, et al. Whole-Organ Magnetic Resonance Imaging Score (WORMS) of the knee in osteoarthritis. Osteoarthritis Cartilage 2004; 12: 177-190.

21. Kornaat PR, Ceulemans RY, Kroon HM, Riyazi N, Kloppenburg M, Carter WO, et al. MRI assessment of knee osteoarthritis: Knee Osteoarthritis Scoring System (KOSS)--inter-observer and intra-observer reproducibility of a compartment-based scoring system. Skeletal Radiol 2005; 34: 95-102.

22. Hunter DJ, Lo GH, Gale D, Grainger AJ, Guermazi A, Conaghan PG. The reliability of a new scoring system for knee osteoarthritis MRI and the validity of bone marrow lesion assessment: BLOKS (Boston Leeds Osteoarthritis Knee Score). Ann Rheum Dis 2008; 67: 206-211.

23. Hunter DJ, Guermazi A, Lo GH, Grainger AJ, Conaghan PG, Boudreau RM, et al. Evolution of semi-quantitative whole joint assessment of knee OA: MOAKS (MRI Osteoarthritis Knee Score). Osteoarthritis Cartilage 2011; 19: 990-1002.

24. Peterfy CG, Gold G, Eckstein F, Cicuttini F, Dardzinski B, Stevens R. MRI protocols for whole-organ assessment of the knee in osteoarthritis. Osteoarthritis Cartilage 2006; 14 Suppl A: A95-111.

25. Guermazi A, Roemer FW, Haugen IK, Crema MD, Hayashi D. MRI-based semiquantitative scoring of joint pathology in osteoarthritis. Nat Rev Rheumatol 2013; 9: 236-251.

26. Burr DB. Anatomy and physiology of the mineralized tissues: role in the pathogenesis of osteoarthrosis. Osteoarthritis Cartilage 2004; 12 Suppl A: S20-30.

27. Imhof H, Sulzbacher I, Grampp S, Czerny C, Youssefzadeh S, Kainberger F. Subchondral bone and cartilage disease: a rediscovered functional unit. Invest Radiol 2000; 35: 581-588.

28. Madry H, van Dijk CN, Mueller-Gerbl M. The basic science of the subchondral bone. Knee Surg Sports Traumatol Arthrosc 2010; 18: 419-433.

29. Sophia Fox AJ, Bedi A, Rodeo SA. The basic science of articular cartilage: structure, composition, and function. Sports Health 2009; 1: 461-468.

30. Castaneda S, Roman-Blas JA, Largo R, Herrero-Beaumont G. Subchondral bone as a key target for osteoarthritis treatment. Biochem Pharmacol 2012; 83: 315-323.

31. Lyons TJ, McClure SF, Stoddart RW, McClure J. The normal human chondro-osseous junctional region: evidence for contact of uncalcified

cartilage with subchondral bone and marrow spaces. BMC Musculoskelet Disord 2006; 7: 52.

32. Carlson CS, Loeser RF, Purser CB, Gardin JF, Jerome CP. Osteoarthritis in cynomolgus macaques. III: Effects of age, gender, and subchondral bone thickness on the severity of disease. J Bone Miner Res 1996; 11: 1209-1217.

33. Patel V, Issever AS, Burghardt A, Laib A, Ries M, Majumdar S. MicroCT evaluation of normal and osteoarthritic bone structure in human knee specimens. J Orthop Res 2003; 21: 6-13.

34. Burr DB, Gallant MA. Bone remodelling in osteoarthritis. Nat Rev Rheumatol 2012; 8: 665-673.

35. Lajeunesse D. Is there a role for bone tissue in osteoarthritis? Therapy 2010; 7: 649+.

36. Cohen-Solal M, Funck-Brentano T, Hay E. Animal models of osteoarthritis for the understanding of the bone contribution. Bonekey Rep 2013; 2: 422.

37. Huebner JL, Hanes MA, Beekman B, TeKoppele JM, Kraus VB. A comparative analysis of bone and cartilage metabolism in two strains of guinea-pig with varying degrees of naturally occurring osteoarthritis. Osteoarthritis Cartilage 2002; 10: 758-767.

38. Libicher M, Ivancic M, Hoffmann M, Wenz W. Early changes in experimental osteoarthritis using the Pond-Nuki dog model: technical procedure and initial results of in vivo MR imaging. Eur Radiol 2005; 15: 390-394.

39. Chen Y, Zhou B, Wang J, Wang T, Zhao W, Cao X, et al. Subchondral trabecular rod loss and trabecular plate stiffening precedes articular cartilage damages in osteoarthritis. Osteoarthritis and Cartilage; 24: S389.

40. Zhao W, Wang T, Luo Q, Chen Y, Leung VY, Wen C, et al. Cartilage degeneration and excessive subchondral bone formation in spontaneous osteoarthritis involves altered TGF-beta signaling. J Orthop Res 2016; 34: 763-770.

41. Hernandez CJ, Majeska RJ, Schaffler MB. Osteocyte density in woven bone. Bone 2004; 35: 1095-1099.

42. Hernandez CJ, van der Meulen MC. Understanding Bone Strength Is Not Enough. J Bone Miner Res 2017; 32: 1157-1162.

43. Licata A. Bone density vs bone quality: what's a clinician to do? Cleve Clin J Med 2009; 76: 331-336.

44. Compston J. Bone quality: what is it and how is it measured? Arquivos Brasileiros de Endocrinologia & Metabologia 2006; 50: 579-585.

45. Parfitt AM. Misconceptions (2): turnover is always higher in cancellous than in cortical bone. Bone 2002; 30: 807-809.

46. Parfitt AM, Mundy GR, Roodman GD, Hughes DE, Boyce BF. A new model for the regulation of bone resorption, with particular reference to the effects of bisphosphonates. J Bone Miner Res 1996; 11: 150-159.

47. Ralston SH. Osteoporosis. BMJ: British Medical Journal 1997; 315: 469-472.

48. Intema F, Hazewinkel HA, Gouwens D, Bijlsma JW, Weinans H, Lafeber FP, et al. In early OA, thinning of the subchondral plate is directly related to cartilage damage: results from a canine ACLT-meniscectomy model. Osteoarthritis Cartilage 2010; 18: 691-698.

49. Zhang R, Fang H, Chen Y, Shen J, Lu H, Zeng C, et al. Gene expression analyses of subchondral bone in early experimental osteoarthritis by microarray. PLoS One 2012; 7: e32356.

50. Bettica P, Cline G, Hart DJ, Meyer J, Spector TD. Evidence for increased bone resorption in patients with progressive knee osteoarthritis: longitudinal results from the Chingford study. Arthritis Rheum 2002; 46: 3178-3184.

51. Kennedy O. The Effect of Bone Turnover on Bone Quality and Material Properties. Trinity College Dublin, vol. Doctor in Philosophy. Dublin: University of Dublin 2007:116.

52. Young MF, Kerr JM, Ibaraki K, Heegaard AM, Robey PG. Structure, expression, and regulation of the major noncollagenous matrix proteins of bone. Clin Orthop Relat Res 1992: 275-294.

53. Baker-LePain JC, Lane NE. Role of bone architecture and anatomy in osteoarthritis. Bone 2012; 51: 197-203.

54. Karsdal MA, Bay-Jensen AC, Lories RJ, Abramson S, Spector T, Pastoureau P, et al. The coupling of bone and cartilage turnover in osteoarthritis: opportunities for bone antiresorptives and anabolics as potential treatments? Ann Rheum Dis 2014; 73: 336-348.

55. Findlay DM, Atkins GJ. Osteoblast-chondrocyte interactions in osteoarthritis. Curr Osteoporos Rep 2014; 12: 127-134.

56. Kumarasinghe DD, Sullivan T, Kuliwaba JS, Fazzalari NL, Atkins GJ. Evidence for the dysregulated expression of TWIST1, TGFbeta1 and SMAD3 in differentiating osteoblasts from primary hip osteoarthritis patients. Osteoarthritis Cartilage 2012; 20: 1357-1366.

57. Soysa NS, Alles N, Aoki K, Ohya K. Osteoclast formation and differentiation: an overview. J Med Dent Sci 2012; 59: 65-74.

58. Muir. Muir's Text Book of Pathology. London, Edward Arnold Ltd 2008.

59. Mills S. Histology for Pathologists, Lippincott Williams&Wilkins 2006.

60. Diarra D, Stolina M, Polzer K, Zwerina J, Ominsky MS, Dwyer D, et al. Dickkopf-1 is a master regulator of joint remodeling. Nat Med 2007; 13: 156-163.

61. Boyle WJ, Simonet WS, Lacey DL. Osteoclast differentiation and activation. Nature 2003; 423: 337-342.

62. Haynes DR, Crotti TN, Loric M, Bain GI, Atkins GJ, Findlay DM. Osteoprotegerin and receptor activator of nuclear factor kappaB ligand (RANKL) regulate osteoclast formation by cells in the human rheumatoid arthritic joint. Rheumatology (Oxford) 2001; 40: 623-630.

63. Haynes DR, Crotti TN, Potter AE, Loric M, Atkins GJ, Howie DW, et al. The osteoclastogenic molecules RANKL and RANK are associated with periprosthetic osteolysis. J Bone Joint Surg Br 2001; 83: 902-911.

64. Schett G, Hayer S, Zwerina J, Redlich K, Smolen JS. Mechanisms of Disease: the link between RANKL and arthritic bone disease. Nat Clin Pract Rheumatol 2005; 1: 47-54.

65. Schett G, Stolina M, Bolon B, Middleton S, Adlam M, Brown H, et al. Analysis of the kinetics of osteoclastogenesis in arthritic rats. Arthritis Rheum 2005; 52: 3192-3201.

66. Hayami T, Pickarski M, Wesolowski GA, McLane J, Bone A, Destefano J, et al. The role of subchondral bone remodeling in osteoarthritis: reduction of cartilage degeneration and prevention of osteophyte formation by alendronate in the rat anterior cruciate ligament transection model. Arthritis Rheum 2004; 50: 1193-1206.

67. Podworny NV, Kandel RA, Renlund RC, Grynpas MD. Partial chondroprotective effect of zoledronate in a rabbit model of inflammatory arthritis. J Rheumatol 1999; 26: 1972-1982.

68. Bingham CO, 3rd, Buckland-Wright JC, Garnero P, Cohen SB, Dougados M, Adami S, et al. Risedronate decreases biochemical markers of cartilage degradation but does not decrease symptoms or slow radiographic progression in patients with medial compartment osteoarthritis of the knee: results of the two-year multinational knee osteoarthritis structural arthritis study. Arthritis Rheum 2006; 54: 3494-3507.
69. Buckland-Wright JC, Messent EA, Bingham CO, 3rd, Ward RJ, Tonkin C. A 2 yr longitudinal radiographic study examining the effect of a bisphosphonate (risedronate) upon subchondral bone loss in osteoarthritic knee patients. Rheumatology (Oxford) 2007; 46: 257-264.
70. Young B, Heath JW. Wheater's Functional Histology. 4 Edition, Churchill Livingstone 2006.
71. Hernandez CJ, Majeska RJ, Schaffler MB. Osteocyte density in woven bone. Bone 2004; 35: 1095-1099.
72. Buenzli PR, Sims NA. Quantifying the osteocyte network in the human skeleton. Bone 2015; 75: 144-150.
73. Kennedy OD, Laudier DM, Majeska RJ, Sun HB, Schaffler MB. Osteocyte apoptosis is required for production of osteoclastogenic signals following bone fatigue in vivo. Bone 2014; 64: 132-137.
74. Prideaux M, Findlay DM, Atkins GJ. Osteocytes: The master cells in bone remodelling. Curr Opin Pharmacol 2016; 28: 24-30.
75. Seeman E. Osteocytesâ€"martyrs for integrity of bone strength. Osteoporosis International 2006; 17: 1443-1448.
76. Verborgt O, Gibson GJ, Schaffler MB. Loss of osteocyte integrity in association with microdamage and bone remodeling after fatigue in vivo. J Bone Miner Res 2000; 15: 60-67.

77. Bonewald L. Osteocytes as multifunctional cells. Musculosceletal Neuronal Interact 2007; 6: 331-333.

78. Santos A, Bakker AD, Klein-Nulend J. The role of osteocytes in bone mechanotransduction. Osteoporosis International 2009; 20: 1027-1031.

79. Kurata K, Fukunaga T, Matsuda J, Higaki H. Role of mechanically damaged osteocytes in the initial phase of bone remodeling. International Journal of Fatigue 2007; 29: 1010-1018.

80. Lanyon LE. Osteocytes, strain detection, bone modeling and remodeling. Calcified Tissue International 1993; 53: S102-S107.

81. Qiu S, Rao DS, Palnitkar S, Parfitt AM. Reduced Iliac Cancellous Osteocyte Density in Patients With Osteoporotic Vertebral Fracture. Journal of Bone and Mineral Research 2003; 18: 1657-1663.

82. Jaiprakash A, Prasadam I, Feng JQ, Liu Y, Crawford R, Xiao Y. Phenotypic characterization of osteoarthritic osteocytes from the sclerotic zones: a possible pathological role in subchondral bone sclerosis. Int J Biol Sci 2012; 8: 406-417.

83. Chang MK, Raggatt LJ, Alexander KA, Kuliwaba JS, Fazzalari NL, Schroder K, et al. Osteal tissue macrophages are intercalated throughout human and mouse bone lining tissues and regulate osteoblast function in vitro and in vivo. J Immunol 2008; 181: 1232-1244.

84. Miron RJ, Bosshardt DD. OsteoMacs: Key players around bone biomaterials. Biomaterials 2016; 82: 1-19.

85. Seeman E. Essay in Bone Quality. Advances in Osteoporotic Fracture Menagement (AOFM). LONDON: Remedica Publishing 2004:60.

86. Seeman E, Delmas PD. Bone Quality -- The Material and Structural Basis of Bone Strength and Fragility. N Engl J Med 2006; 354: 2250-2261.

87. Leeming DJ, Henriksen K, Byrjalsen I, Qvist P, Madsen SH, Garnero P, et al. Is bone quality associated with collagen age? Osteoporosis International 2009; 20: 1461-1470.

88. Day JS, Van Der Linden JC, Bank RA, Ding M, Hvid I, Sumner DR, et al. Adaptation of subchondral bone in osteoarthritis. Biorheology 2004; 41: 359-368.

89. van der Linden JC, Day JS, Verhaar JA, Weinans H. Altered tissue properties induce changes in cancellous bone architecture in aging and diseases. J Biomech 2004; 37: 367-374.

90. Lavigne P, Benderdour M, Lajeunesse D, Reboul P, Shi Q, Pelletier JP, et al. Subchondral and trabecular bone metabolism regulation in canine experimental knee osteoarthritis. Osteoarthritis Cartilage 2005; 13: 310-317.

91. Hildebrand T, Laib A, Müller R, Dequeker J, Rüegsegger P. Direct Three-Dimensional Morphometric Analysis of Human Cancellous Bone: Microstructural Data from Spine, Femur, Iliac Crest, and Calcaneus. Journal of Bone and Mineral Research 1999; 14: 1167-1174.

92. Odgaard A. Three-dimensional methods for quantification of cancellous bone architecture. Bone 1997; 20: 315-328.

93. Meyer EG, Baumer TG, Slade JM, Smith WE, Haut RC. Tibiofemoral contact pressures and osteochondral microtrauma during anterior cruciate ligament rupture due to excessive compressive loading and internal torque of the human knee. Am J Sports Med 2008; 36: 1966-1977.

94. Batiste DL, Kirkley A, Laverty S, Thain LM, Spouge AR, Holdsworth DW. Ex vivo characterization of articular cartilage and bone lesions in a rabbit

ACL transection model of osteoarthritis using MRI and micro-CT. Osteoarthritis Cartilage 2004; 12: 986-996.

95. Botter SM, van Osch GJ, Waarsing JH, Day JS, Verhaar JA, Pols HA, et al. Quantification of subchondral bone changes in a murine osteoarthritis model using micro-CT. Biorheology 2006; 43: 379-388.

96. Mohan G, Perilli E, Kuliwaba JS, Humphries JM, Parkinson IH, Fazzalari NL. Application of in vivo micro-computed tomography in the temporal characterisation of subchondral bone architecture in a rat model of low-dose monosodium iodoacetate-induced osteoarthritis. Arthritis Res Ther 2011; 13: R210.

97. Bolbos RI, Zuo J, Banerjee S, Link TM, Ma CB, Li X, et al. Relationship between trabecular bone structure and articular cartilage morphology and relaxation times in early OA of the knee joint using parallel MRI at 3 T. Osteoarthritis Cartilage 2008; 16: 1150-1159.

98. Chang G, Xia D, Chen C, Madelin G, Abramson SB, Babb JS, et al. 7T MRI detects deterioration in subchondral bone microarchitecture in subjects with mild knee osteoarthritis as compared with healthy controls. J Magn Reson Imaging 2015; 41: 1311-1317.

99. Ding M. Microarchitectural adaptations in aging and osteoarthrotic subchondral bone issues. Acta Orthop Suppl 2010; 81: 1-53.

100. Bobinac D, Spanjol J, Zoricic S, Maric I. Changes in articular cartilage and subchondral bone histomorphometry in osteoarthritic knee joints in humans. Bone 2003; 32: 284-290.

101. Kamibayashi L, Wyss UP, Cooke TD, Zee B. Trabecular microstructure in the medial condyle of the proximal tibia of patients with knee osteoarthritis. Bone 1995; 17: 27-35.

102. Chappard C, Peyrin F, Bonnassie A, Lemineur G, Brunet-Imbault B, Lespessailles E, et al. Subchondral bone micro-architectural alterations in osteoarthritis: a synchrotron micro-computed tomography study. Osteoarthritis Cartilage 2006; 14: 215-223.

103. Steinbeck MJ, Eisenhauer PT, Maltenfort MG, Parvizi J, Freeman TA. Identifying Patient-Specific Pathology in Osteoarthritis Development Based on MicroCT Analysis of Subchondral Trabecular Bone. J Arthroplasty 2016; 31: 269-277.

104. Finnila MA, Thevenot J, Aho OM, Tiitu V, Rautiainen J, Kauppinen S, et al. Association between subchondral bone structure and osteoarthritis histopathological grade. J Orthop Res 2016.

105. Ding M, Christian Danielsen C, Hvid I. Effects of hyaluronan on three-dimensional microarchitecture of subchondral bone tissues in guinea pig primary osteoarthrosis. Bone 2005; 36: 489-501.

106. Salmon PL, Ohlsson C, Shefelbine SJ, Doube M. Structure Model Index Does Not Measure Rods and Plates in Trabecular Bone. Front Endocrinol (Lausanne) 2015; 6: 162.

107. Fazzalari NL, Forwood MR, Smith K, Manthey BA, Herreen P. Assessment of cancellous bone quality in severe osteoarthrosis: bone mineral density, mechanics, and microdamage. Bone 1998; 22: 381-388.

108. Vashishth D, Koontz J, Qiu SJ, Lundin-Cannon D, Yeni YN, Schaffler MB, et al. In vivo diffuse damage in human vertebral trabecular bone. Bone 2000; 26: 147-152.

109. Diab T, Condon KW, Burr DB, Vashishth D. Age-related change in the damage morphology of human cortical bone and its role in bone fragility. Bone 2006; 38: 427-431.

110. Diab T, Vashishth D. Effects of damage morphology on cortical bone fragility. Bone 2005; 37: 96-102.

111. Poundarik AA, Vashishth D. Multiscale imaging of bone microdamage. Connect Tissue Res 2015; 56: 87-98.

112. Fazzalari NL. Trabecular microfracture. Calcified Tissue International 1993; 53: S143-S147.

113. Burr DB, Radin EL. Microfractures and microcracks in subchondral bone: are they relevant to osteoarthrosis? Rheum Dis Clin North Am 2003; 29: 675-685.

114. Chapurlat RD, Delmas PD. Bone microdamage: a clinical perspective. Osteoporosis International 2009; 20: 1299-1308.

115. Boyce TM, Fyhrie DP, Glotkowski MC, Radin EL, Schaffler MB. Damage type and strain mode associations in human compact bone bending fatigue. J Orthop Res 1998; 16: 322-329.

116. Herman BC, Cardoso L, Majeska RJ, Jepsen KJ, Schaffler MB. Activation of bone remodeling after fatigue: differential response to linear microcracks and diffuse damage. Bone 2010; 47: 766-772.

117. Diab T, Vashishth D. Morphology, localization and accumulation of in vivo microdamage in human cortical bone. Bone 2007; 40: 612-618.

118. Vashishth D, Verborgt O, Divine G, Schaffler MB, Fyhrie DP. Decline in osteocyte lacunar density in human cortical bone is associated with accumulation of microcracks with age. Bone 2000; 26: 375-380.

119. Muir P, Sample SJ, Barrett JG, McCarthy J, Vanderby R, Jr., Markel MD, et al. Effect of fatigue loading and associated matrix microdamage on bone blood flow and interstitial fluid flow. Bone 2007; 40: 948-956.

120. Goldring SR. The osteocyte: key player in regulating bone turnover. RMD Open 2015; 1: e000049.

121. Frost. Presence of microscopic cracks in vio in bone. Medical bullten 1960.

122. Dyke JP, Aaron RK. Noninvasive methods of measuring bone blood perfusion. Ann N Y Acad Sci 2010; 1192: 95-102.

123. Imhof H, Breitenseher M, Kainberger F, Trattnig S. Degenerative joint disease: cartilage or vascular disease? Skeletal Radiol 1997; 26: 398-403.

124. Findlay DM. Vascular pathology and osteoarthritis. Rheumatology (Oxford) 2007; 46: 1763-1768.

125. Malinin T, Ouellette EA. Articular cartilage nutrition is mediated by subchondral bone: a long-term autograft study in baboons. Osteoarthritis Cartilage 2000; 8: 483-491.

126. Temmerman OP, Raijmakers PG, Kloet R, Teule GJ, Heyligers IC, Lammertsma AA. In vivo measurements of blood flow and bone metabolism in osteoarthritis. Rheumatol Int 2013; 33: 959-963.

127. Sengupta M, Zhang YQ, Niu JB, Guermazi A, Grigorian M, Gale D, et al. High signal in knee osteophytes is not associated with knee pain. Osteoarthritis Cartilage 2006; 14: 413-417.

128. Kornaat PR, Bloem JL, Ceulemans RY, Riyazi N, Rosendaal FR, Nelissen RG, et al. Osteoarthritis of the knee: association between clinical features and MR imaging findings. Radiology 2006; 239: 811-817.

129. Bakker AC, van de Loo FA, van Beuningen HM, Sime P, van Lent PL, van der Kraan PM, et al. Overexpression of active TGF-beta-1 in the murine knee joint: evidence for synovial-layer-dependent chondro-osteophyte formation. Osteoarthritis Cartilage 2001; 9: 128-136.

130. Scharstuhl A, Glansbeek HL, van Beuningen HM, Vitters EL, van der Kraan PM, van den Berg WB. Inhibition of endogenous TGF-beta during experimental osteoarthritis prevents osteophyte formation and impairs cartilage repair. J Immunol 2002; 169: 507-514.

131. Nagaosa Y, Lanyon P, Doherty M. Characterisation of size and direction of osteophyte in knee osteoarthritis: a radiographic study. Ann Rheum Dis 2002; 61: 319-324.

132. Pottenger LA, Phillips FM, Draganich LF. The effect of marginal osteophytes on reduction of varus-valgus instability in osteoarthritic knees. Arthritis Rheum 1990; 33: 853-858.

133. Dieppe PA, Cushnaghan J, Shepstone L. The Bristol 'OA500' study: progression of osteoarthritis (OA) over 3 years and the relationship between clinical and radiographic changes at the knee joint. Osteoarthritis Cartilage 1997; 5: 87-97.

134. Wolfe F, Lane NE. The longterm outcome of osteoarthritis: rates and predictors of joint space narrowing in symptomatic patients with knee osteoarthritis. J Rheumatol 2002; 29: 139-146.

135. Felson DT, Gale DR, Elon Gale M, Niu J, Hunter DJ, Goggins J, et al. Osteophytes and progression of knee osteoarthritis. Rheumatology (Oxford) 2005; 44: 100-104.

136. Carrino JA, Blum J, Parellada JA, Schweitzer ME, Morrison WB. MRI of bone marrow edema-like signal in the pathogenesis of subchondral cysts. Osteoarthritis Cartilage 2006; 14: 1081-1085.

137. Crema MD, Roemer FW, Zhu Y, Marra MD, Niu J, Zhang Y, et al. Subchondral cystlike lesions develop longitudinally in areas of bone marrow edema-like lesions in patients with or at risk for knee osteoarthritis:

detection with MR imaging--the MOST study. Radiology 2010; 256: 855-862.

138. Torres L, Dunlop DD, Peterfy C, Guermazi A, Prasad P, Hayes KW, et al. The relationship between specific tissue lesions and pain severity in persons with knee osteoarthritis. Osteoarthritis Cartilage 2006; 14: 1033-1040.

139. Raynauld JP, Martel-Pelletier J, Berthiaume MJ, Abram F, Choquette D, Haraoui B, et al. Correlation between bone lesion changes and cartilage volume loss in patients with osteoarthritis of the knee as assessed by quantitative magnetic resonance imaging over a 24-month period. Ann Rheum Dis 2008; 67: 683-688.

140. Berry PA, Davies-Tuck ML, Wluka AE, Hanna FS, Bell RJ, Davis SR, et al. The natural history of bone marrow lesions in community-based middle-aged women without clinical knee osteoarthritis. Semin Arthritis Rheum 2009; 39: 213-217.

141. Davies-Tuck ML, Wluka AE, Wang Y, English DR, Giles GG, Cicuttini F. The natural history of bone marrow lesions in community-based adults with no clinical knee osteoarthritis. Ann Rheum Dis 2009; 68: 904-908.

142. Roemer FW, Frobell R, Hunter DJ, Crema MD, Fischer W, Bohndorf K, et al. MRI-detected subchondral bone marrow signal alterations of the knee joint: terminology, imaging appearance, relevance and radiological differential diagnosis. Osteoarthritis Cartilage 2009; 17: 1115-1131.

143. Roemer FW, Guermazi A, Javaid MK, Lynch JA, Niu J, Zhang Y, et al. Change in MRI-detected subchondral bone marrow lesions is associated with cartilage loss: the MOST Study. A longitudinal multicentre study of knee osteoarthritis. Ann Rheum Dis 2009; 68: 1461-1465.

144. Beckwee D, Vaes P, Shahabpour M, Muyldermans R, Rommers N, Bautmans I. The Influence of Joint Loading on Bone Marrow Lesions in the Knee: A Systematic Review With Meta-analysis. Am J Sports Med 2015; 43: 3093-3107.

145. McQueen FM. A vital clue to deciphering bone pathology: MRI bone oedema in rheumatoid arthritis and osteoarthritis. Ann Rheum Dis 2007; 66: 1549-1552.

146. Wilson AJ, Murphy WA, Hardy DC, Totty WG. Transient osteoporosis: transient bone marrow edema? Radiology 1988; 167: 757-760.

147. Taljanovic MS, Graham AR, Benjamin JB, Gmitro AF, Krupinski EA, Schwartz SA, et al. Bone marrow edema pattern in advanced hip osteoarthritis: quantitative assessment with magnetic resonance imaging and correlation with clinical examination, radiographic findings, and histopathology. Skeletal Radiol 2008; 37: 423-431.

148. Leydet-Quilici H, Le Corroller T, Bouvier C, Giorgi R, Argenson JN, Champsaur P, et al. Advanced hip osteoarthritis: magnetic resonance imaging aspects and histopathology correlations. Osteoarthritis Cartilage 2010; 18: 1429-1435.

149. Roemer FW, Hunter DJ, Winterstein A, Li L, Kim YJ, Cibere J, et al. Hip Osteoarthritis MRI Scoring System (HOAMS): reliability and associations with radiographic and clinical findings. Osteoarthritis Cartilage 2011; 19: 946-962.

150. Haugen IK, Lillegraven S, Slatkowsky-Christensen B, Haavardsholm EA, Sesseng S, Kvien TK, et al. Hand osteoarthritis and MRI: development and first validation step of the proposed Oslo Hand Osteoarthritis MRI score. Ann Rheum Dis 2011; 70: 1033-1038.

151. de Abreu MR, Chung CB, Wesselly M, Jin-Kim H, Resnick D. Acromioclavicular joint osteoarthritis: comparison of findings derived from MR imaging and conventional radiography. Clin Imaging 2005; 29: 273-277.

152. Valderrabano V, Horisberger M, Russell I, Dougall H, Hintermann B. Etiology of ankle osteoarthritis. Clin Orthop Relat Res 2009; 467: 1800-1806.

153. Schmid MR, Hodler J, Vienne P, Binkert CA, Zanetti M. Bone marrow abnormalities of foot and ankle: STIR versus T1-weighted contrast-enhanced fat-suppressed spin-echo MR imaging. Radiology 2002; 224: 463-469.

154. Martig S, Boisclair J, Konar M, Spreng D, Lang J. MRI characteristics and histology of bone marrow lesions in dogs with experimentally induced osteoarthritis. Vet Radiol Ultrasound 2007; 48: 105-112.

155. d'Anjou MA, Troncy E, Moreau M, Abram F, Raynauld JP, Martel-Pelletier J, et al. Temporal assessment of bone marrow lesions on magnetic resonance imaging in a canine model of knee osteoarthritis: impact of sequence selection. Osteoarthritis Cartilage 2008; 16: 1307-1311.

156. Hayashi D, Guermazi A, Hunter DJ. Osteoarthritis year 2010 in review: imaging. Osteoarthritis Cartilage 2011; 19: 354-360.

157. Kijowski R, Blankenbaker DG, Klaers JL, Shinki K, De Smet AA, Block WF. Vastly undersampled isotropic projection steady-state free precession imaging of the knee: diagnostic performance compared with conventional MR. Radiology 2009; 251: 185-194.

158. Kijowski R, Blankenbaker DG, Woods MA, Shinki K, De Smet AA, Reeder SB. 3.0-T evaluation of knee cartilage by using three-dimensional IDEAL

GRASS imaging: comparison with fast spin-echo imaging. Radiology 2010; 255: 117-127.

159. Hayashi D, Guermazi A, Kwoh CK, Hannon MJ, Moore C, Jakicic JM, et al. Semiquantitative assessment of subchondral bone marrow edema-like lesions and subchondral cysts of the knee at 3T MRI: a comparison between intermediate-weighted fat-suppressed spin echo and Dual Echo Steady State sequences. BMC Musculoskelet Disord 2011; 12: 198.

160. Roemer FW, Hunter DJ, Crema MD, Kwoh CK, Ochoa-Albiztegui E, Guermazi A. An illustrative overview of semi-quantitative MRI scoring of knee osteoarthritis: lessons learned from longitudinal observational studies. Osteoarthritis Cartilage 2016; 24: 274-289.

161. Roemer FW, Neogi T, Nevitt MC, Felson DT, Zhu Y, Zhang Y, et al. Subchondral bone marrow lesions are highly associated with, and predict subchondral bone attrition longitudinally: the MOST study. Osteoarthritis Cartilage 2010; 18: 47-53.

162. Foong YC, Khan HI, Blizzard L, Ding C, Cicuttini F, Jones G, et al. The clinical significance, natural history and predictors of bone marrow lesion change over eight years. Arthritis Res Ther 2014; 16: R149.

163. Phan CM, Link TM, Blumenkrantz G, Dunn TC, Ries MD, Steinbach LS, et al. MR imaging findings in the follow-up of patients with different stages of knee osteoarthritis and the correlation with clinical symptoms. Eur Radiol 2006; 16: 608-618.

164. Hunter DJ, Zhang Y, Niu J, Goggins J, Amin S, LaValley MP, et al. Increase in bone marrow lesions associated with cartilage loss: a longitudinal magnetic resonance imaging study of knee osteoarthritis. Arthritis Rheum 2006; 54: 1529-1535.

165. Garnero P, Peterfy C, Zaim S, Schoenharting M. Bone marrow abnormalities on magnetic resonance imaging are associated with type II collagen degradation in knee osteoarthritis: a three-month longitudinal study. Arthritis Rheum 2005; 52: 2822-2829.

166. Felson DT, Parkes MJ, Marjanovic EJ, Callaghan M, Gait A, Cootes T, et al. Bone marrow lesions in knee osteoarthritis change in 6-12 weeks. Osteoarthritis Cartilage 2012; 20: 1514-1518.

167. Zanetti M, Bruder E, Romero J, Hodler J. Bone marrow edema pattern in osteoarthritic knees: correlation between MR imaging and histologic findings. Radiology 2000; 215: 835-840.

168. Hunter DJ, Gerstenfeld L, Bishop G, Davis AD, Mason ZD, Einhorn TA, et al. Bone marrow lesions from osteoarthritis knees are characterized by sclerotic bone that is less well mineralized. Arthritis Res Ther 2009; 11: R11.

169. Saadat E, Jobke B, Chu B, Lu Y, Cheng J, Li X, et al. Diagnostic performance of in vivo 3-T MRI for articular cartilage abnormalities in human osteoarthritic knees using histology as standard of reference. Eur Radiol 2008; 18: 2292-2302.

170. Zubler V, Mengiardi B, Pfirrmann CW, Duc SR, Schmid MR, Hodler J, et al. Bone marrow changes on STIR MR images of asymptomatic feet and ankles. Eur Radiol 2007; 17: 3066-3072.

171. Driban JB, Price L, Lo GH, Pang J, Hunter DJ, Miller E, et al. Evaluation of bone marrow lesion volume as a knee osteoarthritis biomarker--longitudinal relationships with pain and structural changes: data from the Osteoarthritis Initiative. Arthritis Res Ther 2013; 15: R112.

172. Hayes CW, Jamadar DA, Welch GW, Jannausch ML, Lachance LL, Capul DC, et al. Osteoarthritis of the knee: comparison of MR imaging findings with radiographic severity measurements and pain in middle-aged women. Radiology 2005; 237: 998-1007.

173. Lo GH, McAlindon TE, Niu J, Zhang Y, Beals C, Dabrowski C, et al. Bone marrow lesions and joint effusion are strongly and independently associated with weight-bearing pain in knee osteoarthritis: data from the osteoarthritis initiative. Osteoarthritis Cartilage 2009; 17: 1562-1569.

174. Sowers MF, Hayes C, Jamadar D, Capul D, Lachance L, Jannausch M, et al. Magnetic resonance-detected subchondral bone marrow and cartilage defect characteristics associated with pain and X-ray-defined knee osteoarthritis. Osteoarthritis Cartilage 2003; 11: 387-393.

175. Walsh DA, McWilliams DF, Turley MJ, Dixon MR, Franses RE, Mapp PI, et al. Angiogenesis and nerve growth factor at the osteochondral junction in rheumatoid arthritis and osteoarthritis. Rheumatology (Oxford) 2010; 49: 1852-1861.

176. Davies-Tuck ML, Wluka AE, Forbes A, Wang Y, English DR, Giles GG, et al. Development of bone marrow lesions is associated with adverse effects on knee cartilage while resolution is associated with improvement--a potential target for prevention of knee osteoarthritis: a longitudinal study. Arthritis Res Ther 2010; 12: R10.

177. Felson DT, Niu J, Guermazi A, Roemer F, Aliabadi P, Clancy M, et al. Correlation of the development of knee pain with enlarging bone marrow lesions on magnetic resonance imaging. Arthritis Rheum 2007; 56: 2986-2992.

178. Zhang Y, Nevitt M, Niu J, Lewis C, Torner J, Guermazi A, et al. Fluctuation of knee pain and changes in bone marrow lesions, effusions, and synovitis on magnetic resonance imaging. Arthritis Rheum 2011; 63: 691-699.

179. Guymer E, Baranyay F, Wluka AE, Hanna F, Bell RJ, Davis SR, et al. A study of the prevalence and associations of subchondral bone marrow lesions in the knees of healthy, middle-aged women. Osteoarthritis Cartilage 2007; 15: 1437-1442.

180. Xu L, Hayashi D, Roemer FW, Felson DT, Guermazi A. Magnetic resonance imaging of subchondral bone marrow lesions in association with osteoarthritis. Semin Arthritis Rheum 2012; 42: 105-118.

181. Kothari A, Guermazi A, Chmiel JS, Dunlop D, Song J, Almagor O, et al. Within-subregion relationship between bone marrow lesions and subsequent cartilage loss in knee osteoarthritis. Arthritis Care Res (Hoboken) 2010; 62: 198-203.

182. Wluka AE, Hanna F, Davies-Tuck M, Wang Y, Bell RJ, Davis SR, et al. Bone marrow lesions predict increase in knee cartilage defects and loss of cartilage volume in middle-aged women without knee pain over 2 years. Ann Rheum Dis 2009; 68: 850-855.

183. Kazakia GJ, Kuo D, Schooler J, Siddiqui S, Shanbhag S, Bernstein G, et al. Bone and cartilage demonstrate changes localized to bone marrow edema-like lesions within osteoarthritic knees. Osteoarthritis Cartilage 2013; 21: 94-101.

184. Driban JB, Tassinari A, Lo GH, Price LL, Schneider E, Lynch JA, et al. Bone marrow lesions are associated with altered trabecular morphometry. Osteoarthritis Cartilage 2012; 20: 1519-1526.

185. Lo GH, Hunter DJ, Zhang Y, McLennan CE, Lavalley MP, Kiel DP, et al. Bone marrow lesions in the knee are associated with increased local bone density. Arthritis Rheum 2005; 52: 2814-2821.

186. Dore D, Quinn S, Ding C, Winzenberg T, Jones G. Correlates of subchondral BMD: a cross-sectional study. J Bone Miner Res 2009; 24: 2007-2015.

187. Ahedi H, Aitken D, Blizzard L, Cicuttini F, Jones G. The association between hip bone marrow lesions and bone mineral density: a cross-sectional and longitudinal population-based study. Osteoarthritis Cartilage 2013; 21: 1545-1549.

188. Lowitz T, Museyko O, Bousson V, Laouisset L, Kalender WA, Laredo JD, et al. Bone marrow lesions identified by MRI in knee osteoarthritis are associated with locally increased bone mineral density measured by QCT. Osteoarthritis Cartilage 2013; 21: 957-964.

189. Kornaat PR, Kloppenburg M, Sharma R, Botha-Scheepers SA, Le Graverand MP, Coene LN, et al. Bone marrow edema-like lesions change in volume in the majority of patients with osteoarthritis; associations with clinical features. Eur Radiol 2007; 17: 3073-3078.

190. Bennell KL, Creaby MW, Wrigley TV, Bowles KA, Hinman RS, Cicuttini F, et al. Bone marrow lesions are related to dynamic knee loading in medial knee osteoarthritis. Ann Rheum Dis 2010; 69: 1151-1154.

191. Kean CO, Hinman RS, Bowles KA, Cicuttini F, Davies-Tuck M, Bennell KL. Comparison of peak knee adduction moment and knee adduction moment impulse in distinguishing between severities of knee osteoarthritis. Clin Biomech (Bristol, Avon) 2012; 27: 520-523.

192. Eriksen EF, Ringe JD. Bone marrow lesions: a universal bone response to injury? Rheumatol Int 2012; 32: 575-584.

193. Dore D, de Hoog J, Giles G, Ding C, Cicuttini F, Jones G. A longitudinal study of the association between dietary factors, serum lipids, and bone marrow lesions of the knee. Arthritis Res Ther 2012; 14: R13.

194. Davies-Tuck ML, Hanna F, Davis SR, Bell RJ, Davison SL, Wluka AE, et al. Total cholesterol and triglycerides are associated with the development of new bone marrow lesions in asymptomatic middle-aged women - a prospective cohort study. Arthritis Res Ther 2009; 11: R181.

195. Wang Y, Davies-Tuck ML, Wluka AE, Forbes A, English DR, Giles GG, et al. Dietary fatty acid intake affects the risk of developing bone marrow lesions in healthy middle-aged adults without clinical knee osteoarthritis: a prospective cohort study. Arthritis Res Ther 2009; 11: R63.

196. Bonadio MB, Filho AGO, Helito CP, Stump XM, Demange MK. Bone Marrow Lesion: Image, Clinical Presentation, and Treatment. Magn Reson Insights 2017; 10: 1178623X17703382.

197. Bonadio MB, Giglio PN, Helito CP, Pecora JR, Camanho GL, Demange MK. Subchondroplasty for treating bone marrow lesions in the knee - initial experience. Rev Bras Ortop 2017; 52: 325-330.

198. Cohen SB, Sharkey PF. Subchondroplasty for Treating Bone Marrow Lesions. J Knee Surg 2016; 29: 555-563.

199. Laslett LL, Dore DA, Quinn SJ, Boon P, Ryan E, Winzenberg TM, et al. Zoledronic acid reduces knee pain and bone marrow lesions over 1 year: a randomised controlled trial. Ann Rheum Dis 2012; 71: 1322-1328.

200. Pelletier JP, Roubille C, Raynauld JP, Abram F, Dorais M, Delorme P, et al. Disease-modifying effect of strontium ranelate in a subset of patients

from the Phase III knee osteoarthritis study SEKOIA using quantitative MRI: reduction in bone marrow lesions protects against cartilage loss. Ann Rheum Dis 2015; 74: 422-429.

Chapter 2

Bone marrow lesions detected by specific combination of MRI sequences are associated with severity of osteochondral degeneration

Dzenita Muratovic, Flavia Cicuttini, Anita Wluka, David Findlay, Yuanyuan Wang, Sophia Otto, David Taylor, Julia Humphries, Yea-Rin Lee, Agatha Labrinidis, Ruth Williams and Julia Kuliwaba.

Discipline of Orthopaedics and Trauma, The University of Adelaide, Adelaide, Australia.
Bone and Joint Research Laboratory, SA Pathology, Adelaide, Australia.
Department of Epidemiology & Preventive Medicine, Monash University, Melbourne, Australia.
Anatomical Pathology, SA Pathology, Adelaide, Australia.
Department of Radiology, Royal Adelaide Hospital, Adelaide, Australia.
Adelaide Microscopy, The University of Adelaide, Adelaide, Australia.

Arthritis Research &Therapy (2016); 18:54.

Statement of Authorship

Title of Paper	**Bone Marrow Lesions Detected by Specific Combination of MRI Sequences are Associated with Severity of Osteochondral Degeneration**
Publication Status	Published
Publication Details	Muratovic et al. Arthritis Research &Therapy (2016); 18:54 DOI: 10.1186/s13075-016-0953-x

Principal Author

Name of Principal Author (Candidate)	Dzenita Muratovic		
Contribution to the Paper	Designed the study, performed the experiments and analysis of the results, interpreted the data, wrote themanuscript and acted as corresponding author.		
Certification:	This paper reports on original research I conducted during the period of my Higher Degree by Research candidature and is not subject to any obligations or contractual agreements with a third party that would constrain its inclusion in this thesis. I am the primary author of this paper.		
Signature		Date	2/2/2016

Co-Author Contributions

By signing the Statement of Authorship, each author certifies that:

i. the candidate's stated contribution to the publication is accurate (as detailed above);

ii. permission is granted for the candidate in include the publication in the thesis; and the sum of all co-author contributions is equal to 100% less the candidate's stated contribution.

Name of Co-Author	Prof David Findlay		
Contribution to the Paper	Designed the study, interpreted the data, provided overall supervision and wrote the manuscript.		
Signature		Date	2/2/2016

Name of Co-Author	A/Prof Anita Wluka		
Contribution to the Paper	Designed the study, interpreted the data, provided overall supervision and wrote the manuscript.		
Signature		Date	2/2/2016

Name of Co-Author	Prof Flavia Cicuttini		
Contribution to the Paper	Designed the study, interpreted the data, provided overall supervision and wrote the manuscript.		
Signature		Date	2/2/2016

Name of Co-Author	Dr. Yuan Yuan Wang		
Contribution to the Paper	Analysed, advised on interpretation of the MRI data and critically revised the manuscript.		
Signature		Date	2/2/2016

Name of Co-Author	Dr Sophia Otto		
Contribution to the Paper	Analysed histopathology, interpreted the data and critically revised the manuscript.		
Signature		Date	2/2/2016

Name of Co-Author	David Taylor		
Contribution to the Paper	Analysed, advised on interpretation of the MRI data and critically revised the manuscript.		
Signature		Date	2/2/2016

Name of Co-Author	Julia Humphries		
Contribution to the Paper	Contributed to collection of specimens from patients, performed the experiments and critically revised the manuscript.		
Signature		Date	2/2/2016

Name of Co-Author	Yea Rin Lee		
Contribution to the Paper	Contributed to collection of specimens from patients, performed the experiments and critically revised the manuscript.		
Signature		Date	2/2/2016

Name of Co-Author	Dr Agatha Labrinidis		
Contribution to the Paper	Contributed to development of methods and critically revised the manuscript.		
Signature		Date	2/2/2016

Name of Co-Author	Ms Ruth Williams		
Contribution to the Paper	Contributed to development of methods and critically revised the manuscript.		
Signature		Date	2/2/2016

Name of Co-Author	Dr Julia Kuliwaba		
Contribution to the Paper	Designed the study, interpreted the data, provided overall supervision and wrote the manuscript.		
Signature		Date	2/2/2016

Muratovic *et al. Arthritis Research & Therapy* (2016) 18:54
DOI 10.1186/s13075-016-0953-x

Arthritis Research & Therapy

RESEARCH ARTICLE Open Access

Bone marrow lesions detected by specific combination of MRI sequences are associated with severity of osteochondral degeneration

Dzenita Muratovic[1,2*], Flavia Cicuttini[3], Anita Wluka[3], David Findlay[1], Yuanyuan Wang[3], Sophia Otto[4], David Taylor[5], Julia Humphries[2], Yearin Lee[2], Agatha Labrinidis[6], Ruth Williams[6] and Julia Kuliwaba[1,2]

Abstract

Background: Bone marrow lesions (BMLs) are useful diagnostic and prognostic markers in knee osteoarthritis (OA), but what they represent at the tissue level remains unclear. The aim of this study was to provide comprehensive tissue characterization of BMLs detected using two specific MRI sequences.

Methods: Tibial plateaus were obtained from 60 patients (29 females, 31 males), undergoing knee arthroplasty for OA. To identify BMLs, MRI was performed *ex vivo* using T1 and PDFS-weighted sequences. Multi-modal tissue level analyses of the osteochondral unit (OCU) were performed, including cartilage volume measurement, OARSI grading, micro-CT analysis of bone microstructure, routine histopathological assessment and quantitation of bone turnover indices.

Results: BMLs were detected in 74 % of tibial plateaus, the remainder comprising a No BML group. Of all BMLs, 59 % were designated BML 1 (detected only by PDFS) and 41 % were designated BML 2 (detected by both PDFS + T1). The presence of a BML was related to degeneration of the OCU, particularly within BML 2. When compared to No BML, BML 2 showed reduced cartilage volume ($p = 0.008$), higher OARSI scores ($p = 0.004$), thicker subchondral plate ($p = 0.002$), increased trabecular bone volume and plate-like structure ($p = 0.0004$), increased osteoid volume ($p = 0.002$) and thickness ($p = 0.003$), more bone marrow oedema ($p = 0.03$), fibrosis ($p = 0.002$), necrosis ($p = 0.01$) and fibrovascular cysts ($p = 0.04$). For most measures, BML 1 was intermediate between No BML and BML 2.

Conclusions: BMLs detected by specific MRI sequences identify different degrees of degeneration in the OCU. This suggests that MRI characteristics of BMLs may enable identification of different BML phenotypes and help target novel approaches to treatment and prevention of OA.

Keywords: Knee osteoarthritis, Bone marrow lesion, MRI, Osteochondral unit, Subchondral bone, Cartilage

Background

Knee osteoarthritis (OA), a painful degenerative condition with no effective treatment, is one of the leading causes of human suffering. It is widely accepted that OA is a disease of the whole joint, with particular involvement of the articular cartilage and subchondral bone. In fact, these two tissues act as a functional unit, the osteochondral unit (OCU), to maintain joint homeostasis [1]. Pathological changes in either the bone or the cartilage seem to predict degenerative changes in the other.

Focal changes in the subchondral bone, termed bone marrow lesions (BMLs), are features detected by magnetic resonance imaging (MRI) that have been reported to be closely associated with the severity of symptoms of OA such as pain [2–4] and OCU degeneration (e.g., loss of the overlying cartilage) [5–8]. Clinical studies have reported BMLs in both patients with early asymptomatic OA [9–12] and in those with severe late-stage OA [6,

* Correspondence: dzenita.muratovic@adelaide.edu.au
[1]Discipline of Orthopaedics and Trauma, The University of Adelaide, Adelaide, Australia
[2]Bone and Joint Research Laboratory, SA Pathology, Frome Road, Adelaide 5000, Australia
Full list of author information is available at the end of the article

13–15]. In patients with early OA and in individuals who do not have OA, BMLs can decrease in size or resolve completely [2, 5, 16]. Hunter et al. reported that in progressive OA, BMLs are more likely to persist and to enlarge in size [6]. Previous human histological studies examined small numbers of samples and found mixed pathological findings of bone marrow and sclerotic bone in BMLs [17–19]. Similar histopathological findings have been reported for animal models of OA [20].

BMLs are conventionally assessed using fat-suppressed or proton-dense T2-weighted MRI, although they may also be detected using other MRI sequences. Within fat-suppressed T2-weighted and/or proton density-weighted sequences they appear as areas of ill-defined hyperintensity (high signal) in subchondral bone, and in T1-weighted sequences they appear hypointense (low signal) [21–25]. Thus, although fat-suppressed T2-weighted and/or proton density-weighted sequences are recommended for the assessment of BMLs as they depict lesions to their maximum extent, T1-weighted sequences are predominantly used for assessment of the cartilage. Preferably, a combination of sequences should be used to evaluate the extent of OA disease progression [5, 14, 26, 27].

There is extensive debate about the optimal way to image BMLs but it remains unknown whether BMLs detected by different MRI sequences differ at the tissue level. Thus, it is possible that amongst BMLs identified by conventional T2-weighted images, some may also be detectable using another MRI sequence, but others may not. This would suggest that the underlying tissues in these groups are not the same and may thus relate to different clinical outcomes. As BMLs are closely associated with pain and loss of cartilage [12, 14, 28, 29], they are emerging as promising targets for monitoring progression of knee OA [30] and the effects of treatment [31]. Therefore, a comprehensive understanding of the underlying pathology of BMLs is important.

The aim of this study was to comprehensively investigate histological changes in all components of the OCU (cartilage, subchondral bone and subchondral bone marrow) based on the presence or absence of a BML detected by two specific MRI sequences, in tibial plateau tissue obtained during knee replacement surgery.

Methods

Patient samples

Tibial plateaus (TP) were obtained from 60 patients undergoing knee arthroplasty surgery (29 female patients aged 51 to 87 years, body mass index (BMI) range 24.1–41.4 and 31 male patients aged 42 to 86 years, BMI range 22.6–45.7). Written consent was obtained from all patients and the study received prior approval from the Human Research Ethics Committee at the Repatriation General Hospital, Royal Adelaide Hospital and The University of Adelaide, South Australia, in accordance with the Declaration of Helsinki 1975.

Inclusion criteria were: radiographic evidence of OA with severe symptomatic disabilities, such as severe pain and limited mobility. Exclusion criteria were secondary OA of the knee due to trauma or rheumatoid arthritis, evidence of bone-related chronic debilitating disease and/or history of any medication that may have affected bone turnover.

Macroscopic evaluation

All retrieved TP were examined and graded macroscopically according to the Outerbridge Classification [26, 32] by two experienced orthopedic surgeons (DM and CW), for whom the intraclass correlation coefficient (ICC) for inter-observer reproducibility was 0.81 (95 % CI 0.79, 0.84).

Radiographic evaluation of knee OA

Standing anteroposterior, posteroanterior and lateral projection radiographs were taken prior to surgery. The extent of radiographic evidence of progression of OA was assessed according to the Kellgren and Lawrence (K&L) grade, the current standard radiologic grading system for OA. All radiographs were scored by two experienced assessors (AW and YW) with 5 % disagreement. Assessors were blinded to the presence of BMLs in the knee joint.

Magnetic resonance imaging

Specimens were scanned ex vivo using an MRI scanner with an 8-channel wrist coil (3 T MRI Siemens TRIO, Berlin, Germany), with two specific sequences: fat-suppressed (FS) fast spin-echo proton density-weighted (PDFS) and T1-weighted spin echo in the sagittal and coronal planes. Sagittal slice thickness was 1.6 mm with a distance factor of 25 %; coronal slice thickness was 3.0 mm with a 10 % distance factor. We confirmed that ex vivo MRI information corresponded to pre-operative imaging, by comparing pre- and post-operative MRI data for a subset of five patients, consistent with previous reports [20, 33, 34].

The definition for identification of BMLs was by mutual agreement between two radiologists with musculoskeletal MRI expertise (DT and YW). A BML is defined as a zone of altered signal intensity in the bone and marrow, located immediately beneath the articular cartilage and visible on at least two consecutive slices [7, 13, 35]. Based on the presence and/or absence of signal, two subtypes of BML were defined. BMLs detected using the PDFS sequence only and with absent signal on T1-weighted sequence in the same area are referred to as BML 1; BMLs detected by both PDFS and T1 sequences

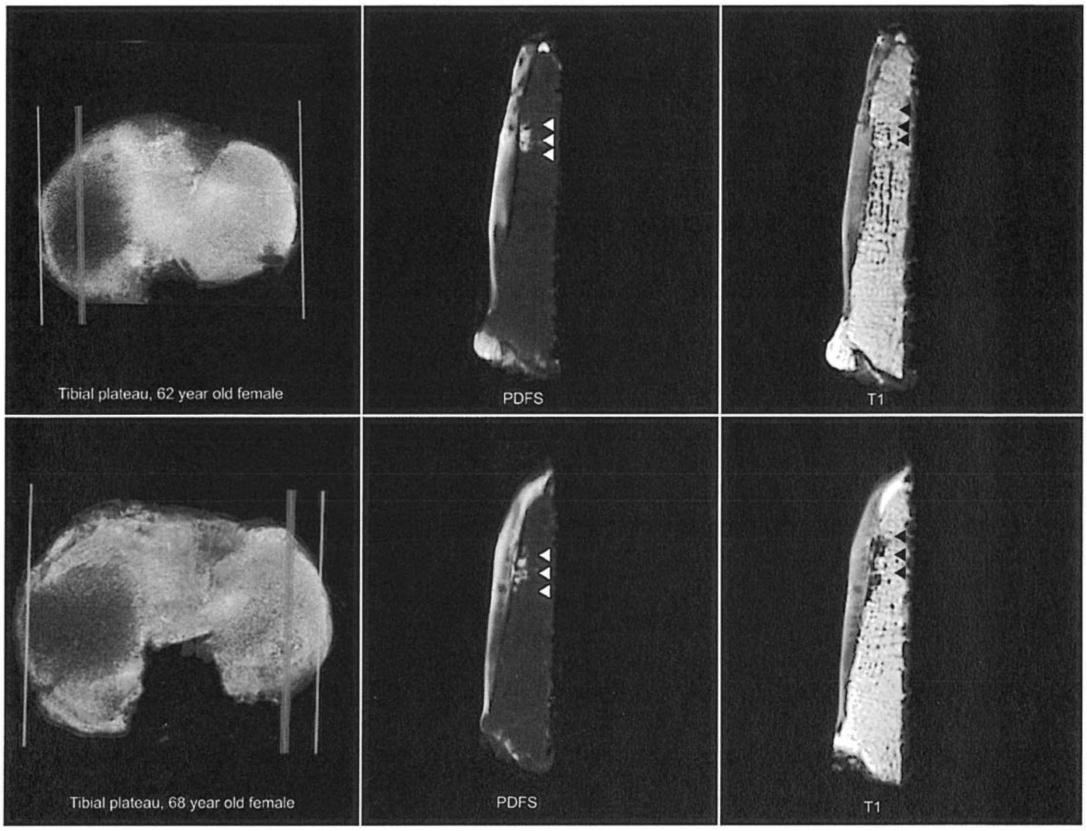

Fig. 1 *Left*, *upper* and *lower panels* show tibial plateaus in the transaxial plane. *Right*, *green line* is the sagittal slice. *Upper panel*, *middle*, the signal of the bone marrow lesion (BML) is detected by fast spin-echo proton density-weighted (PDFS) sequence (*arrows* identify signal), and *right* the signal is not detected by T1-weighted sequence. *Lower panel*, *middle*, the signal of the BML is detected by PDFS sequence (*arrows* identify signal), and *right* the signal is detected by T1-weighted sequence

are referred to as BML 2. (Fig. 1 shows examples of BML 1 and BML 2).

After identification of a BML the external contours of the BMLs were marked in both planes by two researchers (DzM and YRL) blinded to the presence of BMLs. The volume and precise location of each BML was determined, enabling the creation of a two-dimensional (2D) axial map of all BMLs (Fig. 2 demonstrates the approximate size and location of both BMLs). Cartilage volume in the medial compartment was determined as described previously [7, 25]. The coefficient of variation for the measurement of cartilage volume at the medial tibia was 2.2 %.

Micro-computed tomography (micro-CT)

A subset of 36 TP (6 mm minimal thickness) was scanned by micro-CT (Skyscan model 1076, Kontic, Belgium). Images were obtained at isotropic resolution of 17.4 μm. Using AVIZO® Fire software (Zuse Institute, Berlin, Germany), and three-dimensional (3D) volumes of TP were generated using both MRI and micro-CT images. Then, the BML signal location was identified from MRI and aligned onto the 3D volume of micro-CT. A cylindrical region of interest (ROI) containing the volume of the BML, diameter 10 mm × depth 6 mm, was used for analysis of BML bone microstructure. As BMLs were found predominantly on the medial side, the same size and shape ROI was used in the medial compartment of the TP without BMLs. These ROIs were further divided into the subchondral plate and subchondral trabecular bone regions and analyzed separately, using CT-An analyzer software (SkyScan).

Microscopic evaluation

A cuboidal block of cartilage-subchondral bone (10 × 10 × 5 mm), representing the area containing a BML

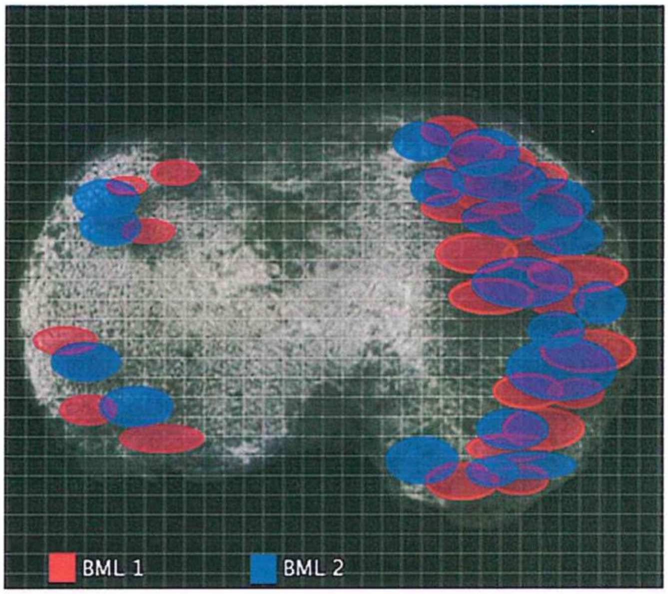

Fig. 2 The approximate external contour of each bone marrow lesion (*BML*) area was marked. The precise map location was placed by identifying the number of sagittal and coronal slices with measurement of distance from the external tibial contour. After marking the position of the BML for all specimens, a distribution map of both types of BML was found. *BML 1* bone marrow lesion detected using the fast spin-echo proton density-weighted sequence only, with absent signal on T1-weighted sequence in the same area, *BML 2* bone marrow lesions detected by both fast spin-echo proton density-weighted and T1 sequences

(named BML), was dissected from the TP using a low-speed diamond saw (Model 660, South Bay Technology, San Clemente, US). A tissue block of the same size and shape was cut from the medial compartment of the TP without BMLs (no BML). Each cube was divided equally, with one half formalin-fixed, processed and embedded in methyl-methacrylate resin. The block was cut into 5-μm-thick sections and stained with von Kossa silver/hematoxylin and eosin (H&E) for histomorphometric analysis of bone remodeling. The other half of the block was formalin-fixed, decalcified in 5 % hydrochloric acid, paraffin-embedded, sectioned 5-μm-thick and stained with H&E and Safranin-O/Fast Green. A senior pathologist (SO) with over 10 years of experience in the field, blinded to the MRI findings, used a 1–5 scoring system to semiquantitatively evaluate the presence and extent of pathological findings in the tissue on the H&E slides, where 1 = <5 % (minimal presence), 2 = 5–14 %, 3 = 15–25 % (moderate presence), 4 = 25–50 % and 5 = >50 % (prominent presence). The intra-observer reproducibility of the histological scores (assessed by SO) was measured at separate times for ten sections (ICC 0.98 (95 % CI 0.95, 0.98)). Safranin-O/Fast Green was used for Osteoarthritis Research Society International (OARSI) grading [36, 37]. Consensus between three assessors (DzM, EG and YRL) determined the grading. The ICC for inter-observer reproducibility was 0.82 (95 % CI 0.80, 0.84).

Statistical analysis

The Shapiro–Wilk test was used to determine normality of the data distribution. Differences between the no BML and the BML (BML 1 + BML 2) groups were described using the unpaired *t* test for parametric distribution or the Mann–Whitney *U* test for non-parametric data distribution. Differences between three groups (no BML (no BML detected), BML 1 (BML detected only by PDFS sequence) and BML 2 (BML detected by both PDFS and T1 sequences)) were described using analysis of variance (ANOVA). For parametric data, ANOVA and the Holm–Sidak comparison test with single pooled variance were performed. For non-parametric data, the Kruskal–Wallis test and Dunn's multiple comparison test were performed. An adjusted model was then performed for all outcome parameters versus BML group, adjusting for age, sex and BMI. P values <0.05 were considered to be statistically significant.

Results

Demographic characteristics of the participating individuals were grouped according to the presence or absence of BML on specific MRI sequences, and are

Table 1 Patient demographic characteristics

	No BML (n = 12)	Total BML (1 + 2) (n = 44)	*P* value
Age[a]	69.8 ± 1.4	68.3 ± 1.2	0.5
Male, number (%)	3 (25 %)	25 (57 %)	0.06
Female, number (%)	9 (75 %)	19 (43 %)	0.1
BMI[a]	31.3 ± 6.4	33.4 ± 5.1	0.2
K&L grade[b]	2 (1, 4)	3 (2, 4)	0.7
Medial OA, number of patients (%)	6 (50 %)	34 (77 %)	0.07
Lateral OA, number of patients (%)	2 (16 %)	6 (14 %)	0.5
Patello-femoral OA, number of patients (%)	4 (33 %)	4 (9 %)	*0.04*
Subchondral cyst present, number of patients (%)	0 (0 %)	12 (27 %)	*0.03*
Outerbridge classification[b]	3 (3, 4)	4 (3, 4)	*0.04*
Cartilage volume[a]	1.3 ± 0.2	0.9 ± 0.3	*0.01*
OARSI score[a]	3.7 ± 1.2	5 ± 0.9	*0.004*

[a]Values presented with mean ± standard deviation. [b]Values presented with median (25[th], 75th percentiles). *P* values are for difference between the group with no bone marrow lesions (No BML) and the group with BML (BML 1 + BML 2). *BMI* body mass index, *K&L* Kellgren and Lawrence, *OA* osteoarthritis, *OARSI* Osteoarthritis Research Society International

summarized in Table 1. There were no significant differences between the two groups in patient age, gender, BMI or K&L grade.

BMLs were detected in 44 (73 %) of TP; 12 (20 %) of TP were without BML and/or subchondral cysts (the no BML group). Of the TP with a BML, 12 (27 %) also had a subchondral cyst present in the intercondylar space. Furthermore, 4 TP (6 % of all subjects) had cysts but without BML and therefore were excluded from further analysis. BMLs detected using the PDFS sequence only (BML 1) represented 59 % of all BMLs. The signal intensity in these lesions was either moderate or diffuse in the PDFS sequence and by definition there was no signal on the T1-weighted sequence in the same areas. BMLs detected by both PDFS and T1 sequences (BML 2) represented 41 % of all BMLs. The signal intensity in BML 2 was hyperintense on the PDFS sequence and hypointense on the T1-weighted sequence. Preoperative radiographs indicated that 77 % of TP with BML were diagnosed with medial OA, 14 % with lateral OA and 9 % with patellofemoral OA (Table 1). Furthermore, both BML types were present predominantly in the medial compartment of TP (87 %), with their anatomical distribution aligning closely with the menisci (Fig. 2).

Firstly, we examined whether structural changes in all components of the OCU (cartilage, subchondral bone and subchondral bone marrow) differed based on the presence or absence of a BML detected by two specific MRI sequences. In TP with BML, areas corresponding to a BML, either BML 1 or BML 2, were compared to anatomically matched areas in TP without BML, and progressive degenerative changes were found in BML areas for all tested parameters. These included a higher Outerbridge score, reduced cartilage volume, higher OARSI score (Table 1), more histopathological abnormalities such as tidemark duplication, penetration of vascular cones into calcified cartilage, edema, necrosis, fibrosis, the presence of thick-walled arterioles, and small fibrovascular cystic formations (Table 2). BML containing subchondral bone had thicker subchondral plate, increased trabecular bone volume, more trabeculae that were predominantly plate-like, increased osteoid volume and thickness of both plate and trabeculae and decreased eroded surface in trabecular bone (Table 3).

We then examined whether the extent of these changes was different depending on the BML subtype. BMLs detected by both PDFS and T1 sequences (BML 2) were identified as lesions having the most advanced degenerative changes throughout the whole OCU. In fact, they displayed all the changes described above for subchondral bone with BML signal (Figs. 3 and 4). In contrast, BMLs detected only by the PDFS sequence (BML 1) displayed a subset of the intermediate degenerative changes when compared to TP with no BML and those with BML 2 (Figs. 3 and 4).

To assess whether the histological composition of BML visualized by different sequences differed, we compared BML 1 and BML 2. The BML 2 were associated with reduced cartilage volume ($p = 0.007$) more fibrosis ($p = 0.006$) and necrosis ($p = 0.01$) in the bone marrow (Fig. 3), thicker subchondral bone plate ($p = 0.002$), with higher osteoid thickness (O.Th) ($p = 0.04$) in trabecular bone and with no differences between histomorphometric parameters besides higher osteoid volume/bone volume (OV/BV) ($p = 0.02$) compared to BML 1 (Fig. 4).

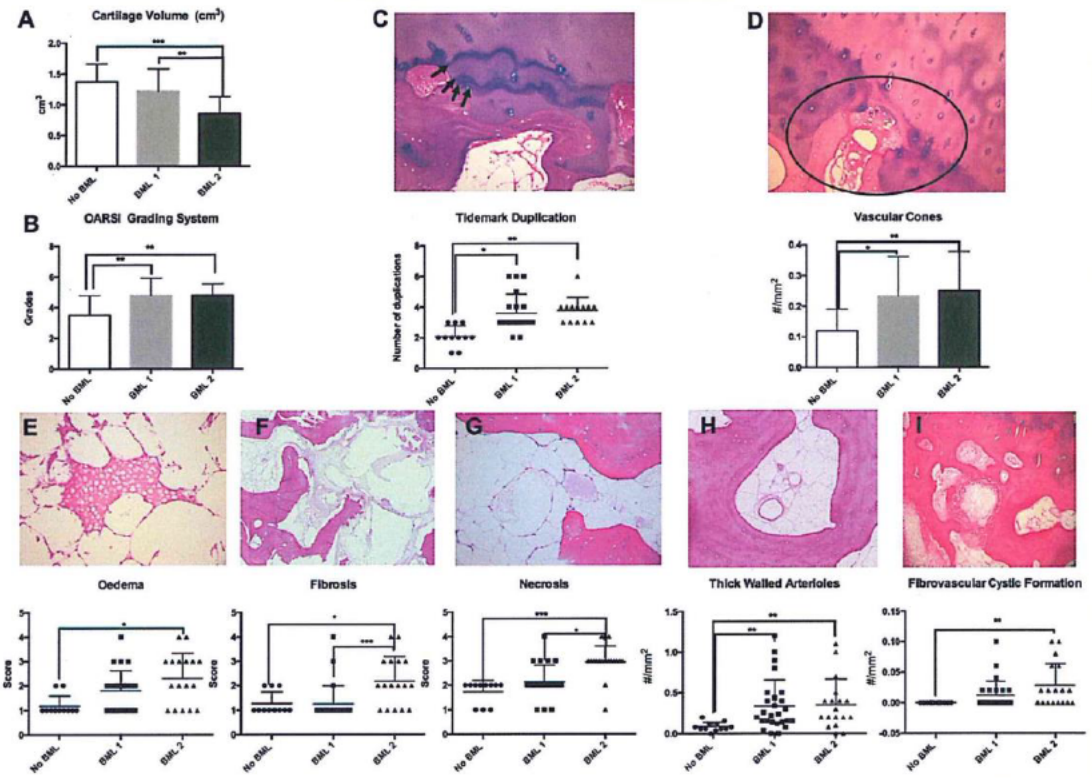

Fig. 3 Comparison of cartilage volume **(a)**, Osteoarthritis Research Society International; (OARSI) grades **(b)**, cartilage tidemark progression (*arrows* identify tidemarks) **(c)**, penetration of vascular cones (*circled*) **(d)**. Histopathology of bone marrow; bone marrow edema **(e)**, fibrosis **(f)**, necrosis **(g)**, thick-walled arterioles **(h)** and fibrovascular cystic formation **(i)**. Represented histologically and graphically for specimens with no bone marrow lesions evident (*No BML*), bone marrow lesions evident only in fast spin-echo proton density-weighted (PDFS) sequences (*BML 1*), and bone marrow lesions evident in both PDFS and T1-weighted sequences (*BML 2*): $^{*}p = 0.05$, $^{**}p = 0.005$, $^{***}p = 0.0005$

Our findings of histological differences between BMLs detected by different MRI sequences are intriguing. The study by Zanetti et al. was one of the first to describe the histology of BMLs and in that study it was found that edema is minimally present, suggesting the term "bone marrow lesion" is used for these features [17]. Our results showed that BML 2 had significantly greater edema, fibrosis and necrosis present in bone marrow compared to the no BML group and BML 1. Other human and animal histological studies [18–20] confirmed that BMLs are characterized by mixed pathological appearances and have not found specific histopathological changes in BML to explain the MRI signal, although it was suggested by Saadat et al. that the hyperintense MRI signal might result from increased blood flow [40]. We analyzed the density of vascular cones in the subchondral plate and the number of small thick-walled arterioles in the bone marrow corresponding to the BML signal in ex vivo samples. We found that the subchondral plate and the marrow of both BML 1 and BML 2 contained significantly more vascular cones and small thick-walled arterioles compared to the no BML group. Therefore, although there was obviously no blood flow in the ex vivo samples, it remains possible that the signals relate somehow to the altered vascular structures associated with BMLs.

Guymer et al. found that the presence of BMLs is closely associated with high BMI and suggested that obesity might be an important factor in their formation [10]. Similarly, Felson et al. found that knee malalignment and high loading of the joint associate with the presence of BMLs [28]. In this study, we did not find a significant relationship between BMI and the presence of BMLs but we did not measure knee malalignment. It is likely that knee loading is not simply a function of BMI, but involves both the frequency and manner of loading. By creating a distribution map of lesions in the tibial plateau, we found that both types of BML are consequences of TGF-β over-expression. The authors suggested that the osteoid islets might correspond to the BML signal detected by MRI [50]. Although this is possible, we have not been able to unequivocally assign the BML signals to any specific feature in the subchondral bone.

Our data suggest that the use of specific MRI sequences offers potential application for OA disease staging and to identify individuals with more advanced structural progression of disease. In particular, BML 2 appears to represent subchondral tissue and cartilage with more degenerative structural changes and therefore less ability to resolve or repair (Table 4). As we found intermediate differences between BML 1 and BML 2, we propose that BML 1 might be an early or transitional stage of BML. In both human and animal studies it has been found that BMLs in the early stage of disease are dynamic and can resolve within time. Perhaps BMLs seen only by PDFS MRI sequences are those that have the ability to resolve [16, 51], making them a potential target for early diagnosis and potential therapy. Further studies of early-stage OA are needed to confirm this possibility and to investigate modifiable risk factors for the initiation of BMLs. The importance of BMLs as therapeutic targets has been recognized, and there are current studies in which BML size and frequency are serving as an outcome measure [39, 52]. Therapies that target BMLs as biomarkers of the initiation and/or progression of knee OA might be more effective than those targeting cartilage repair, as cartilage degradation might be a consequence of failed repair mechanisms in subchondral bone and/or bone marrow. We therefore propose that BML 1 may be a better candidate for targeted treatments and as an outcome measure, than BML 2.

Table 4 Group with no bone marrow lesions (No BML) vs. groups with BML 1 and BML 2

	No BML vs. BML 1	No BML vs. BML 2
Cartilage		
MRI cartilage volume	Not different	Low
OARSI histology score	High	High
Bone marrow pathology		
Edema	Not different	High
Fibrosis	Not different	High
Necrosis	Not different	High
Vascularity	High	High
Subchondral bone		
Plate thickness	High	Very high
Trabecular bone volume	Not different	High
Osteoid volume and thickness	Not different	High

Changes at tissue level between the No BML group vs. group with BML detected using the fast spin-echo proton density-weighted sequence only, with absent signal on T1-weighted sequence in the same area (BML 1) and the group with BML detected by both fast spin-echo proton density-weighted and T1 sequences (BML 2). *MRI* magnetic resonance imaging, *OARSI* Osteoarthritis Research Society International

This study has several limitations. First, we have only examined ex vivo tibial plateau samples from patients with advanced and painful knee OA. However, this limitation will be present for any human OA histopathological studies. It may be important that our recent clinical study broadly supports our ex vivo findings, namely that BML 2 was associated with greater cartilage volume loss and more incident pain [38]. Second, BMLs were identified post-operatively and damage during handling could possibly have led to altered signal on the post-operative MRI. We have taken care to minimize potential artifacts in post-operative MRI by using the same handling protocol for all specimens and by excluding the cut surfaces from our analysis. Third, we only investigated BMLs from knee OA and findings might differ for other skeletal joints. We believe that the strength of this study is that we have analyzed a large number of specimens compared to previous studies, using a comprehensive multi-modal analysis of changes in cartilage, bone and bone marrow in association with BMLs. Fourth, the thickness of our specimens was between 5 and 15 mm, and clinically BMLs may be considerably larger than this and might expand to a greater depth within the tibia. On the other hand, it has been found that bone structural changes are most prominent in the first 6 mm of depth beneath the cartilage [42].

Conclusion

The presence of BMLs detected by specific MRI sequences is strongly associated with the degree of structural change in the OCU in knee OA. Furthermore, different MRI sequences appear able to differentiate different degrees of structural damage in knee OA. Therefore, BMLs detected with specific sequences could act as potential MRI biomarkers for the identification of individuals at high risk of progressive OA or for development and monitoring of new therapies for this condition.

Abbreviations

ANOVA: analysis of variance; BMI: body mass index; BML: bone marrow lesion; BML 1: bone marrow lesion detected using the fast spin-echo proton density-weighted sequence only, with absent signal on T1-weighted sequence in the same area; BML 2: bone marrow lesions detected by both fast spin-echo proton density-weighted and T1 sequences; BS: bone surface; BV: bone volume; cl.pores: closed pores; ES: erosion surface; FS: fat suppressed; H&E: hematoxylin and eosin; ICC: intraclass correlation coefficient; K&L: Kellgren and Lawrence; micro-CT: micro-computed tomography; MRI: magnetic resonance imaging; OA: osteoarthritis; OARSI: Osteoarthritis Research Society International; OCU: osteochondral unit; OS: osteoid surface; O.Th: osteoid thickness; OV: osteoid volume; PDFS: fast spin-echo proton density-weighted; ROI: region of interest; SMI: structural model index; Tb.N: trabecular number; Tb.Sp: trabecular separation; Tb.Th: trabecular thickness; TP: tibial plateau; TV: tissue volume.

Competing interests
The authors declare that they have no competing interests.

Authors' contributions
All authors meet criteria for authorship. DM designed the study, performed the experiments and analysis of the results, interpreted the data and wrote the manuscript. FC, AW, DF and JK designed the study, interpreted the data, provided overall supervision and wrote the manuscript. SO analyzed histopathology, interpreted the data and critically revised the manuscript. DT and YW analyzed, advised on interpretation of the MRI data and critically revised the manuscript. JH and Y-RL contributed to collection of specimens from patients, performed the experiments and critically revised the manuscript. AL and RW contributed to development of methods and critically revised the manuscript. All authors read and approved the manuscript.

Acknowledgements
The authors wish to thank Ms Sue Collins and Ms Emma Giersch for technical assistance, Dr Graham Mercer, Dr Chris Wilson, and Dr Dai Morgan for helping to obtain specimens. The authors wish to acknowledge the staff support from Adelaide Microscopy, Anatomical Pathology at SA Pathology, and Department of Radiology, Royal Adelaide Hospital. A National Health and Medical Research Council of Australia (NHMRC) Project Grant (1042482) and support from the Rebecca Cooper Foundation funded this work. DM is the recipient of an NHMRC scholarship; AEW is the recipient of an NHMRC Career Development Fellowship (Clinical level 2, 1063574).

Author details
[1]Discipline of Orthopaedics and Trauma, The University of Adelaide, Adelaide, Australia. [2]Bone and Joint Research Laboratory, SA Pathology, Frome Road, Adelaide 5000, Australia. [3]Department of Epidemiology & Preventive Medicine, Monash University, Melbourne, Australia. [4]Anatomical Pathology, SA Pathology, Adelaide, Australia. [5]Department of Radiology, Royal Adelaide Hospital, Adelaide, Australia. [6]Adelaide Microscopy, The University of Adelaide, Adelaide, Australia.

Received: 2 December 2015 Accepted: 9 February 2016
Published online: 24 February 2016

References

1. Mahjoub M, Berenbaum F, Houard X. Why subchondral bone in osteoarthritis? The importance of the cartilage bone interface in osteoarthritis. Osteoporos Int. 2012;23 Suppl 8:S841–6.
2. Davies-Tuck ML, Wluka AE, Wang Y, English DR, Giles GG, Cicuttini F. The natural history of bone marrow lesions in community-based adults with no clinical knee osteoarthritis. Ann Rheum Dis. 2009;68(6):904–8.
3. Felson DT, Chaisson CE, Hill CL, Totterman SM, Gale ME, Skinner KM, et al. The association of bone marrow lesions with pain in knee osteoarthritis. Ann Intern Med. 2001;134(7):541–9.
4. Zhai G, Blizzard L, Srikanth V, Ding C, Cooley H, Cicuttini F, et al. Correlates of knee pain in older adults: Tasmanian Older Adult Cohort Study. Arthritis Rheum. 2006;55(2):264–71.
5. Roemer FW, Guermazi A, Javaid MK, Lynch JA, Niu J, Zhang Y, et al. Change in MRI-detected subchondral bone marrow lesions is associated with cartilage loss: the MOST Study. A longitudinal multicentre study of knee osteoarthritis. Ann Rheum Dis. 2009;68(9):1461–5.
6. Hunter DJ, Zhang Y, Niu J, Goggins J, Amin S, LaValley MP, et al. Increase in bone marrow lesions associated with cartilage loss: a longitudinal magnetic resonance imaging study of knee osteoarthritis. Arthritis Rheum. 2006;54(5): 1529–35.
7. Wluka AE, Wang Y, Davies-Tuck M, English DR, Giles GG, Cicuttini FM. Bone marrow lesions predict progression of cartilage defects and loss of cartilage volume in healthy middle-aged adults without knee pain over 2 yrs. Rheumatology (Oxford). 2008;47(9):1392–6.
8. Wluka AE, Hanna F, Davies-Tuck M, Wang Y, Bell RJ, Davis SR, et al. Bone marrow lesions predict increase in knee cartilage defects and loss of cartilage volume in middle-aged women without knee pain over 2 years. Ann Rheum Dis. 2009;68(6):850–5.
9. Zubler V, Mengiardi B, Pfirrmann CW, Duc SR, Schmid MR, Hodler J, et al. Bone marrow changes on STIR MR images of asymptomatic feet and ankles. Eur Radiol. 2007;17(12):3066–72.
10. Guymer E, Baranyay F, Wluka AE, Hanna F, Bell RJ, Davis SR, et al. A study of the prevalence and associations of subchondral bone marrow lesions in the knees of healthy, middle-aged women. Osteoarthritis Cartilage. 2007;15(12):1437–42.
11. Baranyay FJ, Wang Y, Wluka AE, English DR, Giles GG, Sullivan RO, et al. Association of bone marrow lesions with knee structures and risk factors for bone marrow lesions in the knees of clinically healthy, community-based adults. Semin Arthritis Rheum. 2007;37(2):112–8.
12. Sowers MF, Hayes C, Jamadar D, Capul D, Lachance L, Jannausch M, et al. Magnetic resonance-detected subchondral bone marrow and cartilage defect characteristics associated with pain and X-ray-defined knee osteoarthritis. Osteoarthritis Cartilage. 2003;11(6):387–93.
13. Roemer FW, Neogi T, Nevitt MC, Felson DT, Zhu Y, Zhang Y, et al. Subchondral bone marrow lesions are highly associated with, and predict subchondral bone attrition longitudinally: the MOST study. Osteoarthritis Cartilage. 2010;18(1):47–53.
14. Link TM, Steinbach LS, Ghosh S, Ries M, Lu Y, Lane N, et al. Osteoarthritis: MR imaging findings in different stages of disease and correlation with clinical findings. Radiology. 2003;226(2):373–81.
15. Kamibayashi L, Wyss UP, Cooke TD, Zee B. Trabecular microstructure in the medial condyle of the proximal tibia of patients with knee osteoarthritis. Bone. 1995;17(1):27–35.
16. Berry PA, Davies-Tuck ML, Wluka AE, Hanna FS, Bell RJ, Davis SR, et al. The natural history of bone marrow lesions in community-based middle-aged women without clinical knee osteoarthritis. Semin Arthritis Rheum. 2009; 39(3):213–7.
17. Zanetti M, Bruder E, Romero J, Hodler J. Bone marrow edema pattern in osteoarthritic knees: correlation between MR imaging and histologic findings. Radiology. 2000;215(3):835–40.
18. Taljanovic MS, Graham AR, Benjamin JB, Gmitro AF, Krupinski EA, Schwartz SA, et al. Bone marrow edema pattern in advanced hip osteoarthritis: quantitative assessment with magnetic resonance imaging and correlation with clinical examination, radiographic findings, and histopathology. Skeletal Radiol. 2008;37(5):423–31.
19. Hunter DJ, Gerstenfeld L, Bishop G, Davis AD, Mason ZD, Einhorn TA, et al. Bone marrow lesions from osteoarthritis knees are characterized by sclerotic bone that is less well mineralized. Arthritis Res Ther. 2009;11(1):R11.
20. Martig S, Boisclair J, Konar M, Spreng D, Lang J. MRI characteristics and histology of bone marrow lesions in dogs with experimentally induced osteoarthritis. Vet Radiol Ultrasound. 2007;48(2):105–12.
21. Loeuille D, Chary-valckenaere I. MRI in OA: from cartilage to bone marrow lesion. Osteoporos Int. 2012;23(8):867–9.
22. Roemer FW, Khrad H, Hayashi D, Jara H, Ozonoff A, Fotinos-Hoyer AK, et al. Volumetric and semiquantitative assessment of MRI-detected subchondral bone marrow lesions in knee osteoarthritis: a comparison of contrast-enhanced and non-enhanced imaging. Osteoarthritis Cartilage. 2010;18(8):1062–6.
23. Raynauld JP, Martel-Pelletier J, Berthiaume MJ, Abram F, Choquette D, Haraoui B, et al. Correlation between bone lesion changes and cartilage volume loss in patients with osteoarthritis of the knee as assessed by quantitative magnetic resonance imaging over a 24-month period. Ann Rheum Dis. 2008;67(5):683–8.
24. Carrino JA, Blum J, Parellada JA, Schweitzer ME, Morrison WB. MRI of bone marrow edema-like signal in the pathogenesis of subchondral cysts. Osteoarthritis Cartilage. 2006;14(10):1081–5.
25. Dore D, Martens A, Quinn S, Ding C, Winzenberg T, Zhai G, et al. Bone marrow lesions predict site-specific cartilage defect development and volume loss: a prospective study in older adults. Arthritis Res Ther. 2010; 12(6):R222.
26. Driban JB, Tassinari A, Lo GH, Price LL, Schneider E, Lynch JA, et al. Bone marrow lesions are associated with altered trabecular morphometry. Osteoarthritis Cartilage. 2012;20(12):1519–26.
27. Hayashi D, Guermazi A, Kwoh CK, Hannon MJ, Moore C, Jakicic JM, et al. Semiquantitative assessment of subchondral bone marrow edema-like lesions and subchondral cysts of the knee at 3T MRI: a comparison between intermediate-weighted fat-suppressed spin echo and Dual Echo Steady State sequences. BMC Musculoskelet Disord. 2011;12:198.
28. Felson DT, McLaughlin S, Goggins J, LaValley MP, Gale ME, Totterman S, et al. Bone marrow edema and its relation to progression of knee osteoarthritis. Ann Intern Med. 2003;139(5 Pt 1):330–6.
29. Kijowski R, Stanton P, Fine J, De Smet A. Subchondral bone marrow edema in patients with degeneration of the articular cartilage of the knee joint. Radiology. 2006;238(3):943–9.

30. Lowitz T, Museyko O, Bousson V, Laouisset L, Kalender WA, Laredo JD, et al. Bone marrow lesions identified by MRI in knee osteoarthritis are associated with locally increased bone mineral density measured by QCT. Osteoarthritis Cartilage. 2013;21(7):957–64.
31. Laslett LL, Dore DA, Quinn SJ, Boon P, Ryan E, Winzenberg TM, et al. Zoledronic acid reduces knee pain and bone marrow lesions over 1 year: a randomised controlled trial. Ann Rheum Dis. 2012;71(8):1322–8.
32. Kleemann RU, Krocker D, Cedraro A, Tuischer J, Duda GN. Altered cartilage mechanics and histology in knee osteoarthritis: relation to clinical assessment (ICRS Grade). Osteoarthritis Cartilage. 2005;13(11):958–63.
33. Zanetti M, Steiner CL, Seifert B, Hodler J. Clinical outcome of edema-like bone marrow abnormalities of the foot. Radiology. 2002;222(1):184–8.
34. Kazakia GJ, Kuo D, Schooler J, Siddiqui S, Shanbhag S, Bernstein G, et al. Bone and cartilage demonstrate changes localized to bone marrow edema-like lesions within osteoarthritic knees. Osteoarthritis Cartilage. 2013;21(1):94–101.
35. Driban JB, Lo GH, Lee JY, Ward RJ, Miller E, Pang J, et al. Quantitative bone marrow lesion size in osteoarthritic knees correlates with cartilage damage and predicts longitudinal cartilage loss. BMC Musculoskelet Disord. 2011;12:217.
36. Pritzker KPH, Gay S, Jimenez SA, Ostergaard K, Pelletier JP, Revell PA, et al. Osteoarthritis cartilage histopathology: grading and staging. Osteoarthr Cartil. 2006;14(1):13–29.
37. Pauli C, Whiteside R, Heras FL, Nesic D, Koziol J, Grogan SP, et al. Comparison of cartilage histopathology assessment systems on human knee joints at all stages of osteoarthritis development. Osteoarthritis Cartilage. 2012;20(6):476–85.
38. Wluka ATA, Maulana R, Liu B, Wang Y, Giles G, O'Sullivan R, et al. Bone Marrow Lesions can be subtyped into groups with different clinical outcomes using 2 Magnetic Resonance imaging (MRI) sequences. Arthr Res Ther. 2015;17:270. doi:10.1186/s13075-015-0780-5.
39. Roemer FW, Kwoh CK, Hannon MJ, Hunter DJ, Eckstein F, Fujii T, et al. What comes first? Multitissue involvement leading to radiographic osteoarthritis: magnetic resonance imaging-based trajectory analysis over four years in the Osteoarthritis Initiative. Arthritis Rheumatol. 2015;67(8):2085–96.
40. Saadat E, Jobke B, Chu B, Lu Y, Cheng J, Li X, et al. Diagnostic performance of in vivo 3-T MRI for articular cartilage abnormalities in human osteoarthritic knees using histology as standard of reference. Eur Radiol. 2008;18(10):2292–302.
41. Donahue TL, Hull ML, Rashid MM, Jacobs CR. A finite element model of the human knee joint for the study of tibio-femoral contact. J Biomech Eng. 2002;124(3):273–80.
42. Patel V, Issever AS, Burghardt A, Laib A, Ries M, Majumdar S. MicroCT evaluation of normal and osteoarthritic bone structure in human knee specimens. J Orthop Res. 2003;21(1):6–13.
43. Bobinac D, Spanjol J, Zoricic S, Maric I. Changes in articular cartilage and subchondral bone histomorphometry in osteoarthritic knee joints in humans. Bone. 2003;32(3):284–90.
44. Messent EA, Ward RJ, Tonkin CJ, Buckland-Wright C. Tibial cancellous bone changes in patients with knee osteoarthritis. A short-term longitudinal study using Fractal Signature Analysis. Osteoarthritis Cartilage. 2005;13(6):463–70.
45. Burr DB, Radin EL. Microfractures and microcracks in subchondral bone: are they relevant to osteoarthrosis? Rheum Dis Clin N Am. 2003;29(4):675–85.
46. Burr DB. Anatomy and physiology of the mineralized tissues: role in the pathogenesis of osteoarthrosis. Osteoarthritis Cartilage. 2004;12 Suppl A: S20–30.
47. Milz S, Putz R. Quantitative morphology of the subchondral plate of the tibial plateau. J Anat. 1994;185(Pt 1):103–10.
48. Sharma AR, Jagga S, Lee SS, Nam JS. Interplay between cartilage and subchondral bone contributing to pathogenesis of osteoarthritis. Int J Mol Sci. 2013;14(10):19805–30.
49. Crane JL, Cao X. Bone marrow mesenchymal stem cells and TGF-beta signaling in bone remodeling. J Clin Invest. 2014;124(2):466–72.
50. Zhen G, Wen C, Jia X, Li Y, Crane JL, Mears SC, et al. Inhibition of TGF-beta signaling in mesenchymal stem cells of subchondral bone attenuates osteoarthritis. Nat Med. 2013;19(6):704–12.
51. Davies-Tuck ML, Hanna F, Davis SR, Bell RJ, Davison SL, Wluka AE, et al. Total cholesterol and triglycerides are associated with the development of new bone marrow lesions in asymptomatic middle-aged women - a prospective cohort study. Arthritis Res Ther. 2009;11(6):R181.
52. Driban JB, Price L, Lo GH, Pang J, Hunter DJ, Miller E, et al. Evaluation of bone marrow lesion volume as a knee osteoarthritis biomarker–longitudinal relationships with pain and structural changes: data from the Osteoarthritis Initiative. Arthritis Res Ther. 2013;15(5):R112.

Chapter 3

Bone Matrix Microdamage and Vascular Changes Characterize Bone Marrow Lesions in the Subchondral Bone of Knee Osteoarthritis

Dzenita Muratovic, David Findlay Flavia Cicuttini, Anita Wluka, Yea-Rin Lee, and Julia Kuliwaba.

Discipline of Orthopaedics and Trauma, The University of Adelaide, Adelaide, Australia.
Department of Epidemiology & Preventive Medicine, Monash University, Melbourne, Australia.

Bone 2018

Statement of Authorship

Title of Paper	**Bone Matrix Microdamage and Vascular Changes Characterize Bone Marrow Lesions in the Subchondral Bone of Knee Osteoarthritis**
Publication Status	Published
Publication Details	Muratovic et al. BONE (2018) DOI: 10.1016/j.bone.2018.01.012

Principal Author

Name of Principal Author (Candidate)	Dzenita Muratovic		
Contribution to the Paper	Designed the study, performed the experiments and analysis of the results, interpreted the data, wrote the manuscript and acted as corresponding author.		
Certification:	This paper reports on original research I conducted during the period of my Higher Degree by Research candidature and is not subject to any obligations or contractual agreements with a third party that would constrain its inclusion in this thesis. I am the primary author of this paper.		
Signature		Date	17/10/2017

Co-Author Contributions

By signing the Statement of Authorship, each author certifies that:

i. the candidate's stated contribution to the publication is accurate (as detailed above);

ii. permission is granted for the candidate in include the publication in the thesis; and the sum of all co-author contributions is equal to 100% less the candidate's stated contribution.

Name of Co-Author	Prof David Findlay		
Contribution to the Paper	Designed the study, interpreted the data, provided overall supervision and wrote the manuscript.		
Signature		Date	17/10/2017

Name of Co-Author	A/Prof Anita Wluka		
Contribution to the Paper	Designed the study, interpreted the data, provided overall supervision and wrote the manuscript.		
Signature		Date	17/10/2017

Name of Co-Author	Prof Flavia		
Contribution to the Paper	Designed the study, interpreted the data, provided overall supervision and wrote the manuscript.		
Signature		Date	17/10/2017

Name of Co-Author	Yea Rin Lee		
Contribution to the Paper	Contributed to collection of specimens from patients, performed the experiments and critically revised the manuscript.		
Signature		Date	17/10/2017

Name of Co-Author	Dr Julia Kuliwaba		
Contribution to the Paper	Designed the study, interpreted the data, provided overall supervision and wrote the manuscript.		
Signature		Date	17/10/2017

Bone 108 (2018) 193–201

Contents lists available at ScienceDirect

Bone

journal homepage: www.elsevier.com/locate/bone

Full Length Article

Bone matrix microdamage and vascular changes characterize bone marrow lesions in the subchondral bone of knee osteoarthritis

Dzenita Muratovic [a,b,*], David M. Findlay [a], Flavia M. Cicuttini [c], Anita E. Wluka [c], Yea-Rin Lee [a,b], Julia S. Kuliwaba [a,b]

[a] Discipline of Orthopaedics and Trauma, The University of Adelaide, Adelaide, Australia
[b] Bone and Joint Research Laboratory, SA Pathology, Adelaide, Australia
[c] Department of Epidemiology and Preventive Medicine, Monash University, Melbourne, Australia

ARTICLE INFO

Article history:
Received 3 August 2017
Revised 6 December 2017
Accepted 9 January 2018
Available online 10 January 2018

Keywords:
Bone marrow lesions
knee osteoarthritis
subchondral bone
vascular
microdamage
osteocytes

ABSTRACT

Introduction: Bone marrow lesions (BMLs) in the subchondral bone in osteoarthritis (OA) are suggested to be multifactorial, although the pathogenic mechanisms are unknown. Bone metabolism and cardiovascular risk factors associate with BML in epidemiologic studies. However, there are no studies at the tissue level investigating the relationship between these processes and BML. The aim of this study was to investigate the relationship between BMLs in the tibial plateau (TP) of knee OA and bone matrix microdamage, osteocyte density and vascular changes.

Methods: TP were obtained from 73 patients at total knee replacement surgery and BMLs were identified ex vivo in TP tissue using MRI. Comparator 'No BML' tissue was from matched anatomical sites to the BMLs. Quantitative assessment was made of subchondral bone microdamage, bone resorption indices, osteocyte cellularity, and vascular features.

Results: Several key parameters were different between BML and No BML tissue. These included increased microcrack burden ($p = .01$, $p = .0001$), which associated positively with bone resorption and negatively with cartilage volume, and greater osteocyte numerical density ($p = .02$, $p = .01$), in the subchondral bone plate and subchondral trabeculae, respectively. The marrow tissue within BML zones contained increased arteriolar density ($p = .04$, $p = .0006$), and altered vascular characteristics, in particular increased wall thickness ($p = .007$) and wall:lumen ratio (wall thickness over internal lumen area) ($p = .001$), compared with No BML bone.

Conclusions: Increased bone matrix microdamage and altered vasculature in the subchondral bone of BMLs is consistent with overloading and vascular contributions to the formation of these lesions. Given the important role of BMLs in knee OA, these contributing factors offer potential targets for the treatment and prevention of knee OA.

1. Introduction

Bone marrow lesions (BMLs), identified by MRI, are frequently found in the subchondral bone (SCB) in knee osteoarthritis (KOA). They associate strongly with knee pain [2–4], structural degeneration of the articular cartilage, and predict progression to joint replacement [5]. In animal models of OA, BMLs precede cartilage degeneration, thus providing an early indication of OA [6, 7]. In humans, when found in early OA, they predict regional cartilage loss [8].

Evidence suggests that BML are multifactorial, being affected by metabolic bone factors and cardiovascular risk factors. Understanding of the pathological processes underway in BML, and how these relate to their risk factors is poor. Recently, we reported that the subchondral bone within BML zone has specific bone changes: thicker subchondral plate, increased trabecular bone volume and more trabeculae that are

Abbreviations: KOA, knee osteoarthritis; OA, osteoarthritis; OCU, osteochondral unit; SCB, subchondral bone; BMLs, bone marrow lesions; OARSI grade, Osteoarthritis Research Society International; MRI, magnetic resonance imaging; TP, tibial plateau; BMI, body mass index; K&L grade, Kellgren and Lawrence; PDFS, proton density fat suppressed weighted sequences; H&E, hematoxylin and eosin; DD.Ar, diffuse damage density area; DD.Dn, diffuse damage density; Cr.S.Dn, linear microcrack surface density; Cr.Dn, linear microcrack density; Cr.Le, average linear microcrack length; ES.S.Dn, eroded surface density; ES.Le, average eroded surface length; ES.Dn, eroded density; TL.Dn, total lacunar density; Ot.Dn, osteocyte density; EL.Dn, empty lacunar density; EL/TL, percent of empty lacunae.

* Corresponding author at: Discipline of Orthopaedics and Trauma, Level 7, Adelaide Health & Medical Sciences Building, Corner North Terrace & George Street, Adelaide, South Australia 5000, Australia

E-mail addresses: dzenita.muratovic@adelaide.edu.au (D. Muratovic), david.findlay@adelaide.edu.au (D.M. Findlay), flavia.cicuttini@monash.edu (F.M. Cicuttini), anita.wluka@monash.edu (A.E. Wluka), olivia.lee@sa.gov.au (Y.-R. Lee), julia.kuliwaba@adelaide.edu.au (J.S. Kuliwaba).

https://doi.org/10.1016/j.bone.2018.01.012

predominantly plate-like, compared with non-BML regions [9]. Previously, it was found that BMLs represent zones of altered bone mineralization and active remodeling [10]. There is some evidence that patients with KOA and BML respond to bone targeting therapy, such as bisphosphonates and strontium ranelate with a reduction in size of BMLs, reduced pain and cartilage loss, and delayed need for total knee replacement [11, 12].

Also, it has been suggested that changes in the rate of bone remodeling in OA subchondral bone might be a response to an accumulation of microdamage. To our knowledge, the microdamage burden in human KOA has not been reported, and potential relationships between the accumulation of microdamage in BMLs and other disease features have not been explored. Osteocytes have been shown to have essential roles in the repair of microdamage [13] and altered morphology and viability of osteocytes in sclerotic regions of the SCB in OA has been reported [14] However, osteocyte number and viability in relation to the progression of OA and BML presence, have not been investigated.

Vascular changes are common in OA and have been suggested as a possible factor leading to the initiation and/or progression of the disease [15]. BMLs have been identified as areas of reduced vascular perfusion in humans [16]. However, examination of the vasculature within BMLs is incomplete.

The aim of this study was therefore to examine the relationship between BMLs in the tibial plateau of knee OA and bone matrix microdamage, and osteocyte and vascular parameters.

2. Methods

2.1. Patient samples

Seventy-three patients were included in the study, of whom 40 (55%) were females, aged 48 to 86 years, and 33 (45%) were males, aged 49 to 87 years, who all underwent knee arthroplasty surgery. Eleven patients had bilateral arthroplasty, thus a total of 84 tibial plateaus (TP) were collected over an 18-month period. Informed written consent was obtained from all patients and the study received prior approval from the Human Research Ethics Committee at the Repatriation General Hospital, the Royal Adelaide Hospital and The University of Adelaide, South Australia, in accordance with the Declaration of Helsinki 1975. Inclusion criteria were: radiographic OA with severe symptomatic disabilities, such as severe pain and limited mobility. Exclusion criteria were: secondary OA of the knee due to trauma, rheumatoid arthritis, osteoporosis and/or evidence of bone-related chronic debilitating disease. For each patient, clinical data of age, sex and body mass index (BMI) were recorded. BMI was calculated from height and weight information, using the formula weight (kg) divided by the square of height (m).

2.2. Radiographic assessment

Standing antero-posterior, postero-anterior and lateral view radiographs were taken prior to surgery. The extent of radiographic progression was assessed according to the Kellgren and Lawrence (K&L) grade, the current standard radiologic grading system for OA. All radiographs were scored by two experienced assessors (AW and YW) with 5% disagreement. Assessors were blinded for the presence of BMLs in the knee joint.

2.3. MRI assessment

To identify BMLs in TP specimens, each TP was MR imaged ex vivo in an 8-channel wrist coil (3T MRI Siemens TRIO, Royal Adelaide Hospital, Adelaide), using two specific sequences: fat-suppressed (FS) fast spin-echo proton density-weighted (PDFS) and T1 weighted spin echo in the sagittal and coronal plane. Sagittal slice thickness was 1.6 mm with distance factor of 25%. Coronal slice thickness was 1.6 mm with 10% distance factor. A BML was defined as an area of altered signal intensity in the bone and marrow on PDFS and/or T1 weighted sequences (Fig. 1A). The definition and location of BML were by mutual agreement between two investigators (AW and YW) with musculoskeletal MRI expertise. MRI images were used to obtain cartilage and BML volume by two researchers (DzM and YRL), who were blinded to the BML status. The cartilage volume of the medial and/or lateral tibial compartments was measured by manually drawing a contour around the cartilage boundary over 12 consecutive slices in T1 weighted sagittal images [19]. After identification of a BML, the external contour of the BML was marked in both planes. An automatic volume rendering function from OsiriX software (Pixmeo-SARL, Switzerland) was used to calculate the value of cartilage and BML volume in cm^3. The coefficient of variation for the measurement of cartilage volume was 2.2% and 2.4% for BML volume.

2.4. Histological sample collection and processing

For a subset of 54 TPs (40 BML and 14 No BML), a cuboidal block of cartilage-subchondral bone (10 × 10 × 10 mm), containing the BML (BML samples), was dissected using a low-speed diamond wheel saw (Model 660, South Bay Technology). 85% of BML were found in the anterior aspect of the medial compartment in TP Fig. 1A & B. Thus, to match the BML samples, the same size and shape (i.e. cuboidal) block of tissue was cut from the anterior medial compartment of TP from the subjects undergoing knee arthroplasty surgery having no MRI evidence of BMLs ('No BML' samples). Each cartilage-subchondral bone tissue block was divided equally, by a sagittal plane cut, with one half formalin-fixed, *en bloc* stained in basic fuchsin, embedded in methylmethacrylate resin and cut into 70 μm thick sections (Leica SP1600, Nussloch, Germany) for assessment of microdamage accumulation. The other half of the block was formalin-fixed, decalcified in 5% hydrochloric acid, paraffin-embedded, sectioned 5 μm thick and stained with: hematoxylin and eosin (H&E) for assessment of arteriolar density, Miller's elastic stain to identify and assess the integrity of elastic lamina in arteriolar walls, and Safranin-O/Fast Green for assessment of Osteoarthritis Research Society International (OARSI) grade. For a subset of 30 TPs (22 BML and 8 No BML), tissue blocks were formalin-fixed and then slowly decalcified in 10% ethylenediaminetetraacetic acid to preserve nuclear integrity, paraffin-embedded, sectioned 5 μm thick and stained with H&E for a histomorphometric study of osteocyte-lacunar density.

2.5. Cartilage histological grading

OARSI grades ranged from 0 to 6.5, with 0 indicating healthy cartilage with no degradation and 6–6.5 indicating complete cartilage degradation with bone involvement [20], Fig. 1C. Grading was performed using an Olympus BX45 light microscope by three assessors (DM, EG and YRL), blinded to BML status of the samples and with extensive experience in quantitative histopathology. The intra-class correlation coefficient (ICC) for inter-observer reproducibility was 0.82 (95% CI 0.80, 0.84).

2.6. Histoquantitative analysis of microdamage accumulation

Two distinct types of bone microdamage, linear microcracks and diffuse damage, and indices of bone resorption (Fig. 2A–C), classified as we have described previously [21], were quantified for both the subchondral bone plate and subchondral trabeculae. To avoid damage artifact due to sample collection, processing and sectioning, only microdamage >1 mm from the edge of the sample was measured. The quantitation of microdamage was performed in duplicate sections by two assessors (DM and YRL), who were blinded to BML status and with extensive experience in hard tissue histopathology. The ICC for inter-observer reproducibility was 0.85 (95% CI 0.82, 0.86).

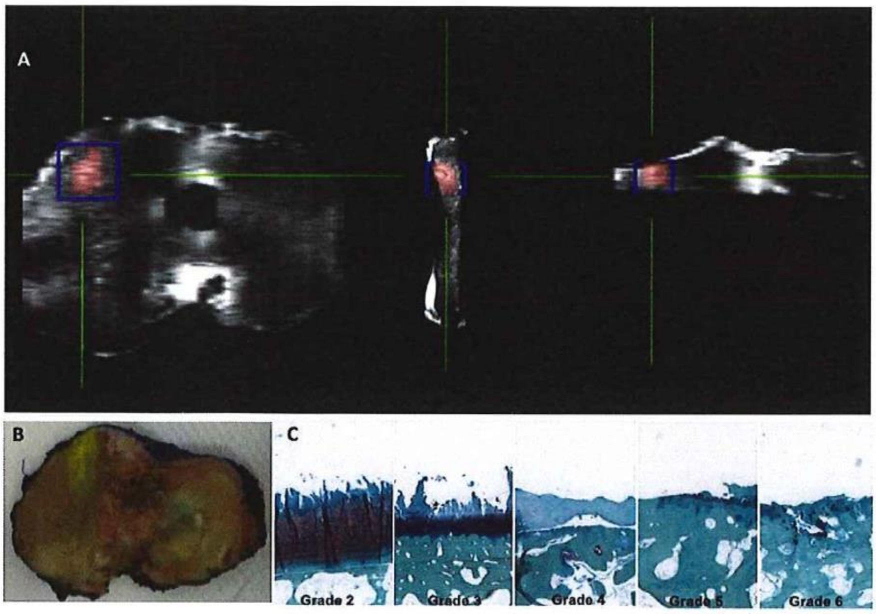

Fig. 1. A) Upper panel shows a tibial plateau with a bone marrow lesion (BML) detected by MRI, shaded pink in transaxial (left), sagittal (centre) and coronal (right) planes. The purple square shape represents a cuboidal block of cartilage-subchondral bone (10x10mm), containing a BML. Lower left, B) panel shows a tibial plateau with a region containing a BML marked in yellow to aid tissue dissection using a low-speed diamond wheel saw. C) Representative images of OARSI histological grades (from 2 to 6) seen in BML samples.

2.7. Histoquantitative analysis of osteocyte density

Two H&E sections per case were used to determine osteocyte density by counting cells and lacunar numbers, using the Quantimet 550 IW Image Analyser (Leica DM 6000B, Cambridge, UK) at 20× objective magnification. The quantitation of osteocyte and lacunar densities was performed by one assessor (DM), who was blinded to BML status and repeated the assessment in duplicate sections. The ICC for intra-observer reproducibility was 0.92 (95% CI 0.90, 0.94).

2.8. Vascular assessment

Duplicate sections per case were used for quantitative assessment of blood vessels and performed separately in the subchondral bone plate

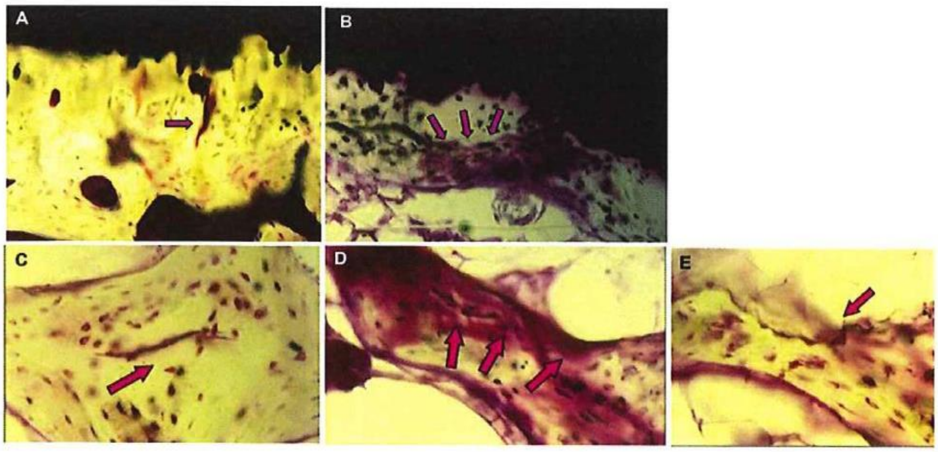

Fig. 2. Microdamage morphological features identified in undecalcified subchondral bone stained by basic fuchsin (objective magnification ×20). A) linear microcrack in subchondral plate, B) diffuse damage in subchondral plate, C) linear microcrack in subchondral trabeculae, D) diffuse damage in subchondral trabeculae, E) eroded surface on subchondral trabeculae.

and in the bone marrow between subchondral trabeculae. In the subchondral plate, the number and length of vascular channels was quantified. The vascular channels were defined as cylindrical cavities larger than 40 μm in diameter containing capillaries and/or thin-walled vessels with endothelial cell membrane. As the subchondral plate lies between the articular cartilage and the bone marrow, quantification was performed separately for the zone of the subchondral plate close to the cartilage (named zone 1) and zone of the subchondral plate close to the bone marrow (named zone 2), (Fig. 3A). Subchondral plate thickness for each sample was >800 μm thick. To ensure that the two zones did not overlap each other, zone 1 was defined as the area of the subchondral plate starting from the tidemark and extending 350 μm downwards into the depth of the subchondral plate (Fig. 3A). Zone 2 was defined as the area of the subchondral plate, starting from the bone marrow and extending 350 μm upwards toward the tidemark (Fig. 3A). Vascular channels were considered to be present in a zone if at least two thirds of the channel were seen in that zone. In addition, the density of vascular channels, expressed as the number of vascular channels penetrating the tidemark per 1 mm, and the proportion of vascular channels penetrating tidemark over total number of vascular channels in zone 1, were reported separately. In bone marrow, between the subchondral trabeculae, arteriolar density (number/cm^2), average arteriolar wall thickness (μm), arteriolar lumen diameter (μm) and ratio of wall thickness over internal lumen area were quantified (Fig. 3B & C), since these vessels are likely important determinants of subchondral blood flow. The integrity of the elastic lamina was observed qualitatively (Fig. 3D), since its changes can lead to atherosclerosis. To ensure visibility of all histological features in the arteriolar wall, only arterioles >70 μm in lumen diameter were studied. The quantitation of vascular densities was performed on duplicate sections by one assessor (DM), who was blinded to BML status. The ICC for intra-observer reproducibility was (ICC 0.98 (95% CI 0.95)).

2.9. Statistical analysis

The histomorphometric data were both normally and non-normally distributed (Shapiro–Wilk). To identify group differences, the unpaired Student's t-test was performed if the data were normally distributed; if the data were non-normally distributed, the Mann–Whitney U test was performed instead. Parametric data are expressed as the mean ± standard deviation, and non-parametric data as the median (25th, 75th quartiles). The critical value for statistical significance was chosen as $p < .05$. The analyses were performed using the GraphPad Prism software (GraphPad Software, Inc., USA).

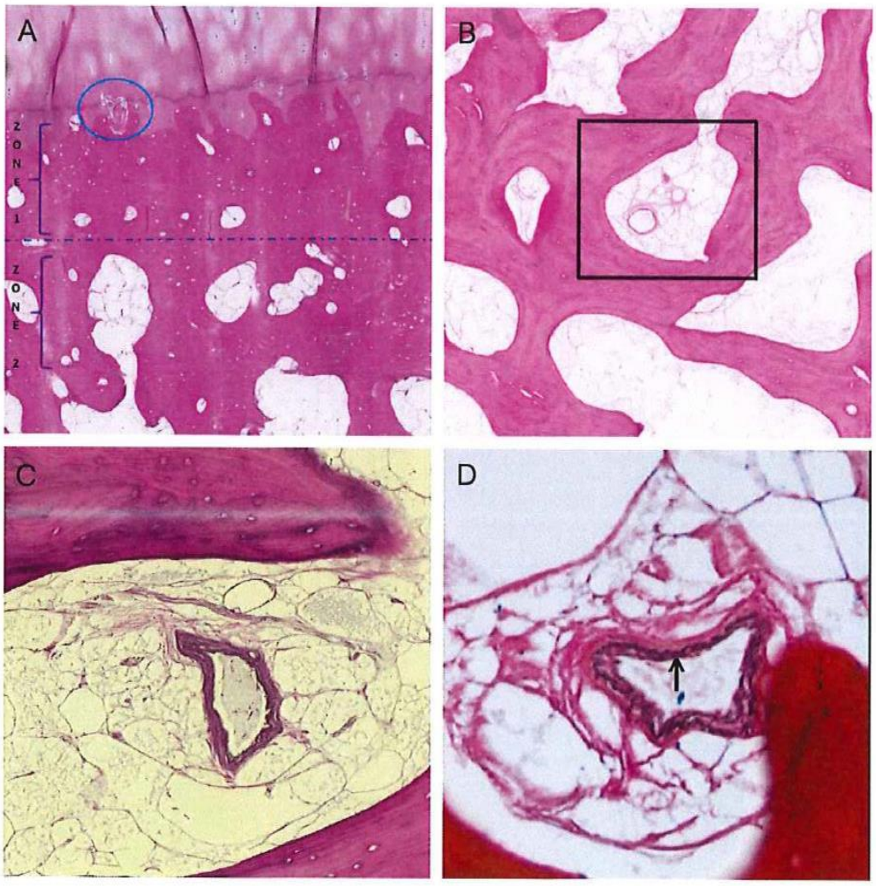

Fig. 3. A) The subchondral bone plate was divided into 2 zones: zone 1- from tidemark 350 μm downwards into the depth of the subchondral plate, zone 2- from bone marrow 350 μm upwards toward tidemark. The blue circle indicates a vascular channel penetrating the tidemark. B) In bone marrow between the subchondral trabeculae, indicated by a black square, quantitative and qualitative study of arterioles was performed. C) H&E staining of arterioles was used to measure wall thickness, lumen size and lumen ratio (wall thickness over internal lumen area). D) Miller's elastic stain was used to demonstrate integrity of elastic lamina (black arrow).

Using a Two-Sample *t*-Test for Mean Difference, the power of the study was calculated, using mean and standard deviation in No BML and BML groups for the clinical outcome cartilage volume. 90% of the sample size of 84 (No BML = 0.9 ∗ 22 = 19, BML = 0.9 ∗ 62 = 55) was considered to be the effective sample size due to correlation of outcome within patient (some patients had two TPs tested due to bilateral knee arthroplasty). Therefore, for a sample size of 74 (No BML = 19, BML = 55), mean clinical difference = 0.3 and standard deviation = 0.3 the power to detect that clinical difference is 96.0%. For the sample size of 54 (No BML = 14, BML = 40), the 90% effective sample size of 48 (No BML = 12, BML = 36) with mean clinical difference = 0.3 and standard deviation = 0.3 has 83.6% power to detect that clinical difference. For the sample size of 30 (No BML = 8, BML = 22), the 90% effective sample size of 26 (No BML = 7, BML = 19) with mean clinical difference = 0.3 and standard deviation = 0.3 has 58.3% power to detect that clinical difference.

Both adjusting for clustering on subject (multiple regions of interest and two possible sides) and controlling for the confounders age, sex and BMI were performed in the linear mixed-effects models. Linear mixed-effects models were also used to investigate the association between cartilage volume vs. microdamage, OARSI grade vs. microdamage and erosion surface vs. microdamage. As all data were non-normally distributed (Shapiro–Wilk), the Spearman rank for correlation was used. These analyses were performed using statistical software SAS 9.4 (SAS Institute Inc., Cary, NC, USA).

3. Results

3.1. Population characteristics

A total of 84 TP from 73 subjects were included in the analysis (11 patients had bilateral surgery). The groups were organized based on the presence or absence of a tibial BML, and no significant difference between groups was found in the patient age or gender. Demographic characteristics of the participating individuals (74), are summarized in Table 1.

3.2. Radiographic assessment

No significant difference in the K&L grade between the BML and No BML group was found.

3.3. MRI assessment

MRI assessment indicated that out of 84 TP samples, 62 (74%) contained a BML detected by one or both MRI sequences. Loss of cartilage volume was significantly higher in TP with a BML compared to TP with No BML ($p = .01$) (Table 1). The BML volume ranged from 0.1 to 2.4 mm^3, with an average BML volume of 0.52 mm^3.

Table 1
Patient data.

	No BML (n = 22)[c]	BML (n = 62)[d]	p value
Age (years)[a]	77 ± 6.3	68.7 ± 9.3	.3
Male [n (%)]	5 (28%)	28 (51%)	.08
Female [n (%)]	13 (72%)	27 (49%)	.08
BMI[a]	31.3 ± 6.4	33.4 ± 5.1	**.01**
K&L grade[b]	2 (1–4)	3 (2–4)	.7
Cartilage volume (mm^3)[a]	1.3 ± 0.2	1.0 ± 0.3	**.01**
BML volume (mm^3)	NA	0.5 (0.1–0.6)	NA
OARSI grade (0–6.5)[a]	3.7 ± 1.3	4.7 ± 1.0	**.03**

Abbreviations: BMI - body mass index, K&L - Kellgren and Lawrence, OARSI grade - Osteoarthritis Research Society International (OARSI) grade.
[a] Values presented as mean ± standard deviation.
[b] Values presented as median (25th, 75th percentiles).
[c] Four patients from No BML group had bilateral total knee replacement.
[d] Seven patients in BML group had bilateral total knee replacement.

3.4. Cartilage histological grading

TP with No BML had moderate histological changes, OARSI grades ranged from 2 to 5. In contrast, TP with BML had more severe histological changes and OARSI grades ranging from 3 to 6.5, ($p = .03$ for BML vs. No BML).

3.5. Histoquantitative analysis of microdamage accumulation

The histoquantitative analyses of microdamage and resorption are listed in Table 2. Microdamage levels were found to be very low in No BML subchondral bone [1 out of 14 samples (7%)]. BML SCB tissue contained widely variant amounts of microdamage [21 out of 40 samples (52%)], which was considerable in some samples, with linear microcracks predominating. There was an increased burden of linear microcracks (Cr.Dn) in both the subchondral bone plate ($p = .01$) and subchondral trabeculae ($p = .0001$) of BML regions, compared to No BML regions. Moreover, in the subchondral plate of BML regions, we found evidence of increased bone resorption, with a greater eroded surface density (ES.S.Dn) ($p = .02$), eroded density (ES.Dn) ($p = .04$) and eroded surface length (ES.Le) ($p = .04$) compared to No BML, where none of the 14 samples had evidence of bone resorption. It was also notable that BML samples contained microdamage and bone erosion in both the subchondral plate and trabeculae. In No BML samples, evidence of bone erosion was seen only in subchondral trabeculae.

3.5.1. Correlations between microdamage density, cartilage volume and OARSI grade

In the BML group we identified an association between the accumulation of microdamage and degenerative changes in the cartilage (loss of cartilage volume and histological evidence of cellular integrity loss). Specifically, in the BML group, we found a negative correlation between diffuse damage density (DD.Dn) and OARSI grade in trabecular bone ($r = -0.47$, $p = .01$) and a negative correlation between Cr.Dn and cartilage volume in both the subchondral plate and subchondral trabeculae ($r = -0.40$, $p = .03$ and $r = -0.42$, $p = .02$, respectively). Also for BML, in both subchondral plate and trabeculae, a positive association was found between Cr.Dn and ES.S.Dn ($r = 0.41$, $p = .04$ and $r = 0.34$, $p = .04$, respectively), and between DD.Dn and ES.S.Dn ($r = 0.42$, $p = .01$ and $r = 0.61$, $p = .0003$, respectively). No other significant correlations were

Table 2
Histoquantitative analysis of bone microdamage accumulation and eroded surface.

	No BML (n = 14)	BML (n = 40)	p value
Subchondral bone plate			
DD.Ar (μm²)	1.26[a]	0 (0–1.35)	.3
DD.Dn (#/mm²)	0.62[a]	0 (0–0.75)	.3
Cr.S.Dn (μm/mm²)	160.9[a]	0 (0–246.5)	**.05**
Cr.Dn (#/mm²)	0.3[a]	0 (0–0.9)	**.01**
Cr.Le (μm)	50.1[a]	53.3 (45.1–63.3)	.8
ES.S.Dn (μm/mm²)	0	0 (0–200.9)	**.02**
ES.Le (μm)	0	0 (0–397.9)	**.04**
ES.Dn (#/mm²)	0	0 (0–0.94)	**.04**
Subchondral bone trabeculae			
DD.Ar (μm²)	0 (0–0.008)	0 (0–0.05)	.2
DD.Dn (#/mm²	0 (0–0.15)	0.08 (0–0.89)	**.05**
Cr.S.Dn (μm/mm²)	950.1[a]	315.7 (0–1842)	**.001**
Cr.Dn (#/mm²)	0.08[a]	0.1 (0–0.8)	**.0001**
Cr.Le (μm)	86.3 (84–88.5)	76.5 (30.3–131.9)	.7
ES.S.Dn (μm/mm²)	0 (0–46.9)	11.9 (0–194.6)	.3
ES.Le (μm)	149 (74–172.9)	110 (70.7–186.7)	.3
ES.Dn (#/mm²)[b]	0 (0–0.19)	0 (0–0.22)	.2

Abbreviations: DD.Ar diffuse damage density area (μm²), DD.Dn diffuse damage density (#/mm²), Cr.S.Dn linear microcrack surface density (μm/mm²), Cr.Dn linear microcrack density (#/mm²), Cr.Le average linear microcrack length, ES.S.Dn eroded surface density (μm/mm²), ES.Le (μm) average eroded surface length, ES.Dn eroded density (#/mm²). Values are presented as median (lower-upper level).
[a] Detected only in one case.

observed between microdamage, osteocyte or vascular parameters for BML or No BML bone.

3.6. Histoquantitative analysis of osteocyte density

The osteocyte and lacunar parameter data are presented in Table 3. Osteocyte cell density (Ot.Dn) was significantly higher in BML compared to No BML regions of the subchondral plate. In subchondral trabeculae, both total lacunar density (TL.Dn) and Ot.Dn were increased in BML compared to No BML.

3.7. Vascular assessment

Significant differences were observed in vascularity between BML and No BML SCB tissue; these are summarized in Table 4. Here we report that in osteochondral zones containing a BML, zone 1 of the subchondral bone plate (closer to calcified cartilage) had a greater density of vascular channels (p = .04), compared to No BML; while in zone 2 (closer to marrow) we found increased length of vascular channels (p = .001) compared to No BML. The density of vascular channels penetrating the tidemark (expressed per 1 mm of tidemark) was significantly higher in the BML group compared to the No BML group (p = .04). In addition, the proportion of vascular channels penetrating the tidemark, compared to the total number of vascular channels in zone 1, was significantly higher in the BML group compared to the No BML group (p = .04).

In trabecular bone marrow within BML areas, we found significantly increased thick-walled arteriolar density (p = .0006), with significant changes in arteriolar wall architecture, which included thickening in the smooth muscle layer of the tunica media (p = .007), and increased wall/lm ratio (wall thickness over internal lumen area) (p = .001), when compared to No BML areas. There were no significant differences in diameter of arteriolar lumen between groups and there was no change in the integrity of the elastic lamina observed.

Table 4
Histoquantitative vascular assessment.

Subchondral bone plate	No BML (n = 14)	BML (n = 40)	p value
Zone 1			
Vas. channel density (#/cm^2)	8 (5–10)	12 (8–18)	**.04**
Length of vas. channels (μm)[b]	85.7 (72.0–104).	118.2 (70.4–54.3)	.2
Vas. channel penetrating TM density (#/mm)	0.12 (±0.07)	0.20 (0.1)	**.04**
No. vas. channels penetrating TM/total vas. channels in zone (%)	19.5 (11–25)	34 (16.2–42)	**.04**
Zone 2			
Vas. channel density (#/cm^2)[b]	6 (0–13)	10 (4–16)	.2
Length of vas. channels (μm)[a]	68.7 ± 59.8	150 ± 59.8	**.001**
Trabecular bone marrow			
Arteriolar density (#/cm^2)[b]	7 (6–18)	34 (22–81)	**.0006**
Arteriolar wall thickness (μm)[a]	6.8 ± 2.4	10.8 ± 3.4	**.007**
Arteriolar lumen diameter (μm)[a]	163.5 ± 73.4	155.5 ± 7.8	.7
Lumen ratio[b,c]	0.04 (0.03–0.04)	0.07 (0.05–0.1)	**.001**

Zone 1, zone from tidemark 350 μm downwards into the depth of subchondral plate. Zone 2, from bone marrow 350 μm upwards into subchondral plate.
[a] Values presented as mean ± standard deviation.
[b] Values presented as median (25th, 75th percentiles).
[c] Wall thickness over internal lumen area.

4. Discussion

The current study provides the first evidence of increased bone matrix microdamage in regions defined as BMLs in the tibial plateau of KOA subjects, compared with anatomically corresponding non-BML zones of the TP. We also observed greater osteocyte numbers, increased arteriolar density and altered vascular characteristics, in particular increased wall thickness and wall:lumen ratio, in regions within BMLs compared to no BML regions, suggesting a vascular contribution to BMLs.

Previous histological studies exploring BMLs described changes in the bone marrow, with zones of fatty marrow, necrosis, oedema and bone marrow fibrosis [22, 23]. In our recent study, we reported that the subchondral bone within BMLs typically has a thicker subchondral plate, increased trabecular bone volume and more trabeculae that are predominantly plate-like in structure [9]. Hunter et al. reported BMLs as areas of altered bone mineralization and active remodeling [10]. Taljanovic et al. reported earlier the presence of micro-fractures within BMLs in histological sections of hip OA [24]. Micro-fractures can only be seen when they begin to heal with a structure analogous to a fracture callus. We focused on linear microcracks and diffuse damage, which represent fatigue damage in the bone matrix due to repeat mechanical over-loading [25].

In this study, an increased density of microdamage was seen in both the subchondral plate and trabeculae of BMLs, suggesting that both compartments are exposed to mechanical loading at damage-inducing levels. However, we found that the subchondral plate corresponding to BML zones contained predominantly linear cracks, which are known to associate with compressive loading [26–28], while diffuse microdamage, associated with tensile loading [26, 29, 30], was also seen in the subchondral trabeculae. Interestingly, we found relatively small (<100 μm) average crack lengths in both the subchondral plate and trabeculae. This is possibly explained by previous reports that BMLs are characterized by a hypo-mineralized bone [10], where the microstructure of the matrix may minimize formation of longer cracks.

The majority of BMLs were located in the anterior aspect of the medial tibial compartment, known to be a region of high contact pressure [9]. It is believed that BMLs occur at sites of maximal loading within the knee but the mechanism of their formation is not known. Moreover, the accumulation of microdamage in bone is generally accepted to be an indicator of repetitive loading, which exceeds the healing capacity of the bone tissue. There is also good evidence for a role of mechanical loading in the initiation and progression of KOA [31]. Thus, obesity has been widely accepted as a major risk factor for the initiation and progression of KOA [32]. However, only weak to moderate associations have been reported previously between obesity and the presence of BMLs [33, 34]. In our study, BMI ≥ 30 kg/m^2 as a measure of obesity, was present in both BML and No BML OA groups, suggesting that body weight per se might not be the key factor for BML presence and/or formation. However, loading of the knee joint is a function of walking gait and the way that the joint is loaded [35], together with the amount and frequency of loading. These data were not available for the current study.

Recent experiments in the mouse have produced data suggesting that changes in the SCB, which include BMLs, are causative of OA in that species [18, 36]. Specifically, the over-expression of transforming growth factor-β (TGFβ) in bone gave rise to spontaneous changes in

Table 3
Group mean values for osteocyte morphometric parameters.

	No BML (n = 8)	BML (n = 22)	p value
Subchondral bone plate			
TL.Dn (#/mm^2)	293.4 ± 51.1	338.0 ± 45.7	.07
Ot.Dn (#/mm^2)	80.4 ± 16.7	108.9 ± 28.2	**.02**
EL.Dn (#/mm^2)	212.8 ± 44.0	234.4 ± 35.1	.2
EL/TL (%)	72.3 ± 5.1	68.4 ± 8.4	.2
Subchondral bone trabeculae			
TL.Dn (#/mm^2)	222.8 ± 103.8	288.8 ± 47.6	**.006**
Ot.Dn (#/mm^2)	68.1 ± 34.2	99.9 ± 20.8	**.01**
EL.Dn (#/mm^2)	180.0 ± 42.0	188.8 ± 40.4	.6
EL/TL (%)	69.6 ± 4.9	65.1 ± 6.2	.1

Abbreviations: TL.Dn total lacunar density (#/mm^2), Ot.Dn osteocyte density (#/mm^2), EL.Dn empty lacunar density (#/mm^2) and EL/TL percent of empty lacunae (%). Values presented as mean ± standard deviation.

the SCB, accompanied by degradation of the overlying articular cartilage. Importantly, TGFβ neutralizing antibody treatment of surgically induced mouse models of OA protected against disease development. It is not clear what would be driving the aberrant expression of TGFβ in the mouse models or whether the mouse will be informative of human OA. However, sequestered TGFβ is released in active form by osteoclastic bone resorption [37] and elevated TGFβ has been reported in human OA bone [38]. This link between bone resorption/remodeling and TGFβ activation in bone may provide clues to the formation of BMLs, given the additional links between microdamage in bone and resorption [29, 39, 40]. Importantly, we found increased bone resorption in the subchondral plate of the BML group, as shown by the presence of erosion surfaces, compared to the subchondral plate of No BML, which showed little evidence of erosion. This suggests that the subchondral bone plate might undergo a higher rate of bone turnover, perhaps as an adaptation to repair damage. Furthermore, a positive correlation between microdamage accumulation and increased resorption in both the subchondral plate and trabeculae may indicate an active repair response in BMLs. However, further studies to investigate specifically osteoclast activity in subchondral bone of BML would be beneficial to confirm this association. Collectively, these results are consistent with BMLs forming in highly loaded bone, and suggest a sequence of events starting with the creation of microdamage, repair by osteoclastic resorption, release of growth factors such as TGFβ from the bone matrix, and finally new bone formation.

Osteocytes act as mechanosensors and are able to integrate the mechanical and biochemical signals that regulate osteoblastogenesis and osteoclastogenesis, and they have a primary role in regulating bone homeostasis [41]. Thus, osteocytes may have an important role in subchondral bone remodeling and mineral metabolism in OA pathogenesis [14]. It has also been shown that osteocytes are essential for repair of linear microcracks in a process that recruits osteoclasts to sites of damage, initiated by osteocyte apoptosis [42, 43]. Contrast to linear microcracks, Herman et al. showed in a rat model that diffuse damage did not cause osteocyte apoptosis or recruitment of osteoclasts but was repaired by an unknown osteocyte-mediated mechanism [39].

The majority of identified osteocyte lacunae (~70%) in both subchondral plate and trabeculae were empty in both groups. This finding is not surprising, as previously an increase of empty lacunae in both aged [44] and osteoarthritic bone [45] has been reported. However, the increased density of viable osteocytes found in BML areas compared to No BML is a novel finding. This might indicate that OA No BML and BML bone respond differently in the pathogenesis of the disease. Also, a higher osteocyte content has been observed in the more rapidly formed bone of Osteogenesis Imperfecta type V patients, in which the bone had a woven appearance, consistent with disturbed lamellation [46].

Previously, we found that BML bone from the same patient cohort is characterized by increased osteoid thickness and volume, which is indicative of new non-mineralized bone. Collectively, our data suggest that BML areas of bone correspond to localized areas of active repair response and remodeling. In this context, the dynamic nature of BMLs and their ability to resolve up to 50% over two years in asymptomatic populations [47] may be explained. Moreover, it is of interest that bisphosphonates, which act by inhibiting osteoclastic bone resorption and bone turnover, may decrease pain in OA, reduce BML size, and have a chondroprotective action [11, 12].

Seah et al. suggested that BMLs might arise due to altered fluid dynamics and perfusion in subchondral bone, resulting in intraosseous hypertension, ischemia, bone necrosis, and cartilage breakdown [48]. Lee et al. supported those theories by finding significantly lower blood perfusion in BML areas compared to normal bone [49]. Consistent with a vascular link with OA initiation and/or progression, as suggested previously [15], our study found vascular structure abnormalities in BMLs. We have already reported the unique presence of fibrovascular cystic structures in BMLs [9]. We have extended these findings to report here thickening of the arteriolar smooth muscle layer and increased wall:lumen ratio in vessels within BMLs. These changes could be associated with arteriolosclerosis, and there are population data suggesting links between, and common mechanisms for, cardiovascular disease and OA [15]. Importantly, structural changes of the arteriolar wall can lead to vasoconstriction and ischemic events in tissues [15], which subsequently result in tissue vulnerability and reduced repair ability. Also, it has been reported that TGFβ can regulate blood vessels in OA bone. In the mouse model of OA produced by over-expression of active TGFβ described above, increased angiogenesis and vascular changes were prominent [18]. A four-fold increase in angiogenesis markers was reported in BMLs in hip OA [50]. Most recently, a gene expression study reported increased vascular proliferation within BML zones, accompanied by genes in the angiogenic pathway being amongst the most upregulated genes in BMLs [51]. Our data add to the proposal that pathological changes of the microvasculature contribute to the formation of BMLs in KOA [15, 52, 53].

A limitation of this study is that our examination of end stage disease does not allow determination of cause and effect. In addition, data on patient activity type and amount, osteoclast–osteoblast activity, and immunohistochemical detection of small caliber vascular profiles were not available. Furthermore, our comparisons were between BMLs and No BML bone and therefore do not allow comparison with healthy SCB. However, our results are consistent with the notion that overloading-induced microdamage and vascular changes contribute to the formation of BMLs.

In conclusion, our data suggest that change in subchondral bone is intimately involved in the progression of OA. The accumulation of microdamage in BMLs supports the notion that excessive and biomechanically unfavorable loading contributes to the occurrence of BMLs in tibial SCB tissue. Since these factors are modifiable, our findings suggest that an early focus on reducing joint loading, and using BML as an outcome measure, might provide effective intervention for OA progression and might aid the development of more individualized OA treatments.

Acknowledgements

The authors wish to thank Ms. Sue Collins and Ms. Emma Giersch (EG) for technical assistance, Dr. Jamie Taylor and Dr. Yuan-Yuan Wang (YW) for assistance and advice on measurement and interpretation of the radiographic and MRI data, and Dr. Graham Mercer, Dr. Chris Wilson, and Dr. Dai Morgan for providing TP specimens. The authors wish to acknowledge support from Adelaide Microscopy at The University of Adelaide, Anatomical Pathology at SA Pathology, and the Department of Radiology, Royal Adelaide Hospital.

Authors contributions

All authors meet the criteria for authorship. DM designed the study, performed the experiments and analysis of the results, interpreted the data and wrote the manuscript. DF, FC, AW, and JK designed the study, interpreted the data, provided overall supervision and wrote the manuscript. YL contributed to the collection of specimens from patients, performed the experiments and critically revised the manuscript. All authors read and approved the manuscript.

The authors declare no conflicts of interest.

Funding

The authors acknowledge funding from the National Health and Medical Research Council of Australia (NHMRC, Project Grant 1042482) and support from the Rebecca Cooper Foundation. DM is the recipient of an NHMRC postgraduate scholarship; AW is the recipient of an NHMRC Career Development Fellowship (Clinical level 2, 1063574).

Conflict of interest

None

References

[2] D.T. Felson, C.E. Chaisson, C.L. Hill, S.M. Totterman, M.E. Gale, K.M. Skinner, L. Kazis, D.R. Gale, The association of bone marrow lesions with pain in knee osteoarthritis, Ann. Intern. Med. 134 (2001) 541–549.

[3] D.T. Felson, J. Niu, A. Guermazi, F. Roemer, P. Aliabadi, M. Clancy, J. Torner, C.E. Lewis, M.C. Nevitt, Correlation of the development of knee pain with enlarging bone marrow lesions on magnetic resonance imaging, Arthritis Rheum. 56 (2007) 2986–2992.

[4] M.F. Sowers, C. Hayes, D. Jamadar, D. Capul, L. Lachance, M. Jannausch, G. Welch, Magnetic resonance-detected subchondral bone marrow and cartilage defect characteristics associated with pain and X-ray-defined knee osteoarthritis, Osteoarthr. Cartil. 11 (2003) 387–393.

[5] S.K. Tanamas, A.E. Wluka, J.P. Pelletier, J.M. Pelletier, F. Abram, P.A. Berry, Y. Wang, G. Jones, F.M. Cicuttini, Bone marrow lesions in people with knee osteoarthritis predict progression of disease and joint replacement: a longitudinal study, Rheumatology (Oxford) 49 (2010) 2413–2419.

[6] M. Libicher, M. Ivancic, M. Hoffmann, W. Wenz, Early changes in experimental osteoarthritis using the Pond-Nuki dog model: technical procedure and initial results of in vivo MR imaging, Eur. Radiol. 15 (2005) 390–394.

[7] J.L. Huebner, M.A. Hanes, B. Beekman, J.M. TeKoppele, V.B. Kraus, A comparative analysis of bone and cartilage metabolism in two strains of guinea-pig with varying degrees of naturally occurring osteoarthritis, Osteoarthr. Cartil. 10 (2002) 758–767.

[8] E.G. Meyer, T.G. Baumer, J.M. Slade, W.E. Smith, R.C. Haut, Tibiofemoral contact pressures and osteochondral microtrauma during anterior cruciate ligament rupture due to excessive compressive loading and internal torque of the human knee, Am. J. Sports Med. 36 (2008) 1966–1977.

[9] D. Muratovic, F. Cicuttini, A. Wluka, D. Findlay, Y. Wang, S. Otto, D. Taylor, J. Humphries, Y. Lee, A. Labrinidis, R. Williams, J. Kuliwaba, Bone marrow lesions detected by specific combination of MRI sequences are associated with severity of osteochondral degeneration, Arthritis Res. Ther. 18 (2015) 54.

[10] D.J. Hunter, L. Gerstenfeld, G. Bishop, A.D. Davis, Z.D. Mason, T.A. Einhorn, R.A. Maciewicz, P. Newham, M. Foster, S. Jackson, E.F. Morgan, Bone marrow lesions from osteoarthritis knees are characterized by sclerotic bone that is less well mineralized, Arthritis Res. Ther. 11 (2009) R11.

[11] L.L. Laslett, D.A. Dore, S.J. Quinn, P. Boon, E. Ryan, T.M. Winzenberg, G. Jones, Zoledronic acid reduces knee pain and bone marrow lesions over 1 year: a randomised controlled trial, Ann. Rheum. Dis. 71 (8) (2012) 1322.

[12] J.P. Pelletier, C. Roubille, J.P. Raynauld, F. Abram, M. Dorais, P. Delorme, J. Martel-Pelletier, Disease-modifying effect of strontium ranelate in a subset of patients from the Phase III knee osteoarthritis study SEKOIA using quantitative MRI: reduction in bone marrow lesions protects against cartilage loss, Ann. Rheum. Dis. 74 (2015) 422–429.

[13] O.D. Kennedy, D.M. Laudier, R.J. Majeska, H.B. Sun, M.B. Schaffler, Osteocyte apoptosis is required for production of osteoclastogenic signals following bone fatigue in vivo, Bone 64 (2014) 132–137.

[14] A. Jaiprakash, I. Prasadam, J.Q. Feng, Y. Liu, R. Crawford, Y. Xiao, Phenotypic characterization of osteoarthritic osteocytes from the sclerotic zones: a possible pathological role in subchondral bone sclerosis, Int. J. Biol. Sci. 8 (2012) 406–417.

[15] D.M. Findlay, Vascular pathology and osteoarthritis, Rheumatology (Oxford) 46 (2007) 1763–1768.

[16] R.K. Aaron, J.P. Dyke, D.M. Ciombor, D. Ballon, J. Lee, E. Jung, G.A. Tung, Perfusion abnormalities in subchondral bone associated with marrow edema, osteoarthritis, and avascular necrosis, Ann. N. Y. Acad. Sci. 1117 (2007) 124–137.

[18] G. Zhen, C. Wen, X. Jia, Y. Li, J.L. Crane, S.C. Mears, F.B. Askin, F.J. Frassica, W. Chang, J. Yao, J.A. Carrino, A. Cosgarea, D. Artemov, Q. Chen, Z. Zhao, X. Zhou, L. Riley, P. Sponseller, M. Wan, W.W. Lu, X. Cao, Inhibition of TGF-beta signaling in mesenchymal stem cells of subchondral bone attenuates osteoarthritis, Nat. Med. 19 (2013) 704–712.

[19] A.E. Wluka, Y. Wang, M. Davies-Tuck, D.R. English, G.G. Giles, F.M. Cicuttini, Bone marrow lesions predict progression of cartilage defects and loss of cartilage volume in healthy middle-aged adults without knee pain over 2 yrs, Rheumatology (Oxford) 47 (2008) 1392–1396.

[20] K.P. Pritzker, S. Gay, S.A. Jimenez, K. Ostergaard, J.P. Pelletier, P.A. Revell, D. Salter, W.B. van den Berg, Osteoarthritis cartilage histopathology: grading and staging, Osteoarthr. Cartil. 14 (2006) 13–29.

[21] N.L. Fazzalari, J.S. Kuliwaba, M.R. Forwood, Cancellous bone microdamage in the proximal femur: influence of age and osteoarthritis on damage morphology and regional distribution, Bone 31 (2002) 697–702.

[22] H. Leydet-Quilici, T. Le Corroller, C. Bouvier, R. Giorgi, J.N. Argenson, P. Champsaur, T. Pham, A. Maues de Paula, P. Lafforgue, Advanced hip osteoarthritis: magnetic resonance imaging aspects and histopathology correlations, Osteoarthr. Cartil. 18 (2010) 1429–1435.

[23] M. Zanetti, E. Bruder, J. Romero, J. Hodler, Bone marrow edema pattern in osteoarthritic knees: correlation between MR imaging and histologic findings, Radiology 215 (2000) 835–840.

[24] M.S. Taljanovic, A.R. Graham, J.B. Benjamin, A.F. Gmitro, E.A. Krupinski, S.A. Schwartz, T.B. Hunter, D.L. Resnick, Bone marrow edema pattern in advanced hip osteoarthritis: quantitative assessment with magnetic resonance imaging and correlation with clinical examination, radiographic findings, and histopathology, Skelet. Radiol. 37 (2008) 423–431.

[25] Z. Seref-Ferlengez, O.D. Kennedy, M.B. Schaffler, Bone microdamage, remodeling and bone fragility: how much damage is too much damage? Bonekey Rep. 4 (644) (2015).

[26] T. Diab, D. Vashishth, Effects of damage morphology on cortical bone fragility, Bone 37 (2005) 96–102.

[27] T. Diab, K.W. Condon, D.B. Burr, D. Vashishth, Age-related change in the damage morphology of human cortical bone and its role in bone fragility, Bone 38 (2006) 427–431.

[28] T.M. Boyce, D.P. Fyhrie, M.C. Glotkowski, E.L. Radin, M.B. Schaffler, Damage type and strain mode associations in human compact bone bending fatigue, J. Orthop. Res. 16 (1998) 322–329.

[29] Z. Seref-Ferlengez, J. Basta-Pljakic, O.D. Kennedy, C.J. Philemon, M.B. Schaffler, Structural and mechanical repair of diffuse damage in cortical bone in vivo, J. Bone Miner. Res. 29 (2014) 2537–2544.

[30] X. Wang, D.B. Masse, H. Leng, K.P. Hess, R.D. Ross, R.K. Roeder, G.L. Niebur, Detection of trabecular bone microdamage by micro-computed tomography, J. Biomech. 40 (2007) 3397–3403.

[31] D.T. Felson, Osteoarthritis as a disease of mechanics, Osteoarthr. Cartil. 21 (2013) 10–15.

[32] M. Sowers, C.A. Karvonen-Gutierrez, R. Palmieri-Smith, J.A. Jacobson, Y. Jiang, J.A. Ashton-Miller, Knee osteoarthritis in obese women with cardiometabolic clustering, Arthritis Rheum. 61 (2009) 1328–1336.

[33] B. Antony, A. Venn, F. Cicuttini, L. March, L. Blizzard, T. Dwyer, A. Halliday, M. Cross, G. Jones, C. Ding, Correlates of knee bone marrow lesions in younger adults, Arthritis Res. Ther. 18 (31) (2016).

[34] Y.Z. Lim, Y. Wang, A.E. Wluka, M.L. Davies-Tuck, F. Hanna, D.M. Urquhart, F.M. Cicuttini, Association of obesity and systemic factors with bone marrow lesions at the knee: a systematic review, Semin. Arthritis Rheum. 43 (2014) 600–612.

[35] B.C. Roberts, L.B. Solomon, G. Mercer, K.J. Reynolds, D. Thewlis, E. Perilli, Joint loading and proximal tibia subchondral trabecular bone microarchitecture differ with walking gait patterns in end-stage knee osteoarthritis, Osteoarthr. Cartil. 25 (10) (2017 Oct) 1623–1632, https://doi.org/10.1016/j.joca.2017.06.001.

[36] J.L. Crane, X. Cao, Bone marrow mesenchymal stem cells and TGF-beta signaling in bone remodeling, J. Clin. Invest. 124 (2014) 466–472.

[37] S.L. Dallas, J.L. Rosser, G.R. Mundy, L.F. Bonewald, Proteolysis of latent transforming growth factor-beta (TGF-beta)-binding protein-1 by osteoclasts. A cellular mechanism for release of TGF-beta from bone matrix, J. Biol. Chem. 277 (2002) 21352–21360.

[38] J. Dequeker, S. Mohan, R.D. Finkelman, J. Aerssens, D.J. Baylink, Generalized osteoarthritis associated with increased insulin-like growth factor types I and II and transforming growth factor beta in cortical bone from the iliac crest. Possible mechanism of increased bone density and protection against osteoporosis, Arthritis Rheum. 36 (1993) 1702–1708.

[39] B.C. Herman, L. Cardoso, R.J. Majeska, K.J. Jepsen, M.B. Schaffler, Activation of bone remodeling after fatigue: differential response to linear microcracks and diffuse damage, Bone 47 (2010) 766–772.

[40] M.B. Schaffler, Role of bone turnover in microdamage, Osteoporos. Int. 14 (Suppl. 5) (2003) S73–7 (discussion S77–80).

[41] M. Prideaux, C. Schutz, A.R. Wijenayaka, D.M. Findlay, D.G. Campbell, L.B. Solomon, G.J. Atkins, Isolation of osteocytes from human trabecular bone, Bone 88 (2016) 64–72.

[42] S.R. Goldring, The osteocyte: key player in regulating bone turnover, RMD Open 1 (2015), e000049.

[43] M.B. Schaffler, W.Y. Cheung, R. Majeska, O. Kennedy, Osteocytes: master orchestrators of bone, Calcif. Tissue Int. 94 (2014) 5–24.

[44] D. Vashishth, O. Verborgt, G. Divine, M.B. Schaffler, D.P. Fyhrie, Decline in osteocyte lacunar density in human cortical bone is associated with accumulation of microcracks with age, Bone 26 (2000) 375–380.

[45] V.T. Carpentier, J. Wong, Y. Yeap, C. Gan, P. Sutton-Smith, A. Badiei, N.L. Fazzalari, J.S. Kuliwaba, Increased proportion of hypermineralized osteocyte lacunae in osteoporotic and osteoarthritic human trabecular bone: implications for bone remodeling, Bone 50 (2012) 688–694.

[46] S. Blouin, N. Fratzl-Zelman, F.H. Glorieux, P. Roschger, K. Klaushofer, J.C. Marini, F. Rauch, Hypermineralization and high osteocyte lacunar density in osteogenesis imperfecta type V bone indicate exuberant primary bone formation, J. Bone Miner. Res. 32 (9) (2017 Sep) 1884–1892, https://doi.org/10.1002/jbmr.3180.

[47] M.L. Davies-Tuck, A.E. Wluka, Y. Wang, D.R. English, G.G. Giles, F. Cicuttini, The natural history of bone marrow lesions in community-based adults with no clinical knee osteoarthritis, Ann. Rheum. Dis. 68 (2009) 904–908.

[48] S. Seah, D. Wheaton, L. Li, J.P. Dyke, C. Talmo, W.F. Harvey, D.J. Hunter, The relationship of tibial bone perfusion to pain in knee osteoarthritis, Osteoarthr. Cartil. 20 (2012) 1527–1533.

[49] J.H. Lee, J.P. Dyke, D. Ballon, D.M. Ciombor, M.P. Rosenwasser, R.K. Aaron, Subchondral fluid dynamics in a model of osteoarthritis: use of dynamic contrast-enhanced magnetic resonance imaging, Osteoarthr. Cartil. 17 (2009) 1350–1355.

[50] M. Shabestari, J. Vik, J.E. Reseland, E.F. Eriksen, Bone marrow lesions in hip osteoarthritis are characterized by increased bone turnover and enhanced angiogenesis, Osteoarthr. Cartil. 24 (2016) 1745–1752.

[51] A. Kuttapitiya, L. Assi, K. Laing, C. Hing, P. Mitchell, G. Whitley, A. Harrison, F.A. Howe, V. Ejindu, C. Heron, N. Sofat, Microarray analysis of bone marrow lesions in osteoarthritis demonstrates upregulation of genes implicated in osteochondral

turnover, neurogenesis and inflammation, Ann. Rheum. Dis. 76 (10) (2017 Oct) 1764–1773, https://doi.org/10.1136/annrheumdis-2017-211396.

[52] M.L. Davies-Tuck, R. Kawasaki, A.E. Wluka, T.Y. Wong, L. Hodgson, D.R. English, G.G. Giles, F. Cicuttini, The relationship between retinal vessel calibre and knee cartilage and BMLs, BMC Musculoskelet. Disord. 13 (255) (2012).

[53] G.M. Goldsmith, D. Aitken, F.M. Cicuttini, A.E. Wluka, T. Winzenberg, C.H. Ding, G. Jones, J.E. Sharman, Osteoarthritis bone marrow lesions at the knee and large artery characteristics, Osteoarthr. Cartil. 22 (2014) 91–94.

Chapter 4

Associations between Components of the Metabolic Syndrome and the Presence of Bone Marrow Lesions in Knee Osteoarthritis

Dzenita Muratovic, Flavia Cicuttini, Anita Wluka, David Findlay, Yea-Rin Lee, and Julia Kuliwaba.

Discipline of Orthopaedics and Trauma, The University of Adelaide, Adelaide, Australia.
Department of Epidemiology & Preventive Medicine, Monash University, Melbourne, Australia.

To be submitted to Arthritis Research &Therapy

Statement of Authorship

Title of Paper	**Associations between Components of the Metabolic Syndrome and the Presence of Bone Marrow Lesions in Knee Osteoarthritis**.
Publication Status	Unpublished and unsubmitted work written in manuscript style
Publication Details	To be submited to Arthritis Research &Therapy

Principal Author

Name of Principal Author (Candidate)	Dzenita Muratovic		
Contribution to the Paper	Designed the study, performed the experiments and analysis of the results, interpreted the data, wrote the manuscript and acted as corresponding author.		
Certification:	This paper reports on original research I conducted during the period of my Higher Degree by Research candidature and is not subject to any obligations or contractual agreements with a third party that would constrain its inclusion in this thesis. I am the primary author of this paper.		
Signature		Date	17/10/2017

Co-Author Contributions

By signing the Statement of Authorship, each author certifies that:

i. the candidate's stated contribution to the publication is accurate (as detailed above);

ii. permission is granted for the candidate in include the publication in the thesis; and the sum of all co-author contributions is equal to 100% less the candidate's stated contribution.

Name of Co-Author	Prof David Findlay		
Contribution to the Paper	Designed the study, interpreted the data, provided overall supervision and wrote the manuscript.		
Signature		Date	17/10/2017

Name of Co-Author	A/Prof Anita Wluka		
Contribution to the Paper	Designed the study, interpreted the data, provided overall supervision and wrote the manuscript.		
Signature		Date	17/10/2017

Name of Co-Author	Prof Flavia		
Contribution to the Paper	Designed the study, interpreted the data, provided overall supervision and wrote the manuscript.		
Signature		Date	17/10/2017

Name of Co-Author	Yea Rin Lee
Contribution to the Paper	Contributed to collection of specimens from patients, performed the experiments and critically revised the manuscript.

Signature		Date	17/10/2017

Name of Co-Author	Dr Julia Kuliwaba		
Contribution to the Paper	Designed the study, interpreted the data, provided overall supervision and wrote the manuscript.		
Signature		Date	17/10/2017

Associations between Components of the Metabolic Syndrome and the Presence of Bone Marrow Lesions in Knee Osteoarthritis

[1]Dzenita Muratovic, [1]David M. Findlay, [2]Flavia M. Cicuttini, [2]Anita E. Wluka, [1]Yea Rin Lee, [1]Julia S. Kuliwaba.

Institutes

[1]Discipline of Orthopaedics and Trauma, The University of Adelaide, Adelaide, Australia.

[2]Department of Epidemiology & Preventive Medicine, Monash University, Melbourne, Australia.

E-mails:

dzenita.muratovic@adelaide.edu.au
david.findlay@adelaide.edu.au
flavia.cicuttini@monash.edu
anita.wluka@monash.edu
yea.lee@adelaide.edu.au
julia.kuliwaba@adelaide.edu.au

Corresponding author:
Dzenita Muratovic
Discipline of Orthopaedics and Trauma
Level 7, Adelaide Health & Medical Sciences Building,
Cnr North Tce & George St, Adelaide, South Australia 5000
Tel: +61 431286068
Email: dzenita.muratovic@adelaide.edu.au

Abstract

Introduction: Epidemiological studies demonstrate a link between knee osteoarthritis (KOA) and the metabolic syndrome (MetS) and its components. The presence of a bone marrow lesion (BML) in KOA is a strong predictor of structural degeneration and severity of the symptoms. However, little is known regarding the influence of metabolic factors on BML development in the subchondral bone of the knee. Therefore, this study aimed to investigate association between MetS, its components and BML in KOA subjects.

Methods: Tibial plateaus and medical histories were obtained from 73 patients (41 females, 32 males) aged 48-87 years, undergoing knee arthroplasty for KOA. To identify BMLs in tibial plateaus, MRI scans were performed *ex vivo*, using T1 and PDFS-weighted sequences. For each patient, relevant clinical data of age and body mass index (BMI) were recorded on day of surgery. Data on comorbidities and medication (including antidiabetic treatment, antihypertensive medication and dyslipidaemia treatment) were retrieved from clinical histories and medical records.

Results: An increased prevalence of MetS was found in KOA subjects with BMLs compared to those without BML (p=0.02). Furthermore, high total cholesterol and high body mass index showed significant association with radiographic OA severity (high KL grade and loss of cartilage volume), while high fasting glucose and high triglycerides were significantly associated with larger BML size (higher BML volume).

Discussion: Our data suggest that a combination of specific metabolic factors might promote the occurrence of BMLs in subchondral bone tissue and that metabolic factors might contribute to the progressive osteochondral degeneration of KOA.

4.1 Introduction

Systemic and metabolic factors, such as nutritional intake [1, 2] and serum lipids [3], have been linked with knee osteoarthritis (KOA). In addition, the presence of metabolic syndrome (MetS) and its components might be a causative factor for the initiation and progression of KOA and may influence the enlargement of bone marrow lesions (BMLs) [4-6].

Visualised by magnetic resonance imaging (MRI), BMLs act as a valuable imaging indicator of the structural degenerative progression in KOA [7-9], and as a predictor of future potential intervention outcome such as total knee replacement [10]. At the tissue level, they have been described as areas of subchondral bone with impaired bone quality [7, 8, 11] and nonspecific changes in bone marrow such as fibrotic and necrotic changes, with fatty marrow and numerous vascular infiltrations [7, 11, 12]. An interesting finding for BMLs is that in pre-OA populations BMLs can resolve within two years in up to 50% of individuals [13], while in established OA they are less likely to decrease in size or resolve [14]. Thus, in early OA, MRI identified BMLs might provide potential targets for therapeutic intervention. Further, our recent data indicated that presence of BML subtypes, detected by different MRI sequences, in tibial subchondral bone, identify more or less severe KOA [7]. This further opens the possibility of identifying individuals with less severe KOA, perhaps at an earlier stage of progression, which may be amenable to therapeutic intervention.

It is not known whether metabolic factors have direct or indirect relationship to the formation and presence of BMLs. We hypothesised that individuals with tibial BML suffer from metabolic conditions and have increased incidence of MetS. Therefore, the aim of this study was to explore the relationship between the metabolic syndrome and its components and the presence of BMLs in subjects with KOA. This potentially could uncover modifiable risk factors for BML in KOA, information that could perhaps be used to influence the understanding of KOA pathogenesis and lead to novel and more personalised/individualised treatments for this condition, at least in early disease

4.2 Methodology

4.2.1 Clinical characteristics of the patient cohort

Tibial plateau and medical histories from 73 patients undergoing knee arthroplasty surgery, of whom 41 (56%) were females, aged 48 to 86 years, and 32 (44%) were males, aged 49 to 87 years, were included in the study. Tibial plateaus were scanned *ex vivo* using MRI to detect presence of BMLs as previously described [7]. For each patient, relevant clinical data of age, and body mass index (BMI) were recorded. BMI categories were defined according to the recommendation of the Australian Department of Health: normal BMI range 19-25, overweight BMI 25-30, obese BMI 30-35 and severely obese >35. Patients were fasted overnight, and pre-surgery blood samples were taken for the measurement of glucose, total cholesterol and triglyceride levels. Blood pressure was measured twice, and the average of two measurements was calculated. Data on comorbidities and medication (including antidiabetic treatment, antihypertensive medication and dyslipidaemia treatment) were retrieved from clinical histories and medical records. According to the World Health Organisation (WHO), metabolic syndrome (MetS) was defined as the presence of three or more of the following components: 1) central obesity with BMI 30 or greater, 2) dyslipidaemia or use of medication for dyslipidaemia, 3) blood pressure of 130/85 or greater or use of antihypertensive medication, and 4) fasting glucose level greater than 5.5 mmol/L or medication for diabetes mellitus [15, 16].

Informed written consent was obtained from all patients and the study received prior approval from the Human Research Ethics Committee at the Repatriation General Hospital, the Royal Adelaide Hospital and The University of Adelaide, South Australia, in accordance with the Declaration of Helsinki 1975. Inclusion criteria were: radiographic OA with severe symptomatic disabilities, such as severe pain and limited mobility. Exclusion criteria were: secondary OA of the knee due to trauma, rheumatoid arthritis, osteoporosis, evidence of bone-related chronic debilitating disease and/or history of any medication that may have affected bone turnover.

4.2.2 Radiographic evaluation of knee OA

Standing anteroposterior, posteroanterior and lateral view radiographs were taken of OA subjects prior to surgery. The extent of radiographic progression was assessed according to Kellgren and Lawrence (K&L) grade. All radiographs were scored by two experienced assessors (AW and YW), with 95% agreement. Assessors were blinded for the presence of BMLs in the knee joint.

4.2.3 Magnetic resonance imaging (MRI)

Each TP was MR imaged *ex vivo* in an 8-channel wrist coil (3T MRI Siemens TRIO, Royal Adelaide Hospital, Adelaide), using two specific sequences; fat suppressed fast spin-echo proton density-weighted (PDFS) and T1-weighted spin echo in the sagittal and coronal plane. Sagittal slice thickness was 1.6 mm, with distance factor of 25%. Coronal slice thickness was 1.6 mm, with 10% distance factor. A BML was defined as a zone of altered signal intensity in the bone and marrow located immediately beneath the articular cartilage and visible on at least two consecutive slices [17, 18]. Cartilage volume and BML volume were assessed by two researchers (DM and YL), as described previously [18]. The coefficient of variation for the measurement of cartilage volume in the medial and lateral compartment was 2.2% and for BML volume 2.4%.

4.2.4 Statistical analysis

Student's t test and chi square tests were used to compare the distribution of characteristics between groups. The difference between No BML vs BML (BML 1+BML 2) groups was analysed, followed by analysis of the difference between BML 1 vs BML 2. The critical value for statistical significance was chosen as $P<0.05$. The analyses were performed using the GraphPad Prism software (GraphPad Software, Inc., USA).

Both adjusting for clustering on subject and controlling for the confounders age, sex and BMI and presence of BML, were performed in linear mixed-effects models. Linear mixed-effects models were also used to investigate the association between cartilage volume vs each MetS component separately and as the number of MetS components, K&L grade vs each MetS component separately and as the number of metabolic components present, and BML volume vs each MetS component separately and as the number of MetS components present. Adjustment for multiple comparisons was made using a Sidak adjustment to account for significance of P values by chance due to large numbers of regressions being performed. These analyses were performed using the statistical software SAS 9.4 (SAS Institute Inc., Cary, NC, USA).

4.3 Results

Fifty-five (76%) of the TP samples contained a BML detected with one or both MRI sequences. BMLs detected using the PDFS sequence only (BML 1) represented 62% of all BMLs. BMLs detected by both PDFS and T1 sequences (BML 2) represented 38% of all BMLs.

4.3.1 Demographic characteristics

4.3.1.1 Age and gender

Eighteen patients did not show a BML on MRI (No BML group). This group was composed predominantly of females (13; 72%). The average age for the No BML group was 71.5 years. The female age range was 64 to 84 years, and the male age range was 60 to 80 years. 95% of individuals from the No BML group were 65 to 75 years of age.

The BML group contained almost equal proportions of females and males (51%, 49%, respectively). The average age of the BML group was 68.7 years. The female ages ranged from 49 to 87 years, and the male age range was from 48 to 86 years. In the BML group, 31% of individuals were younger than 65 years and 65% were between 65 and 85 years of age. These data are summarised in Table 1.

4.3.1.2 Body mass index (BMI)

In the No BML group, 11 (61%) were obese or severely obese, with an average BMI of 34. 70% of females were obese or severely obese. The BML group had an average BMI of 30 and approximately 50% were in the obese or severely obese category, while 16% had ideal weight. About 60% of females were obese or severely obese compared to 33% of males. Observing BML 1 and BML 2 separately, we found that both groups had an average BMI of 31. These data are summarised in Table 2.

4.3.1.3 Metabolic Syndrome (MetS)

For each individual, components of the MetS were documented separately and as the co-occurrence of at least 3 components (defined as MetS). Individuals in the No BML group had an average fasting glucose level of 5.9 mmol/L, blood pressure of 140/80, serum total cholesterol level of 4.5 mmol/L and triglycerides of 1.6 mmol/L. Observing females and males separately, elevated levels for some MetS components were detected in the No BML group, with 2/3 of the females having elevated fasting blood glucose and 2/3 of the males having elevated systolic blood pressure. In the BML group, the average fasting glucose level was 6.2 mmol/L, blood pressure of 140/80, serum total cholesterol level of 4.9 mmol/L and total triglycerides of 1.4 mmol/L. More than 50% of the individuals in the BML group had above normal fasting glucose levels (>5.5 mmol/L), elevated systolic blood pressure or use of antihypertensive medication. These data are summarised in Table 3.

4.3.2 Differences between groups

There were no significant differences in the patient's age, gender or K&L grade between the BML and no BML group. Individuals in the no BML group had a higher mean BMI than the BML group (p=0.04). However, when we investigated differences according to BMI category, healthy, overweight, obese and severely obese, no significant difference was found between groups. The volume of cartilage was significantly higher in the No BML than the BML group (p=0.01). Comparing prevalence of metabolic components separately between BML and no BML, a high prevalence of established hypertension (use of antihypertensive medication) was found only in the BML group (74%, 41 out of 55), (p=0.005). MetS prevalence (co-occurrence of at least 3 components) was significantly greater in the BML group compared to the no BML (p= 0.02). This remained significant after adjusting for age, sex and BMI.

In the BML group, a significant difference was found between the BML1 and BML2 subgroups, such that radiographic progression (K&L grade) was lower and cartilage volume was higher in BML 1 compared to BML 2 (p=0.04, 0.006, respectively). In regard to metabolic components, the total cholesterol and the number of patients with elevated total cholesterol were significantly higher in BML 1 compared to BML 2 (p=0.008 and p= 0.02, respectively). These data are summarised in Table 3.

4.3.3 Correlations between each metabolic component separately and as the number of metabolic components present vs. cartilage volume, K&L grade and BML volume

BMI was positively correlated with K&L grade in No BML (r=0.49, p=0.04) and BML 1 (r=0.47, p=0.03). Total cholesterol levels also correlated positively with K&L grade (r=0.66, p=0.001) in the BML group (BML 1+BML 2) and in the BML 1 group (r=0.65, p=0.001), and with cartilage volume in the BML group (r=0.50, p=0.004). There was a positive association between triglyceride level and BML volume in the BML group (r=0.33, p=0.04) and in the BML 1 group (r=0.58, p=0.01). Levels of fasting glucose associated positively with BML volume in the BML 1 group (r=0.33, p= 0.04), and negatively with cartilage volume in the No BML group (r=-0.57, p=0.04). No significant correlation was found between the severity of MetS (represented by the number of MetS components present) with K&L grade, cartilage volume, or BML volume, for any group.

4.4 Discussion

This study is the first to explore the association between the presence of MetS, as a cluster of three or more metabolic disorders [15], and its components, with the presence or absence of BMLs in KOA subjects. We found an increased prevalence of MetS in KOA subjects with BMLs compared to those without a BML. Furthermore, high total cholesterol and high BMI showed significant association with OA severity (high K&L grade and loss of cartilage volume), while high fasting glucose and high triglycerides were significantly associated with larger BML (higher BML volume). These relationships persisted after adjustment for age, sex and BMI. Collectively, these results suggest the possible involvement of metabolic factors in the development of BMLs and the progression of KOA.

Obesity is a major risk factor for the initiation and progression of KOA [19]. However, only a weak association was reported previously between obesity and the presence of BMLs in young individuals [20], and a moderate association was found in an older population [21]. Weight loss did not have a positive impact on tibiofemoral BML size scores, suggesting that BMLs do not respond to a rapidly decreased body weight [22]. The results from the present study indicate that obesity (defined as BMI ≥ 30 kg/m^2) was present in both subjects with BML and in those without BML. Moreover, high BMI associates with higher K&L grade in both no BML and BML, suggesting that BMI might be a contributing factor of radiographic progression in KOA but not the key factor for BML development in the tissue. However, in the knee joint, in addition to excessive and/or misdirected biomechanical load, the way that the joint is loaded, together with the amount and frequency of loading is important to take in consideration. These data were not available for the current study and further study will be required to interrogate this issue.

There is published evidence that obesity and bone metabolism are closely interconnected. Fat cells, the adipocytes, and the bone forming cells, the osteoblasts, share the same origin from multipotent mesenchymal stem cells [23]. Therefore, increased adipocyte differentiation might indirectly decrease osteoblast differentiation and bone formation/mineralisation [24]. Furthermore, it has been reported that high fat intake may affect calcium absorption and decrease bone formation/mineralisation [25]. Animal studies have demonstrated that lipid and lipoprotein oxidation by-products inhibit differentiation and function of osteoblasts [26, 27] and that hypercholesterolemia promotes osteoclastic differentiation and bone resorption. More recent human studies reported that dietary lipids, such as mono-saturated fatty acids, increase the risk of BML in a healthy population [28] and that increased levels of total serum cholesterol and triglycerides were associated with the development of new BMLs in knees over 2 years [29]. Collectively, these data suggest a tight association between dietary fat and bone turnover in health and disease.

Another important aspect of obesity is that fat tissue can produce pro-inflammatory cytokines/adipokines [19, 30, 31]. Synovial fluid and plasma in OA patients contain an increased level of leptin (pro-inflammatory) and decreased level of adiponectin (anti-inflammatory), [32, 33]. Elevated leptin in serum and/or synovia associates with MRI-defined cartilage defects, the presence of BMLs and osteophytes, meniscal abnormalities, and synovitis and therefore thought to play significant roles in bone metabolism and the maintenance of an inflammatory state in the joint [34-37]. On the other hand, leptin is closely associated with the prevalence of cardiovascular diseases, including hypertension, atherosclerosis, and MetS [38, 39]. Interestingly, animal studies indicate leptin as one of the key regulators of TGF-β [32]. TGF-β has a beneficial role in cartilage repair in OA [40], but prolonged exposure has adverse effects on bone remodelling and can trigger degenerative changes in both cartilage and subchondral bone [41]. Also, elevated serum concentrations of TGF-β associate with incidence of type 2 diabetes and play a role in the pathogenesis of hypertension [39]. Recently, in the same patient cohort as reported here, we found thickening of the arteriolar smooth muscle layer and increased lumen ratio in areas of BML (Chapter 3), consistent with arteriolosclerosis. The observed change in wall structure is possibly a compensatory response to sustained hypertension, consistent with our finding that hypertension was significantly more prevalent in subjects with tibial BMLs than in those without BMLs. Structural changes of the arteriolar wall due to hypertension and increased lipid levels can lead to vasoconstriction and ischaemic events in tissues, a possible mechanism of BML development [42]. Moreover, the presence of hypertension and type 2 diabetes mellitus has been linked to aberrant endothelial cell behaviour [43], which in turn could affect osteoblastic function [44-46]. Complementary to this, we reported that BML subchondral bone (subchondral plate and subchondral trabeculae) is characterised by increased osteoid thickness and osteoid volume as well as with higher bone volume [7]. Moreover, Hunter *et. al* reported that BML subchondral bone is sclerotic and hypo-mineralised [8]. Collectively, pathological changes of the microvasculature might be caused by MetS and together contribute to the pathogenesis of BML.

High levels of glucose and/or the presence of diabetes mellitus associates positively with structural degradation in the joint, such as cartilage volume loss and incidence of new BMLs in a non-OA population [47], while in an OA population diabetes associates with OA progression and increased incidence of total joint replacement [48-50]. Our finding of a positive association between increased levels of glucose and higher volume size of BMLs complements those studies. Moreover, many studies indicated that hyperglycaemia could influence bone metabolism at the cellular level by direct reduction in osteoblast maturation, function and viability, causing bone hypomineralisation [51, 52]. A high level of glucose stimulates differentiation of bone marrow mesenchymal cells into adipocytes, which results in an increased rate of adipogenesis and decreased osteogenesis [53]. Insulin and insulin analogue IGF-1 can directly or indirectly induce osteoblast proliferation, increase bone deposition and decrease bone resorption [54-56]. Furthermore, an association between diabetes mellitus and abnormalities in bone metabolism, including increased porosity of the subchondral plate and changes in subchondral trabeculae, reduced serum biomarkers of bone turnover, accumulation of non-healing microfractures and elevated sclerostin levels has been noted [57]. Collectively, those changes are indicative of reduced bone quality in patients with diabetes mellitus [58]. Furthermore, several studies reported that bone healing is prolonged in diabetic patients [57]. The presence of a BML in KOA was considered to be a sign of an active response to acute tissue injury [59]. Therefore, it is possible that the presence of MetS in KOA subjects with BML impairs the process of healing and thus accelerates degenerative changes in both bone and cartilage.

Regarding the association between MetS as a cluster of three or more metabolic disorders and the presence of BML in KOA, our results indicate a higher prevalence of MetS in OA subjects with BMLs. However, there was no association between the number of MetS components, higher K&L grade, lower cartilage volume and BML volume. This might be explained by previous reports, in which an association between the number of components and radiographic progression was found prior to adjustment for BMI, yet after adjustment association was weak [30]. We also found that the majority of significant associations between elevated metabolic components (higher BMI, higher cholesterol, high triglycerides and higher fasting glucose) and higher K&L grade and BML volume were for BML 1. We previously described BML 1 as lesions with less structural degeneration, compared to BML 2, and we proposed that those lesions might characterise OA that has a greater ability to respond to treatment. In addition, results from this study suggest that the negative effect of specific metabolic components might be important in an early stage of OA progression. Hence, targeting those metabolic components might be useful in future choice of OA treatment strategies.

A limitation of this human tissue-level study is that we could sample only at end stage KOA. Therefore, we are unable to comment on the relationship between disease initiation and MetS and its components. Based on the results of this study we can only speculate that targeted treatment of MetS would have a beneficial effect on OA and its symptoms. Also, our study is cross-sectional and we cannot offer conclusion if treatment of MetS abnormalities would act positively on BML resolution or progression of KOA. However, the study suggests that further longitudinal research in a larger population would be beneficial to explore the interaction of metabolic mechanisms in the development of BMLs and OA pathogenesis. The current view is that biomechanical stress is the main causal factor of BML appearance in the tissue. Results from our study are incomplete as we only assessed BMI as an indicator of possible mechanical loading. However, the type and frequency of loading is important to take into consideration. Collecting high definition activity monitoring data, together with data on the metabolic status of the subject, would likely be favourable in terms of identifying links between these parameters and OA/BML development.

In conclusion, our data suggest that a combination of specific metabolic factors might promote the occurrence of BMLs in tibial subchondral bone tissue and that metabolic factors might contribute to the progressive osteochondral degeneration of KOA. Larger longitudinal studies observing BML in individuals with MetS are needed to confirm whether treatment of MetS at an early stage of OA would be valuable for resolution of BML associated clinical symptoms and/or structural degeneration in KOA.

4.5 Acknowledgements

The authors wish to thank Ms. Sue Collins for MRI technical assistance, Dr. Jamie Taylor and Dr. Yuan-Yuan Wang (YW) for assistance and advice on measurement and interpretation of the radiographic and MRI data, and Dr. Graham Mercer, Dr. Chris Wilson, and Dr. Dai Morgan for providing TP specimens. Anatomical Pathology at SA Pathology, and the Department of Radiology, Royal Adelaide Hospital.

4.6 Authors contributions

All authors meet the criteria for authorship. DM designed the study, performed the experiments and analysis of the results, interpreted the data and wrote the manuscript. DF, FC, AW, and JK designed the study, interpreted the data, provided overall supervision and wrote the manuscript. YL contributed to the collection of specimens from patients, performed the experiments and critically revised the manuscript. All authors read and approved the manuscript.
The authors declare no conflicts of interest.

4.7 Funding

The authors acknowledge funding from the National Health and Medical Research Council of Australia (NHMRC, Project Grant 1042482) and support from the Rebecca Cooper Foundation. DM is the recipient of an NHMRC postgraduate scholarship; AW is the recipient of an NHMRC Career Development Fellowship (Clinical level 2, 1063574).

4.8 Conflict of interest

None

4.9 References

1. Wang Y, Wluka AE, Hodge AM, English DR, Giles GG, O'Sullivan R, et al. Effect of fatty acids on bone marrow lesions and cartilage in healthy, middle-aged subjects without clinical knee osteoarthritis. Osteoarthritis Cartilage 2008; 11: R63.

2. Wang Y, Hodge AM, Wluka AE, English DR, Giles FG, O'Sullivan R, et al. Effect of antioxidants on knee cartilage and bone in healthy, middle-aged subjects: a cross sectional study. Arthritis Res Ther 2007; 9: R66.

3. Davies-Tuck ML, Hanna F, Davis SR, Bell RJ, Davison SL, Wluka AE, et al. Total cholesterol and triglycerides are associated with the development of new bone marrow lesions in asymptomatic middle-aged women - a prospective cohort study. . Arthritis Research and Therapy 2009; 11: R181.

4. Yoshimura N, Muraki S, Oka H, Tanaka S, Kawaguchi H, Nakamura K, et al. Accumulation of metabolic risk factors such as overweight, hypertension, dyslipidaemia, and impaired glucose tolerance raises the risk of occurrence and progression of knee osteoarthritis: a 3-year follow-up of the ROAD study. Osteoarthritis Cartilage 2012; 20: 1217-1226.

5. Hussain SM, Cicuttini FM, Bell RJ, Robinson PJ, Davis SR, Giles GG, et al. Incidence of total knee and hip replacement for osteoarthritis in relation to circulating sex steroid hormone concentrations in women. Arthritis Rheumatol 2014; 66: 2144-2151.

6. Shin D. Association between metabolic syndrome, radiographic knee osteoarthritis, and intensity of knee pain: results of a national survey. J Clin Endocrinol Metab 2014; 99: 3177-3183.

7. Muratovic D, Cicuttini F, Wluka A, Findlay D, Wang Y, Otto S, et al. Bone marrow lesions detected by specific combination of MRI sequences are associated with severity of osteochondral degeneration. Arthritis Res Ther 2015; 18: 54.

8. Hunter DJ, Gerstenfeld L, Bishop G, Davis AD, Mason ZD, Einhorn TA, et al. Bone marrow lesions from osteoarthritis knees are characterized by sclerotic bone that is less well mineralized. Arthritis Res Ther 2009; 11: R11.

9. Kazakia GJ, Kuo D, Schooler J, Siddiqui S, Shanbhag S, Bernstein G, et al. Bone and cartilage demonstrate changes localized to bone marrow edema-like lesions within osteoarthritic knees. Osteoarthritis Cartilage 2013; 21: 94-101.

10. Tanamas SK, Wluka AE, Pelletier JP, Pelletier JM, Abram F, Berry PA, et al. Bone marrow lesions in people with knee osteoarthritis predict progression of disease and joint replacement: a longitudinal study. Rheumatology (Oxford) 2010; 49: 2413-2419.

11. Taljanovic MS, Graham AR, Benjamin JB, Gmitro AF, Krupinski EA, Schwartz SA, et al. Bone marrow edema pattern in advanced hip osteoarthritis: quantitative assessment with magnetic resonance imaging and correlation with clinical examination, radiographic findings, and histopathology. Skeletal Radiol 2008; 37: 423-431.

12. Zanetti M, Bruder E, Romero J, Hodler J. Bone marrow edema pattern in osteoarthritic knees: correlation between MR imaging and histologic findings. Radiology 2000; 215: 835-840.

13. Davies-Tuck ML, Wluka AE, Wang Y, English DR, Giles GG, Cicuttin FM. The natural history of bone marrow lesions in community based adults with no clinical knee osteoarthritis. Ann Rheum Dis 2008; 68: 904-908.

14. Hunter DJ, Zhang Y, Niu J, Goggins J, Amin S, LaValley MP, et al. Increase in bone marrow lesions associated with cartilage loss: A longitudinal magnetic resonance imaging study of knee osteoarthritis. Arthritis and Rheumatism 2006; 54: 1529-1535.

15. Day C. Metabolic syndrome, or What you will: definitions and epidemiology. Diab Vasc Dis Res 2007; 4: 32-38.

16. World Health Organization: Geneva SLaoJ. Definition, diagnosis and classification of diabetes mellitus and its complications: . 2011.

17. Wluka AE, Wang Y, Davies-Tuck M, English DR, Giles GG, Cicuttini FM. Bone marrow lesions predict progression of cartilage defects and loss of cartilage volume in healthy middle-aged adults without knee pain over 2 yrs. Rheumatology (Oxford) 2008; 47: 1392-1396.

18. Muratovic D, Cicuttini F, Wluka A, Findlay D, Wang Y, Otto S, et al. Bone marrow lesions detected by specific combination of MRI sequences are associated with severity of osteochondral degeneration. Arthritis Res Ther 2016; 18: 54.

19. Sowers M, Karvonen-Gutierrez CA, Palmieri-Smith R, Jacobson JA, Jiang Y, Ashton-Miller JA. Knee osteoarthritis in obese women with cardiometabolic clustering. Arthritis Rheum 2009; 61: 1328-1336.

20. Antony B, Venn A, Cicuttini F, March L, Blizzard L, Dwyer T, et al. Correlates of knee bone marrow lesions in younger adults. Arthritis Res Ther 2016; 18: 31.

21. Lim YZ, Wang Y, Wluka AE, Davies-Tuck ML, Hanna F, Urquhart DM, et al. Association of obesity and systemic factors with bone marrow lesions at the knee: a systematic review. Semin Arthritis Rheum 2014; 43: 600-612.

22. Gudbergsen H, Boesen M, Christensen R, Bartels EM, Henriksen M, Danneskiold-Samsoe B, et al. Changes in bone marrow lesions in response to weight-loss in obese knee osteoarthritis patients: a prospective cohort study. BMC Musculoskelet Disord 2013; 14: 106.

23. Gregoire FM, Smas CM, Sul HS. Understanding adipocyte differentiation. Physiol Rev 1998; 78: 783-809.

24. Rosen CJ, Bouxsein ML. Mechanisms of disease: is osteoporosis the obesity of bone? Nat Clin Pract Rheumatol 2006; 2: 35-43.

25. Nelson SE, Frantz JA, Ziegler EE. Absorption of fat and calcium by infants fed a milk-based formula containing palm olein. J Am Coll Nutr 1998; 17: 327-332.

26. Parhami F, Jackson SM, Tintut Y, Le V, Balucan JP, Territo M, et al. Atherogenic diet and minimally oxidized low density lipoprotein inhibit

osteogenic and promote adipogenic differentiation of marrow stromal cells. J Bone Miner Res 1999; 14: 2067-2078.

27. Tintut Y, Parhami F, Tsingotjidou A, Tetradis S, Territo M, Demer LL. 8-Isoprostaglandin E2 enhances receptor-activated NFkappa B ligand (RANKL)-dependent osteoclastic potential of marrow hematopoietic precursors via the cAMP pathway. J Biol Chem 2002; 277: 14221-14226.

28. Wang Y, Wluka AE, Hodge AM, English DR, Giles GG, O'Sullivan R, et al. Effect of fatty acids on bone marrow lesions and knee cartilage in healthy, middle-aged subjects without clinical knee osteoarthritis. Osteoarthritis Cartilage 2008; 16: 579-583.

29. Davies-Tuck ML, Hanna F, Davis SR, Bell RJ, Davison SL, Wluka AE, et al. Total cholesterol and triglycerides are associated with the development of new bone marrow lesions in asymptomatic middle-aged women - a prospective cohort study. Arthritis Res Ther 2009; 11: R181.

30. Han CD, Yang IH, Lee WS, Park YJ, Park KK. Correlation between metabolic syndrome and knee osteoarthritis: data from the Korean National Health and Nutrition Examination Survey (KNHANES). BMC Public Health 2013; 13: 603.

31. Scotece M, Mobasheri A. Leptin in osteoarthritis: Focus on articular cartilage and chondrocytes. Life Sci 2015; 140: 75-78.

32. Dumond H, Presle N, Terlain B, Mainard D, Loeuille D, Netter P, et al. Evidence for a key role of leptin in osteoarthritis. Arthritis Rheum 2003; 48: 3118-3129.

33. Chen TH, Chen L, Hsieh MS, Chang CP, Chou DT, Tsai SH. Evidence for a protective role for adiponectin in osteoarthritis. Biochim Biophys Acta 2006; 1762: 711-718.

34. Hoeven TA, Kavousi M, Clockaerts S, Kerkhof HJ, van Meurs JB, Franco O, et al. Association of atherosclerosis with presence and progression of osteoarthritis: the Rotterdam Study. Ann Rheum Dis 2013; 72: 646-651.

35. Grundy SM. Metabolic syndrome: a multiplex cardiovascular risk factor. J Clin Endocrinol Metab 2007; 92: 399-404.

36. Karvonen-Gutierrez CA, Harlow SD, Jacobson J, Mancuso P, Jiang Y. The relationship between longitudinal serum leptin measures and measures of magnetic resonance imaging-assessed knee joint damage in a population of mid-life women. Ann Rheum Dis 2014; 73: 883-889.

37. Zhang P, Zhong ZH, Yu HT, Liu B. Significance of increased leptin expression in osteoarthritis patients. PLoS One 2015; 10: e0123224.

38. Sciarretta S, Ferrucci A, Ciavarella GM, De Paolis P, Venturelli V, Tocci G, et al. Markers of inflammation and fibrosis are related to cardiovascular damage in hypertensive patients with metabolic syndrome. Am J Hypertens 2007; 20: 784-791.

39. Aihara K IY, Yagi S, Akaike M, Matsumoto T. Transforming Growth Factor-β1 as a Common Target Molecule for Development of Cardiovascular Diseases, Renal Insufficiency and Metabolic Syndrome. Cardiology Research and Practice 2011; 2011:175381.

40. Grimaud E, Heymann D, Redini F. Recent advances in TGF-beta effects on chondrocyte metabolism. Potential therapeutic roles of TGF-beta in cartilage disorders. Cytokine Growth Factor Rev 2002; 13: 241-257.

41. Zhen G, Wen C, Jia X, Li Y, Crane JL, Mears SC, et al. Inhibition of TGF-beta signaling in mesenchymal stem cells of subchondral bone attenuates osteoarthritis. Nat Med 2013; 19: 704-712.

42. Findlay DM. Vascular pathology and osteoarthritis. Rheumatology (Oxford) 2007; 46: 1763-1768.

43. Hadi HA, Suwaidi JA. Endothelial dysfunction in diabetes mellitus. Vasc Health Risk Manag 2007; 3: 853-876.

44. Guillotin B, Bourget C, Remy-Zolgadri M, Bareille R, Fernandez P, Conrad V, et al. Human primary endothelial cells stimulate human osteoprogenitor cell differentiation. Cell Physiol Biochem 2004; 14: 325-332.

45. Decker B, Bartels H, Decker S. Relationships between endothelial cells, pericytes, and osteoblasts during bone formation in the sheep femur following implantation of tricalciumphosphate-ceramic. Anat Rec 1995; 242: 310-320.

46. Kular J, Tickner J, Chim SM, Xu J. An overview of the regulation of bone remodelling at the cellular level. Clin Biochem 2012; 45: 863-873.

47. Davies-Tuck ML, Wang Y, Wluka AE, Berry PA, Giles GG, English DR, et al. Increased fasting serum glucose concentration is associated with adverse knee structural changes in adults with no knee symptoms and diabetes. Maturitas 2012; 72: 373-378.

48. King KB, Findley TW, Williams AE, Bucknell AL. Veterans with diabetes receive arthroplasty more frequently and at a younger age. Clin Orthop Relat Res 2013; 471: 3049-3054.

49. Schett G, Kleyer A, Perricone C, Sahinbegovic E, Iagnocco A, Zwerina J, et al. Diabetes is an independent predictor for severe osteoarthritis: results from a longitudinal cohort study. Diabetes Care 2013; 36: 403-409.

50. Eymard F, Parsons C, Edwards MH, Petit-Dop F, Reginster JY, Bruyere O, et al. Diabetes is a risk factor for knee osteoarthritis progression. Osteoarthritis Cartilage 2015; 23: 851-859.

51. Botolin S, McCabe LR. Chronic hyperglycemia modulates osteoblast gene expression through osmotic and non-osmotic pathways. J Cell Biochem 2006; 99: 411-424.

52. Cunha JS, Ferreira VM, Maquigussa E, Naves MA, Boim MA. Effects of high glucose and high insulin concentrations on osteoblast function in vitro. Cell Tissue Res 2014; 358: 249-256.

53. Keats E, Khan ZA. Unique responses of stem cell-derived vascular endothelial and mesenchymal cells to high levels of glucose. PLoS One 2012; 7: e38752.

54. Kasukawa Y, Miyakoshi N, Mohan S. The anabolic effects of GH/IGF system on bone. Curr Pharm Des 2004; 10: 2577-2592.

55. Klein GL. Insulin and bone: Recent developments. World J Diabetes 2014; 5: 14-16.

56. Yang J, Zhang X, Wang W, Liu J. Insulin stimulates osteoblast proliferation and differentiation through ERK and PI3K in MG-63 cells. Cell Biochem Funct 2010; 28: 334-341.

57. King KB, Rosenthal AK. The adverse effects of diabetes on osteoarthritis: update on clinical evidence and molecular mechanisms. Osteoarthritis Cartilage 2015; 23: 841-850.

58. Schwartz AV, Vittinghoff E, Bauer DC, Hillier TA, Strotmeyer ES, Ensrud KE, et al. Association of BMD and FRAX score with risk of fracture in older adults with type 2 diabetes. JAMA 2011; 305: 2184-2192.

59. Eriksen EF, Ringe JD. Bone marrow lesions: a universal bone response to injury? Rheumatol Int 2012; 32: 575-584.

Tables

Table 4-1 Age and gender in the No BML, BML, BML 1 and BML 2 groups

	No BML		BML		BML 1		BML 2	
	Female	Male	Female	Male	Female	Male	Female	Male
N (%)	13 (72%)	5 (28%)	28 (51%)	27 (49%)	18 (53%)	16 (47%)	10 (48%)	11(52%)
Age<65	0	1 (20%)	8 (28%)	9 (33.4%)	6 (33.3%)	6 (38%)	2 (20%)	3 (27.3%)
Age 65-74	10 (75%)	4 (80%)	12 (43%)	9 (33.4%)	8 (44.4%)	4 (25%)	4 (40%)	5 (45.4%)
Age 75-84	3 (25%)	0	7 (25%)	8 (29.5%)	4 (22.3%)	5 (31%)	3 (30%)	3 (27.3%)
Age 85+	0	0	1 (4%)	1 (3.7%)	0	1 (6%)	1 (10%)	0

Table 4-2 Body mass index classification

	No BML		BML		BML 1		BML 2	
Gender	Female	Male	Female	Male	Female	Male	Female	Male
N (%)	13 (72%)	5 (27%)	28 (51%)	27 (49%)	18 (53%)	16 (47%)	10 (47.6)	11 (52.3%)
Ideal BMI (<25)	0	1 (20%)	3 (10.7%)	6 (22.2%)	2 (11.1%)	4 (25%)	1 (10%)	2 (18.1%)
Overweight (25-30)	4 (30.7%)	2 (40%)	8 (28.1%)	12 (44.4%)	5 (27.7%)	8 (50%)	3 (30%)	4 (36.6%)
Obese (>30)	3 (23%)	0	8 (28.1%)	5 (18.4%)	5 (27.7%)	2 (12.5%)	3 (30%)	3 (27.2%)
Severely Obese (>35)	6 (47.7%)	2 (40%)	9 (32.1)	4 (15%)	6 (33.3%)	2 (12.5%)	3 (30%)	2 (18.1%)

Table 4-3 Difference between patient characteristics among groups

	No BML	BML	p value	BML 1	BML 2	p value
Age (years)	77±6.3	68.7±9.3	0.3	68±1.7	69.8±1.6	0.5
Male [n (%)]	5 (28%)	28 (51%)	0.08	16 (47%)	12 (57%)	0.4
Female [n (%)]	13 (72%)	27 (49%)	0.08	18 (53%)	9 (43%)	0.4
BMI	33.7± 4.9	30.8± 4.9	**0.04**	30.5± 0.8	31.5±1	0.4
K&L grade	2 (1-4)	3 (1-4)	0.7	2 (1-3)	3 (2-4)	**0.04**
Cartilage Volume (mm^3)	1.3±0.2	1.0±0.3	0.01	1.1±0.3	0.8±0.3	**0.006**
BML volume (mm^3)	NA	0.4 (0.1-0.6)	NA	0.3 (0.1-0.5)	0.3 (0.1-0.4)	0.5

Table 4-4 Metabolic components between groups

Metabolic components	No BML	BML	p value	BML 1	BML 2	p value
Fasting glucose	5.9±1.8	6.2±1.4	0.6	5.3 (4.4-6.4)	3.9 (3.3-4)	0.9
Patients with elevated fasting glucose [n (%)]	7 (38.8%)	27 (49%)	0.9	15 (44.1%)	12 (57%)	0.3
Females [n (%)]	*5 (71%)*	*14 (52%)*	0.3	*9 (60%)*	*5 (42%)*	0.3
Insulin dependent [n (%)]	4 (22.2%)	11 (20%)	0.8	5 (4.7%)	6 (28.5%)	0.2
Females [n (%)]	*2 (50%)*	*4 (36%)*	0.8	*2 (40%)*	*2 (33%)*	0.8
Systolic blood pressure	140 (137-152)	140 (130-150)	0.4	141.5±16	139.2±13	0.6
Elevated systolic blood pressure [n (%)]	11 (61%)	30 (54.5%)	0.6	20 (58.8%)	11 (52.3%)	0.6
Females [n (%)]	*6 (18%)*	*19 (63%)*	0.6	*12 (60%)*	*7 (64%)*	0.8
Diastolic blood pressure	80 (70-80)	80 (70-80)	0.8	76.6±10.6	75.6±8.3	0.3
Elevated diastolic blood pressure [n (%)]	3 (16.6%)	**5 (9%)**	0.3	4 (11.7%)	1 (4.7%)	0.7
Females [n (%)]	*2 (67%)*	*4 (80%)*	0.6	*4 (100%)*	*1 (100%)*	0.4
Antihypertensive medication [n (%)]	7 (38.8%)	41 (74.5%)	**0.005**	26 (76.4%)	15 (71.4%)	0.4
Females [n (%)]	*4 (57%)*	*22 (54%)*	0.8	*15 (58%)*	*7 (46%)*	>0.9
Levels of total cholesterol	4.5±1	4.9±1	0.4	4.4 (3.6-5.3)	3.3 (3-4)	**0.008**
Elevated total cholesterol [n (%)]	1 (5.5%)	10 (18%)	0.1	9 (26.4%)	1 (4.7%)	**0.02**
Females [n (%)]	*1 (100%)*	*4 (40%)*	0.2	*3 (33%)*	*1 (100%)*	0.1

Total triglycerides	1.6±0.9	1.4±0.5	0.5	1.3 (0.9-1)	1.4 (1-2)	0.5
Elevated total serum triglycerides [n (%)]	1 (5.5%)	7 (12.7%)	0.3	3 (8.8%)	4 (19%)	0.2
Females [n (%)]	*1 (100%)*	*2 (28%)*	0.1	*0*	*2 (50%)*	0.1
Hypertriglyceridemia medication [n (%)]	4 (22.2%)	24 (43.6)	0.1	14 (41%)	10 (47.6%)	0.6
Females [n (%)]	*3 (75%)*	*14 (56%)*	0.5	*9 (64%)*	*5 (50%)*	0.4

Table 4-5 Prevalence of MetS between groups

	No BML	BML	p value	BML 1	BML 2	p value
MetS+[n (%)]	6 (33.6%)	35 (63.6%)	**0.02**	25 (65%)	13 (62%)	0.3
Females [n (%)]	*3 (50%)*	*20 (57%)*	0.7	*13 (52%)*	*7 (54%)*	0.9
No Metabolic components [n (%)]	3 (16.6%)	4 (7.2%)	0.3	2 (5.8%)	2 (9.5%)	0.6
1 Metabolic component [n (%)]	3 (16.6%)	7 (12.7%)	0.6	4 (11.7%)	3 (14.2%)	0.7
2 Metabolic components [n (%)]	6 (33.3%)	9 (16.3%)	0.1	6 (17.6%)	3 (14.2%)	0.7
3+ Metabolic components [n (%)]	6 (33.3%)	34 (64%)	**0.03**	24 (70%)	13 (62%)	0.5

Chapter 5

Bone Marrow Lesions in Knee Osteoarthritis: Regional Changes in Subchondral Bone Microstructure and their Association with Cartilage Loss

Dzenita Muratovic, Flavia Cicuttini, Anita Wluka, David Findlay, Yea-Rin Lee, and Julia Kuliwaba.

Discipline of Orthopaedics and Trauma, The University of Adelaide, Adelaide, Australia.
Department of Epidemiology & Preventive Medicine, Monash University, Melbourne, Australia.

To be submitted to Osteoarthritis and Cartilage

Statement of Authorship

Title of Paper	**Bone Marrow Lesions in Knee Osteoarthritis: Regional Changes in Subchondral Bone Microstructure and their Association with Cartilage Loss**
Publication Status	Unpublished and unsubmitted work written in manuscript style
Publication Details	To be submited to Osteoarthritis and Cartilage

Principal Author

Name of Principal Author (Candidate)	Dzenita Muratovic		
Contribution to the Paper	Designed the study, performed the experiments and analysis of the results, interpreted the data, wrote the manuscript and acted as corresponding author.		
Certification:	This paper reports on original research I conducted during the period of my Higher Degree by Research candidature and is not subject to any obligations or contractual agreements with a third party that would constrain its inclusion in this thesis. I am the primary author of this paper.		
Signature		Date	17/10/2017

Co-Author Contributions

By signing the Statement of Authorship, each author certifies that:

i. the candidate's stated contribution to the publication is accurate (as detailed above);

ii. permission is granted for the candidate in include the publication in the thesis; and the sum of all co-author contributions is equal to 100% less the candidate's stated contribution.

Name of Co-Author	Prof David Findlay		
Contribution to the Paper	Designed the study, interpreted the data, provided overall supervision and wrote the manuscript.		
Signature		Date	17/10/2017

Name of Co-Author	A/Prof Anita Wluka		
Contribution to the Paper	Designed the study, interpreted the data, provided overall supervision and wrote the manuscript.		
Signature		Date	17/10/2017

Name of Co-Author	Prof Flavia		
Contribution to the Paper	Designed the study, interpreted the data, provided overall supervision and wrote the manuscript.		
Signature		Date	17/10/2017

Name of Co-Author	Yea Rin Lee
Contribution to the Paper	Contributed to collection of specimens from patients, performed the experiments and critically revised the manuscript.

Signature		Date	17/10/2017

Name of Co-Author	Dr Julia Kuliwaba
Contribution to the Paper	Designed the study, interpreted the data, provided overall supervision and wrote the manuscript.

Signature		Date	17/10/2017

Abstract

Objective: It is not known how tissue level changes within bone marrow lesions (BMLs) relate to the microstructural changes across the human tibial plateau (TP). To address this, we evaluated subchondral bone microarchitecture, and cartilage deterioration, in non-osteoarthritis (OA) and in OA TP with and without BML.

Design: Tibial plateaus were collected from 32 subjects, aged 49 to 79 years, undergoing total knee replacement surgery for knee OA (KOA), and from 12 non-OA control subjects, aged 44 to 89 years. MRI was used to identify BMLs and to quantify cartilage volume. Micro CT was used to quantitate the subchondral plate and subchondral trabecular bone microstructure in seven volumes of interest; two oval cross-section cylinders representing the whole medial and lateral compartments; four circular cross-section cylinders representing anterior medial (AM), posterior medial (PM), anterior lateral (AL) and posterior lateral (PL) subregions of the compartments, and one cylinder representing BML. Cartilage loss and degeneration were evaluated by MRI measurement of cartilage volume and OARSI histological grading.

Results: In non-OA control and OA-no BML groups, parameters describing subchondral bone (plate and trabeculae) showed no significant intragroup variability between compartments or subregions, while in OA-BML differences were evident. The anterior-medial region of OA-no BML did not differ significantly from non-OA controls. In contrast, the OA-BML group had significantly thicker subchondral plate ($p=0.02$, $p=0.004$), and trabeculae that are more numerous ($p=0.03$, $p=0.03$), well connected ($p=0.009$, $p=0.003$), and more plate-like ($p=0.04$, $p=0.01$), compared to both non-OA controls and OA-no BML. Cartilage volume decreased and OARSI grade increased in OA-BML compared with controls, especially in the medial compartment.

Conclusion: In established KOA, both the extent of cartilage damage and microstructural change in the subchondral bone depended on the presence of a BML. Thus, use of BMLs as MRI image-based biomarkers appears to inform on the severity of disease in established OA.

Keywords; knee osteoarthritis, bone marrow lesions, subchondral bone microarchitecture, micro CT, cartilage volume

5.1 Introduction

Knee osteoarthritis (KOA) is a painful and degenerative musculoskeletal condition characterized by loss of osteochondral integrity. Specifically, destruction of cartilage (loss of cellular integrity and cartilage volume) and pathophysiological changes in the underlying subchondral bone, such as subchondral bone sclerosis, osteophytes, bone marrow lesions (BMLs) and bone cysts, are characteristics of advanced KOA. Although cartilage destruction has received the majority of research attention, there is evidence that changes in the subchondral bone may precede cartilage loss, and are thus important to understanding the pathogenesis and progression of OA [1-6].

Animal models of OA have described a predictable disease progression in OA, in which initial loss of subchondral bone is followed by sclerotic changes, increased anisotropy and an increase in the plate:rod ratio, prior to cartilage degeneration [7]. In human patients, since the majority of studies have described late stage OA, the sequence of KOA changes is less well understood.

BMLs could assist in grading clinically important changes in the subchondral bone. BMLs are identified by magnetic resonance imaging (MRI), and are frequently seen in both early and late stage OA. They have acquired considerable clinical interest because their presence is predictive of degenerative changes in cartilage [8, 9] and future joint replacement [9]. Since BMLs can increase or decrease in size, and even resolve over time [10], the notion has developed that BMLs may have utility as biomarkers, both of disease progression and of response to treatment of KOA [11].

Histologically, the subchondral bone contained within BMLs is described as sclerotic, with increased subchondral plate thickness, and trabeculae showing increased bone volume fraction, increased thickness, a more plate-like structure, and increased osteoid volume and thickness but reduced tissue mineral density [12-15]. Although these changes in subchondral bone have been reported as focal [12-15], the association between the presence of BMLs and the bone microstructure of the remainder of the tibial plateau has not been described.

We hypothesized that the presence of a BML in KOA will associate with structural changes across the tibial plateau. Thus, the aim of this study was to comprehensively investigate and compare the subchondral bone microarchitecture of the whole tibial plateau in KOA subjects, with and without tibial BML, and in tibial plateau without OA. Specifically, the purpose of the study was to better understand tibial plateau regional subchondral bone changes in KOA and then to determine the association of the presence of a BML with the type and extent of bone changes. Finally, we determined the microstructural subchondral bone changes in relation to loss of cartilage integrity and volume.

5.2 Materials and Methods

5.2.1 Tibial plateau specimens

Tibial plateaus were obtained from 32 patients, 20 females and 12 males aged 49 to 79 years, undergoing knee arthroplasty surgery. Inclusion criteria were: radiographic OA with severe symptomatic disabilities, such as severe pain and limited mobility. Exclusion criteria were: KOA due to trauma or rheumatoid arthritis, osteoporosis, and metabolic bone disease. Control tibial plateau specimens were obtained from 11 non-OA cadavers, 4 females and 7 males, aged 44 to 89 years with no previous history of bone or joint disease (eg. Paget's disease, malignant tumors, avascular necrosis, rheumatoid arthritis), medication that may have affected bone metabolism, such as steroids and no macroscopic evidence of significant cartilage degeneration (all of the non-OA tibial plateau had Outerbridge score 0-1). Written consent was obtained for all subjects (joint replacement patients and cadavers) and the study received prior approval from the Human Research Ethics Committee at the Repatriation General Hospital, Royal Adelaide Hospital and The University of Adelaide, South Australia, in accordance with the Declaration of Helsinki 1975.

5.2.2 Magnetic resonance imaging (MRI)

Each tibial plateau was MR imaged *ex vivo* in an 8-channel wrist coil (3T MRI Siemens TRIO, Royal Adelaide Hospital, Adelaide), using two specific sequences; fat suppressed fast spin-echo proton density-weighted (PDFS) and T1 weighted spin echo in the sagittal and coronal plane. A BML was defined as a zone of altered signal intensity seen on PDFS +/- T1 weighted sequences in the bone and marrow (Figure 1A), located immediately beneath the articular cartilage and visible on at least two consecutive slices [15, 16]. The definition and location of BML were by mutual agreement between two investigators (AW and YW) with musculoskeletal MRI expertise. After identification of a BML, the external contour of the BML was marked in both planes and the automatic volume rendering function from OsiriX software (Pixmeo-SARL, Switzerland) was used to calculate the BML volume in cm^3. The coefficient of variation for the measurement of BML volume was 2.4%. Cartilage volume was assessed by two researchers (DM and YL), as described previously [15]. The coefficient of variation for the measurement of cartilage volume in the medial and lateral compartments was 2.2%.

5.2.3 Micro CT

To analyse the microstructure of the subchondral bone, whole tibial plateau was scanned by micro CT (SkyScan model 1076, Kontic, Belgium). Images were obtained at 74kV at isotropic resolution of 17.4 μm, with 1.0 mm aluminium filter and 0.8° rotation step. As depicted in Figure 1B, seven volumes of interest (VOI) were selected; two oval shapes to cover the whole medial (M; 45x25mm diameter x 6mm depth) and lateral (L; 40x25mm diameter x 6mm depth) compartments; four circular shapes (20mm diameter x 6mm depth) to cover the anterior medial (AM), posterior medial (PM), anterior lateral (AL) and posterior lateral (PL) subregions of the compartments; and one circular shape (10x10 diameter x 6mm depth) representing BML. The subchondral bone plate was manually segmented from the subchondral trabecular bone compartment for each VOI (Figure 1C). Subchondral plate and subchondral trabeculae were analyzed separately. Using CT-An analyzer software (SkyScan), the following morphometric parameters were determined for subchondral plate: plate thickness (Pl.Th) and plate porosity (Pl.Po) and for subchondral trabeculae: bone volume per total volume (BV/TV), trabecular thickness (Tb.Th), trabecular number (Tb.N), trabecular separation (Tb.Sp), structural model index (SMI) as measure of predominant shapes in the structure (plate-like or rod-like), trabecular bone pattern factor (Tb.Pf) as quantitative ratio of inter-trabecular connectivity, and degree of anisotropy (DA) which reflects the orientation of bone microarchitecture.

5.2.4 Histopathology assessment

Histopathological assessment was performed only for medial tibial plateau, as the majority of BML (75%) were detected in this compartment. Blocks of tissue (10x10x6mm) representing AM and PM (containing the entire BML, if present) were dissected using a low-speed diamond wheel saw (Model 660, South Bay Technology), formalin-fixed, decalcified in 5% hydrochloric acid, paraffin-embedded, sectioned 5 μm-thick and stained with Safranin-O/Fast Green to be used for Osteoarthritis Research Society International (OARSI) grading [17]. Consensus between three assessors (DM, EG and YL) determined the grading. The intra-class correlation coefficient (ICC) for inter-observer reproducibility was 0.82 (95% CI 0.80, 0.84).

5.2.5 Statistical analysis

All data sets were initially analysed by the Shapiro-Wilk test to determine normality of the data distribution. Parametric data are expressed as the mean ± standard deviation and non-parametric data as the median (25th-75th quartiles). The differences across groups for demographic variables, cartilage volume, histological grade, and subchondral bone plate and trabecular microstructure were investigated. For continuous normally-distributed variables a one-way ANOVA was used, for continuous non-normally distributed variables, a Kruskal-Wallis test was used, and for categorical variables, a Fisher's Exact test was used. The critical value for statistical significance was chosen as $P<0.05$. These analyses were performed using the GraphPad Prism software (GraphPad Software, Inc., USA).

Both adjusting for clustering on subject (multiple regions of interest) and controlling for the confounders age, sex and BMI and presence of BML, were performed in linear mixed-effects models. Linear mixed-effects models were also used to investigate the association between subchondral bone microstructural parameters versus cartilage volume, OARSI grade and BML volume. This was because there was clustering on patient ID and knee (multiple regions of interest in the same patient's knee), which could be adjusted for by the use of a mixed-effects model. Adjustment for multiple comparisons was made using a Sidak adjustment to account for significance of P values by chance due to large numbers of regressions being performed. These analyses were performed using statistical software SAS 9.4 (SAS Institute Inc., Cary, NC, USA).

5.3 Results

5.3.1 Demographic characteristics of the cohorts

In the control group, only one subject was detected with a BML, which was located in the AL subregion. This case was excluded from further analysis. In OA subjects, BMLs were detected in 24 (75%) patients. The majority of BMLs were located in the medial compartment [18 out of 24 (75%)], with 12 (67%) located in the AM and 6 (33%) located in the PM. OA-BML subjects were predominantly diagnosed with medial OA (63%) and with varus malalignment (63%). The OA-no BML subjects were a mix of all three compartmental OA types; Medial OA (femoro-tibial compartment), Lateral OA (femoro-tibial compartment) and Patellofemoral OA, and had predominantly neutral alignment (62%).

5.3.2 Cartilage volume and histological grading (intragroup variability)

In controls and in OA-no BML, mean cartilage volumes measured over the whole M and L compartments were not significantly different between M vs. L compartments, while the L compartment of OA-BML had significantly thicker cartilage compared to M (p=0.0001). The mean OARSI grade was not different between AM and PM subregions in controls. In OA-no BML and OA-BML, the AM subregion had significantly higher mean OARSI grade compared to the PM subregion (p=0.001 and p=0.002 respectively, Figure 2B).

5.3.3 Cartilage volume and histological grading between groups

Mean cartilage volume in the M and L compartments was significantly lower in the OA-BML group compared to the M (p=0.0006) and L (p=0.002) of the control group. The mean cartilage volume of the OA-no BML group was intermediate between the control and OA-BML groups, and not significantly different from either group. In both OA-no BML and OA-BML groups, the AM subregion had significantly higher median OARSI grade than the control group (p=0.03 and p=0.0001, respectively). In the posterior medial subregion, the median OARSI grade was higher in OA-BML compared to both control (p=0.0001) and OA-no BML (p=0.03) groups (Figure 2B).

5.3.4 Microstructure of subchondral bone

5.3.4.1 Subchondral bone plate characteristics (intragroup variability)

In controls and in OA-no BML, mean plate thickness did not differ significantly between M vs. L compartments, nor between AM vs. PM and AL vs. PL subregions. In OA-BML, mean plate thickness was significantly greater in AM vs. AL and vs. PL (p=0.0001, 0.002) and in PM vs. AL and vs. PL (p=0.02 and p=0.0005). No difference was observed in mean plate porosity between regions in all groups. Results are presented in Figure 3A.

5.3.4.2 Subchondral bone plate microstructure between groups

Differences in subchondral plate microstructure between groups for each region of interest are presented in Figure 3B.

Medial compartment

The OA-no BML group had decreased median plate thickness compared to OA-BML (p=0.02) and controls (p=0.03). The OA-BML group had increased median plate porosity compared to controls (p=0.02).

Anterior medial subregion

The OA-BML group had increased mean plate thickness compared to controls and OA-no BML (p=0.04, p=0.004, respectively), and increased mean plate porosity compared to controls (p=0.001).

Posterior medial subregion

The OA-BML group had increased mean plate thickness and porosity compared to controls and OA-no BML ($p=0.001$, $p<0.0001$ and $p=0.02$, $p=0.04$, respectively).

Lateral compartment

Median plate thickness was greater in controls for the L compartment, compared with OA-no BML and OA-BML groups. No significant difference was observed in median plate porosity parameters between the three groups in the L, AL or PL.

5.3.4.3 Subchondral trabecular bone microstructure (intragroup variability)

As seen for the subchondral plate, parameters describing subchondral trabecular bone microstructure of non-OA controls and OA-no BML showed no significant intragroup variability between compartments or subregions. However, in OA-BML, differences were evident. These results are presented in Figure 4.

Percent bone volume (BV/TV)

In OA-BML, mean BV/TV was significantly higher in M vs. L ($p=0.03$), in AM vs. PM ($p=0.03$), vs. AL ($p=0.03$) and vs. PL ($p=0.03$).

Trabecular number (Tb.N)

In OA-BML, mean Tb.N was significantly higher in the AM vs. PM ($p=0.04$), vs. AL ($p=0.04$), and vs. PL ($p=0.04$).

Trabecular thickness (Tb.Th)

In OA-BML, mean Tb.Th was significantly higher in M vs. L ($p=0.003$), in AM vs AL ($p=0.001$) and in PM vs AL ($p=0.0003$) and vs. PL ($p=0.03$).

Trabecular separation (Tb.Sp)

Trabecular separation did not differ significantly between compartments and subregions in any group.

Structure model index (SMI)

In OA-BML, mean SMI was significantly lower, indicating more plate-like trabeculae, in M vs. L ($p<0.0001$), in AM vs. PM, vs. AL, vs. PL and ($p=0.0005$, $p<0.0001$, $p<0.0001$, respectively) and in PM vs.AL ($p=0.001$) and vs. PL ($p=0.04$).

Degree of anisotropy (DA)

In OA-BML, median DA was significantly higher in M vs. L ($p=0.02$), in AM vs. AL ($p=0.01$), and vs. PL ($p<0.0001$), and in PM vs.PL ($p=0.002$).

Trabecular pattern factor (Tb.Pf)

In OA-BML, mean Tb.Pf was significantly decreased in M vs. L ($p=0.0008$), and in AM vs. PM, vs. AL and vs. PL ($p=0.002$, $p<0.0001$ and $p<0.0001$, respectively) and in PM vs. AL ($p<0.0001$).

5.3.4.4 Trabecular bone microstructure differences between groups

Results are summarised in Figures 5 and 6.

Medial compartment

M compartment of OA-no BML was similar to controls except that it showed higher mean DA ($p= 0.03$). Compared to the control group, OA-BML had significantly higher mean Tb.Sp ($p=0.01$), and DA ($p=0.0002$) and lower median Tb.Pf ($p=0.005$). Compared to OA-no BML, OA-BML had higher mean BV/TV ($p=0.008$), Tb.N ($p=0.01$), lower mean SMI ($p=0.0004$) and lower median Tb.Pf ($p=0.0002$) in the medial compartment.

Anterior medial subregion

The AM subregion of OA-no BML was similar to controls except that it showed higher median DA ($p= 0.03$). OA-BML had significantly higher mean Tb.N ($p=0.03$), Tb.Sp ($p=0.01$) and median DA ($p<0.0001$) and lower mean SMI ($p=0.04$), and median Tb.Pf ($p=0.003$), compared to controls. OA-BML compared to OA-no BML, had higher mean BV/TV ($p=0.02$) and Tb.N ($p=0.03$), but lower mean SMI ($p=0.01$) and median Tb.Pf ($p=0.02$).

Posterior medial subregion

In the PM, OA-no BML had higher mean SMI ($p=0.004$) and median Tb.Pf ($p=0.006$) compared to controls. OA-BML had higher mean Tb.Th ($p=0.02$) and median DA ($p=0.001$) compared to controls. Comparing OA-BML to OA-no BML, OA-BML had higher mean BV/TV ($p=0.03$) and lower mean SMI ($p=0.01$) and median Tb.Pf ($p=0.01$).

Lateral compartment

Both OA-no BML and OA-BML had higher mean SMI ($p=0.003$, $p<0.0001$, respectively) and median Tb.Pf ($p=0.01$, $p<0.0001$, respectively), compared to controls. No differences were found between OA-no BML and OA-BML.

Anterior lateral subregion

No differences were found between OA-no BML vs. control or between OA-no BML vs. OA-BML. OA-BML had lower median Tb.Sp ($p=0.04$) and higher median Tb.Pf ($p=0.005$), compared to controls.

Posterior lateral subregion

The OA-BML group showed higher median Tb.Pf ($p=0.005$) than controls. No other group differences were observed for the PL parameters between OA-no BML vs. control, or between OA-BML vs. OA-no BML.

5.3.5 Correlation between subchondral bone microstructural parameters, histological OARSI grade, cartilage volume and BML volume.

Correlation analyses were performed between parameters describing subchondral bone microstructure and cartilage volume, obtained from the medial and lateral tibial compartments, and between subchondral bone microstructure and OARSI grade obtained from the anterior medial subregions. In the medial compartment of OA-no BML, Tb.N ($r=-0.65$, $p=0.04$) correlated negatively, and Tb.Sp ($r=0.77$, $p=0.02$) positively, with cartilage volume. In the anterior medial subregion of OA-no BML, Tb.Th ($r=0.78$, $p=0.02$) correlated positively, and DA ($r=-0.85$, $p=0.01$) negatively, with OARSI grade.

In the medial compartment of the OA-BML group, Tb.N ($r=-0.67$, $p=0.003$) and Tb.Th ($r=-0.57$, $p=0.04$) correlated negatively with cartilage volume. In the anterior medial subregion of OA-BML, Pl.Th ($r=0.76$, $p=0.01$), BV/TV ($r=0.65$, $p=0.01$) and Tb.N ($r=0.54$, $p=0.04$) correlated positively with OARSI grade, while Tb.Sp ($r=-0.64$, $p=0.01$) and SMI ($r=-0.61$ $p=0.02$) correlated negatively with OARSI grade.

In the lateral compartment of the control, OA-no BML and OA-BML groups, no correlations were observed between parameters of subchondral bone microstructure cartilage volume and OARSI grade.

Correlation analyses were performed between microstructural parameters of anterior medial and posterior medial subregions in OA-no BML and OA-BML. In OA-BML, no significant correlation was found. In OA-BML, changes in microstructural parameters of the anterior medial subregion correlated positively with changes in the posterior medial subregion; BV/TV (r=0.64, p=0.01), Tb.Th (r=0.78, p=0.001), Tb.N (r=0.69, p=0.008).

Correlation analyses between BML volume and microstructural parameters of the whole medial compartment, and the posterior medial subregion, indicated positive association in both for BVTV (r=0.48, p=0.04 and r=0.51, p=0.04) and Tb.N (r=0.53, p=0.02 and r=0.62, p=0.01), respectively.

5.4 Discussion

To our knowledge, this is the first comprehensive study of the subchondral bone microstructure (subchondral plate and trabeculae) across the whole OA tibial plateau in association with presence/absence of BMLs. In this study, there were three major findings relating to the subchondral bone microarchitecture of the tibial plateau due to KOA. Firstly, similarly as in non-OA (control) subjects, in OA subjects with no BML, bone microstructure of the subchondral plate and trabeculae did not vary significantly between subregions of the tibial plateau, while in OA subjects with detectable tibial BML, differences in microstructure between subregions were evident. Secondly, in KOA subjects, microstructural changes in the subchondral plate and trabeculae were dependent on the presence or absence of a BML in the tibial plateau, which also related to the extent of cartilage degradation. Thirdly, the microstructural changes within a BML often extended well beyond the zone of the BML. These observations suggest that BMLs derived from MRI clinical imaging might serve as an indicative tool of OA severity at the tissue level.

5.4.1 Structural changes in the subchondral bone plate and trabeculae in KOA subjects

The subchondral bone comprises the subchondral plate and the trabeculae. The architectural, biological and biomechanical properties of these two units are different and respond differently during OA progression. The present study demonstrates that subregional differences in control group and OA-No BML were not significant. In comparison, in the OA-BML group, substantial differences in bone microstructure were found between regions.

Consistent with previous studies of the human tibial plateau, we observed that changes of subchondral bone microstructure of the OA-BML group were more pronounced in the medial compartment than in the lateral compartment. Furthermore, and again similar to previous studies, significant differences between the anterior and posterior regions of these compartments were found [18-20]. The most substantial microstructural changes were found in the AM subregion of OA-BML, where the majority of BMLs were found (75%). In the OA-BML group, the AM subregion did not differ in plate characteristics to the PM region. However, trabecular bone of the AM region showed more prominent sclerotic changes, such as higher bone volume, and more numerous and plate-like trabeculae compared to PM. Comparing the AM subregion to AL and PL, significant differences were found in all parameters describing the microstructure of the subchondral plate and trabeculae.

Cox et al. described asymmetric loading between medial and lateral compartments of the knee that might contribute to development of OA [21]. Recently, Roberts et al. suggested that joint alignment influences both medial to lateral and within-condyle distribution of forces across the tibia that results in changes of subchondral bone microstructure, at least in late stage OA. They further showed that regional variation in bone microstructure within tibial compartments likely reflects joint loading history in KOA [22]. In a separate study, the same group identified three subgroups in KOA patients, based on distinct walking gait patterns, suggesting that there might be different mechanisms for generating loads through the tibial plateau, with corresponding microarchitectural adaptation [23]. With respect to BMLs, high peak knee adduction moment and high knee adduction moment impulse, as well as static alignment were significantly related to the presence of BMLs [24]. Lim et al., demonstrated from a systematic review of the literature, a strong relationship between meniscal pathology and mechanical knee alignment and BML in the OA population. Interestingly, the same review suggested that there is no strong association between BML presence and physical activity [25]. The conclusion was that BML areas represent a “hot spot” in the tibial plateau where changes in the bone microstructure might be the result of an acute localised tissue response as well as a pathophysiological interaction between the bone and cartilage [1, 26].

When we compared microstructural parameters between groups, we found substantial thinning of the subchondral plate in the medial compartment of OA-no BML, compared to both control and OA-BML. In contrast, the subchondral plate of OA-BML was thicker in the AM and PM subregions compared to the same subregions of both control and OA-no BML groups. We also found an increased porosity of the subchondral plate in OA-BML compared to controls, likely reflecting altered vascularity and/or bone resorption within the subchondral plate. The increased porosity could also affect the permeability of the osteochondral interface and play a direct role in the pathogenesis of OA. Increasing porosity of the subchondral plate was observed to co-localise with the point of mechanical load during ambulation in a rat knee model of post-traumatic OA [27].

Trabecular bone of medial compartment or its anterior aspect did not differ significantly between OA-no BML and controls beside higher degree of anisotropy in the medial compartment, indicating that OA-no BML has more preferential trabecular alignment compared to controls. In the PM subregion, OA-no BML had higher mean values for SMI and Tb.Pf compared to controls, indicating persistence of a rod-like structure with low connectivity. Furthermore, we found that trabecular bone in the AM subregion of OA-no BML, compared to the same region of OA-BML, was characterised predominantly with lower bone volume and fewer trabeculae that are more rod-like (indicated by increased SMI). While the PM subregion of OA-no BML had lower mean bone volume, more rod-like trabeculae that were more isolated or less connected (indicated by larger Tb.Pf), compared to PM of OA-BML.

The thinning of the subchondral plate and the reduced number of trabeculae both suggest a process of bone attrition at some prior stage of the disease progression. In addition, recently it has been suggested that rod-like structure (indicated by increased SMI) might have a protective effect on cartilage during impact loading [28, 29]. However, in a separate study it has been noted that SMI alone may not be the optimal parameter to make assessment of rod-like and/or plate-like structure [30]). Further clarification and definition of the microstructural parameters representing rod-like and/or plate-like structure is needed.

Previously, similar findings (to OA-no BML) were only reported in animal models such as in the Duncan Hartley guinea pig model of OA, when an early change was described by thickening of the subchondral plate and trabeculae, but the subchondral bone was found to change across time, eventually resembling that of a non-OA guinea pig strain [31]. Also, these alterations in animal bone structure have been found to precede severe cartilage degeneration and to associate with histopathological changes in the cartilage [3-5].

Recently, Chen *et. al*. demonstrated a novel finding in microstructural adaption due to OA disease, in terms of significant loss of rod-like trabeculae and thickening plate-like trabeculae in all regions of the human tibial plateau (with and without severe cartilage loss) providing a valuable insight into the dynamics of subchondral bone microstructural changes in OA. They also confirmed that similar changes preceded cartilage degeneration in the guinea pig model of spontaneous OA. These results suggested that specific trabecular changes might be important during the development and progression of OA [32]. Complementary to those findings, in our study SMI, DA and Tb.Pf, as nonmetric measures of topological structural features and useful determinants of mechanical strength [33], were significantly different in both OA-no BML and OA-BML compared to controls, confirming a lower bone quality of OA subchondral bone and its inability to resist overloading [34].

Collectively, structural alterations found in OA-no BML resemble changes that have been described previously as early OA [3-5, 35-42]. The OA BML group was associated with the greatest degree of sclerotic microstructural changes, cartilage degeneration and loss of cartilage volume, consistent with late stage OA [19, 20, 43].

5.4.2 Presence of BMLs predicts wider microstructural changes in the tibial plateau

The presence and size of BMLs is strongly associated with clinical symptoms (pain) [44] and focal structural degeneration (loss of cartilage and bone sclerosis) [12-15]. The present results suggest that the presence of a BML might be associated with structural changes beyond the BML, particularly in the medial compartment. Moreover, it seems that focal sclerosis of the BML area expands radially to the adjacent subregions (Figure 7). As BML sclerotic changes in a specific compartment are closely related to loss of cartilage volume and higher OARSI grade in the same compartment, BMLs could represent an epicentre of the structural change in the OCU of the tibial plateau. Interestingly, these data suggest that the MRI signal that represents a BML is not due to bone changes, and more likely resides in the inter-trabecular marrow.

Sclerotic changes are widely accepted as a key feature of advanced OA progression, but it is important to point out that these findings have not been consistently reported for end stage OA [45, 46]. A possible explanation for the different observations between studies might be due to the presence or absence of BMLs, since these subchondral bone features appear to segregate with more severe disease. Recently, Steinbeck et al. described two subtypes within a KOA population, defined according to microstructural features of subchondral bone (sclerotic and non-sclerotic trabecular bone), and suggested different mechanisms of disease progression [47]. Finnila et al. also analysed the tibial plateau in late stage of OA and found that bone volume fraction, trabecular thickness and trabecular number increase with OARSI grade, while trabecular separation and structure model index decrease, suggesting that sclerosis might potentially be used in radiological assessment of OA severity [48]. Neither of these studies considered the presence or absence of a BML in the tissue. Our study suggests that OA subjects without a BML belong to a non-sclerotic OA subtype, while those with BML belong to a sclerotic OA subtype. This conclusion will require greater numbers for confirmation.

Our study has several limitations. Firstly, the relatively small and heterogeneous OA-no BML group limits the strength of comparisons with other groups to investigate in more detail the relationship between BML and subchondral bone structure. Further studies are recommended to investigate these relationships. Secondly, as this study is cross-sectional in design, the changes in subchondral bone structure characteristic of early stage disease cannot be confirmed, nor can mechanisms of BML genesis in the tissue be identified. Longitudinal studies would help to clarify this sequence of events. We believe the strength of this study is that we have analysed subchondral bone microstructure for the entire human tibial plateau, while previous studies have mainly investigated bone microstructural changes in specific sub-regions.

5.4.3 Conclusion

Study of the microstructure of tibial plateaus in KOA showed that the presence of a BML defines the changes in both the subchondral bone and cartilage, which in turn relate to the severity of the disease. BMLs may therefore provide surrogate biomarkers that can discriminate OA subtypes or severity, for example helping to triage candidates for joint replacement surgery or conservative, non-surgical treatment, or be used as therapeutic targets, and response to treatment.

5.5 Acknowledgements

The authors wish to thank Ms. Sue Collins and Ms. Emma Giersch for technical assistance, Dr. Graham Mercer, Dr. Chris Wilson, Dr. Dai Morgan for helping obtain tibial plateau specimens, Dr. Yuan-Yuan Wang (YW) for assistance and advice on measurement and interpretation of the radiographic and MRI data, and Ms. Ruth Williams and Dr. Agatha Labrinidis for assisting with micro CT scanning of specimens. The authors wish to acknowledge support from Adelaide Microscopy at The University of Adelaide, Anatomical Pathology at SA Pathology, and the Department of Radiology at the Royal Adelaide Hospital.

5.6 Authors contributions

All authors meet the criteria for authorship. DM designed the study, performed the experiments and analysis of the results, interpreted the data and wrote the manuscript. FC, AW, DF and JK designed the study, interpreted the data, provided overall supervision and wrote the manuscript. YL contributed to the collection of specimens from patients, performed the experiments and critically revised the manuscript. All authors read and approved the manuscript.

5.7 Funding

The authors acknowledge funding from the National Health and Medical Research Council of Australia (NHMRC, Project Grant 1042482) and support from the Rebecca Cooper Foundation. DM is the recipient of an NHMRC postgraduate scholarship; AW is the recipient of an NHMRC Career Development Fellowship (Clinical level 2, 1063574).

5.8 Conflict of interest

The authors declare no conflicts of interest.

5.9 References

1. Goldring MB, Goldring SR. Articular cartilage and subchondral bone in the pathogenesis of osteoarthritis. Ann N Y Acad Sci 2010; 1192: 230-237.

2. Li G, Yin J, Gao J, Cheng TS, Pavlos NJ, Zhang C, et al. Subchondral bone in osteoarthritis: insight into risk factors and microstructural changes. Arthritis Res Ther 2013; 15: 223.

3. Huebner JL, Hanes MA, Beekman B, TeKoppele JM, Kraus VB. A comparative analysis of bone and cartilage metabolism in two strains of guinea-pig with varying degrees of naturally occurring osteoarthritis. Osteoarthritis Cartilage 2002; 10: 758-767.

4. Libicher M, Ivancic M, Hoffmann M, Wenz W. Early changes in experimental osteoarthritis using the Pond-Nuki dog model: technical procedure and initial results of in vivo MR imaging. Eur Radiol 2005; 15: 390-394.

5. Zhao W, Wang T, Luo Q, Chen Y, Leung VY, Wen C, et al. Cartilage degeneration and excessive subchondral bone formation in spontaneous

osteoarthritis involves altered TGF-beta signaling. J Orthop Res 2016; 34: 763-770.

6. Burr DB, Gallant MA. Bone remodelling in osteoarthritis. Nat Rev Rheumatol 2012; 8: 665-673.

7. Wang T, Wen CY, Yan CH, Lu WW, Chiu KY. Spatial and temporal changes of subchondral bone proceed to microscopic articular cartilage degeneration in guinea pigs with spontaneous osteoarthritis. Osteoarthritis Cartilage 2013; 21: 574-581.

8. Raynauld JP, Martel-Pelletier J, Haraoui B, Choquette D, Dorais M, Wildi LM, et al. Risk factors predictive of joint replacement in a 2-year multicentre clinical trial in knee osteoarthritis using MRI: results from over 6 years of observation. Ann Rheum Dis 2011; 70: 1382-1388.

9. Tanamas SK, Wluka AE, Pelletier JP, Pelletier JM, Abram F, Berry PA, et al. Bone marrow lesions in people with knee osteoarthritis predict progression of disease and joint replacement: a longitudinal study. Rheumatology (Oxford) 2010; 49: 2413-2419.

10. Kornaat PR, Kloppenburg M, Sharma R, Botha-Scheepers SA, Le Graverand MP, Coene LN, et al. Bone marrow edema-like lesions change in volume in the majority of patients with osteoarthritis; associations with clinical features. Eur Radiol 2007; 17: 3073-3078.

11. Laslett LL, Dore DA, Quinn SJ, Boon P, Ryan E, Winzenberg TM, et al. Zoledronic acid reduces knee pain and bone marrow lesions over 1 year: a randomised controlled trial. Ann Rheum Dis 2012; 71: 1322-1328.

12. Hunter DJ, Gerstenfeld L, Bishop G, Davis AD, Mason ZD, Einhorn TA, et al. Bone marrow lesions from osteoarthritis knees are characterized by sclerotic bone that is less well mineralized. Arthritis Res Ther 2009; 11: R11.

13. Driban JB, Tassinari A, Lo GH, Price LL, Schneider E, Lynch JA, et al. Bone marrow lesions are associated with altered trabecular morphometry. Osteoarthritis Cartilage 2012; 20: 1519-1526.

14. Kazakia GJ, Kuo D, Schooler J, Siddiqui S, Shanbhag S, Bernstein G, et al. Bone and cartilage demonstrate changes localized to bone marrow edema-like lesions within osteoarthritic knees. Osteoarthritis Cartilage 2013; 21: 94-101.

15. Muratovic D, Cicuttini F, Wluka A, Findlay D, Wang Y, Otto S, et al. Bone marrow lesions detected by specific combination of MRI sequences are associated with severity of osteochondral degeneration. Arthritis Res Ther 2016; 18: 54.

16. Wluka AE, Wang Y, Davies-Tuck M, English DR, Giles GG, Cicuttini FM. Bone marrow lesions predict progression of cartilage defects and loss of cartilage volume in healthy middle-aged adults without knee pain over 2 yrs. Rheumatology (Oxford) 2008; 47: 1392-1396.

17. Pritzker KP, Gay S, Jimenez SA, Ostergaard K, Pelletier JP, Revell PA, et al. Osteoarthritis cartilage histopathology: grading and staging. Osteoarthritis Cartilage 2006; 14: 13-29.

18. Matsui H, Shimizu M, Tsuji H. Cartilage and subchondral bone interaction in osteoarthrosis of human knee joint: a histological and histomorphometric study. Microsc Res Tech 1997; 37: 333-342.

19. Bobinac D, Spanjol J, Zoricic S, Maric I. Changes in articular cartilage and subchondral bone histomorphometry in osteoarthritic knee joints in humans. Bone 2003; 32: 284-290.

20. Kamibayashi L, Wyss UP, Cooke TD, Zee B. Trabecular microstructure in the medial condyle of the proximal tibia of patients with knee osteoarthritis. Bone 1995; 17: 27-35.

21. Cox LG, van Rietbergen B, van Donkelaar CC, Ito K. Bone structural changes in osteoarthritis as a result of mechanoregulated bone adaptation: a modeling approach. Osteoarthritis Cartilage 2011; 19: 676-682.

22. Roberts BC, Thewlis D, Solomon LB, Mercer G, Reynolds KJ, Perilli E. Systematic mapping of the subchondral bone 3D microarchitecture in the human tibial plateau: Variations with joint alignment. J Orthop Res 2016.

23. Roberts BC, Solomon LB, Mercer G, Reynolds KJ, Thewlis D, Perilli E. Joint loading and proximal tibia subchondral trabecular bone microarchitecture differ with walking gait patterns in end-stage knee osteoarthritis. Osteoarthritis Cartilage 2017.

24. Bennell KL, Creaby MW, Wrigley TV, Bowles KA, Hinman RS, Cicuttini F, et al. Bone marrow lesions are related to dynamic knee loading in medial knee osteoarthritis. Ann Rheum Dis 2010; 69: 1151-1154.

25. Lim YZ, Wang Y, Wluka AE, Davies-Tuck ML, Teichtahl A, Urquhart DM, et al. Are biomechanical factors, meniscal pathology, and physical activity risk factors for bone marrow lesions at the knee? A systematic review. Semin Arthritis Rheum 2013; 43: 187-194.

26. Cohen-Solal M, Funck-Brentano T, Hay E. Animal models of osteoarthritis for the understanding of the bone contribution. Bonekey Rep 2013; 2: 422.

27. Iijima H, Aoyama T, Tajino J, Ito A, Nagai M, Yamaguchi S, et al. Subchondral plate porosity colocalizes with the point of mechanical load during ambulation in a rat knee model of post-traumatic osteoarthritis. Osteoarthritis Cartilage 2016; 24: 354-363.

28. Ding M, Christian Danielsen C, Hvid I. Effects of hyaluronan on three-dimensional microarchitecture of subchondral bone tissues in guinea pig primary osteoarthrosis. Bone 2005; 36: 489-501.

29. Chen Y, Zhou B, Wang J, Wang T, Zhao W, Cao X, et al. Subchondral trabecular rod loss and trabecular plate stiffening precedes articular cartilage damages in osteoarthritis. Osteoarthritis and Cartilage; 24: S389.

30. Salmon PL, Ohlsson C, Shefelbine SJ, Doube M. Structure model index does not measure rods and plates in trabecular bone. Front Endocrinol (Lausanne) 2015; 6: 162.

31. Zamli Z, Robson Brown K, Sharif M. Subchondral bone plate changes more rapidly than trabecular bone in osteoarthritis. Int J Mol Sci 2016; 17.

32. Chen Y, Hu Y, Yu YE, Zhang X, Watts T, Zhou B, et al. Subchondral trabecular rod loss and plate thickening in the development of osteoarthritis. J Bone Miner Res 2017.

33. Odgaard A. Three-dimensional methods for quantification of cancellous bone architecture. Bone 1997; 20: 315-328.

34. Kim JE, Shin JM, Oh SO, Yi WJ, Heo MS, Lee SS, et al. The three-dimensional microstructure of trabecular bone: Analysis of site-specific variation in the human jaw bone. Imaging Sci Dent 2013; 43: 227-233.

35. Batiste DL, Kirkley A, Laverty S, Thain LM, Spouge AR, Holdsworth DW. Ex vivo characterization of articular cartilage and bone lesions in a rabbit ACL transection model of osteoarthritis using MRI and micro-CT. Osteoarthritis Cartilage 2004; 12: 986-996.

36. Bettica P, Cline G, Hart DJ, Meyer J, Spector TD. Evidence for increased bone resorption in patients with progressive knee osteoarthritis: longitudinal results from the Chingford study. Arthritis Rheum 2002; 46: 3178-3184.

37. Bolbos RI, Zuo J, Banerjee S, Link TM, Ma CB, Li X, et al. Relationship between trabecular bone structure and articular cartilage morphology and relaxation times in early OA of the knee joint using parallel MRI at 3 T. Osteoarthritis Cartilage 2008; 16: 1150-1159.

38. Botter SM, van Osch GJ, Waarsing JH, Day JS, Verhaar JA, Pols HA, et al. Quantification of subchondral bone changes in a murine osteoarthritis model using micro-CT. Biorheology 2006; 43: 379-388.

39. Chang G, Xia D, Chen C, Madelin G, Abramson SB, Babb JS, et al. 7T MRI detects deterioration in subchondral bone microarchitecture in subjects with mild knee osteoarthritis as compared with healthy controls. J Magn Reson Imaging 2015; 41: 1311-1317.

40. Intema F, Hazewinkel HA, Gouwens D, Bijlsma JW, Weinans H, Lafeber FP, et al. In early OA, thinning of the subchondral plate is directly related to cartilage damage: results from a canine ACLT-meniscectomy model. Osteoarthritis Cartilage 2010; 18: 691-698.

41. Meyer EG, Baumer TG, Slade JM, Smith WE, Haut RC. Tibiofemoral contact pressures and osteochondral microtrauma during anterior cruciate ligament rupture due to excessive compressive loading and internal torque of the human knee. Am J Sports Med 2008; 36: 1966-1977.

42. Mohan G, Perilli E, Kuliwaba JS, Humphries JM, Parkinson IH, Fazzalari NL. Application of in vivo micro-computed tomography in the temporal characterisation of subchondral bone architecture in a rat model of low-dose monosodium iodoacetate-induced osteoarthritis. Arthritis Res Ther 2011; 13: R210.

43. Ding M. Microarchitectural adaptations in aging and osteoarthrotic subchondral bone issues. Acta Orthop Suppl 2010; 81: 1-53.

44. Felson DT, Chaisson CE, Hill CL, Totterman SM, Gale ME, Skinner KM, et al. The association of bone marrow lesions with pain in knee osteoarthritis. Ann Intern Med 2001; 134: 541-549.

45. Chappard C, Peyrin F, Bonnassie A, Lemineur G, Brunet-Imbault B, Lespessailles E, et al. Subchondral bone micro-architectural alterations in

osteoarthritis: a synchrotron micro-computed tomography study. Osteoarthritis Cartilage 2006; 14: 215-223.

46. Patel V, Issever AS, Burghardt A, Laib A, Ries M, Majumdar S. MicroCT evaluation of normal and osteoarthritic bone structure in human knee specimens. J Orthop Res 2003; 21: 6-13.

47. Steinbeck MJ, Eisenhauer PT, Maltenfort MG, Parvizi J, Freeman TA. Identifying patient-specific pathology in osteoarthritis development based on microCT analysis of subchondral trabecular bone. J Arthroplasty 2016; 31: 269-277.

48. Finnila MA, Thevenot J, Aho OM, Tiitu V, Rautiainen J, Kauppinen S, et al. Association between subchondral bone structure and osteoarthritis histopathological grade. J Orthop Res 2016.

Figures

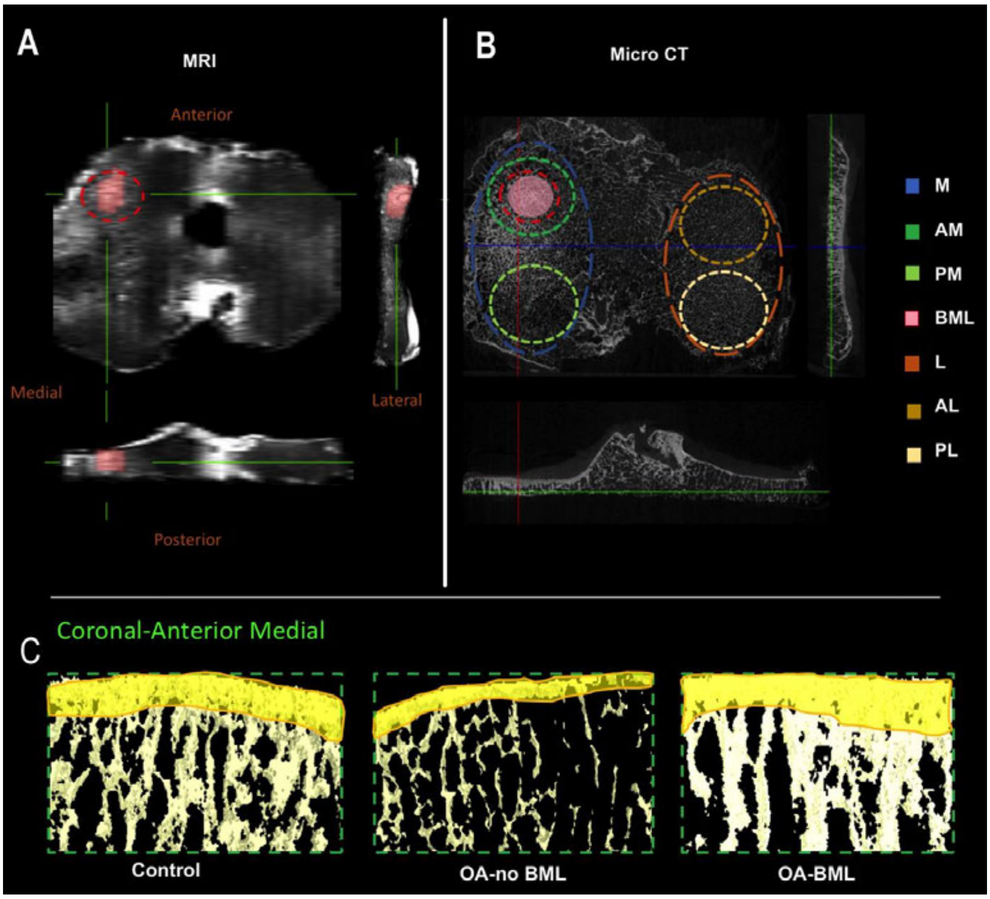

Figure 5-1 Representative cross-section images A) MRI of tibial plateau (upper-transaxial, lower-coronal, right-sagittal views) with BML (pink area enclosed by red dashed line) detected by PDFS+T1 weighted sequences. B) Micro CT of whole tibial plateau (upper-transaxial, lower-coronal, right-sagittal views), regions of interest M-medial (blue oval shape), AM-anterior medial (dark green round shape), PM-posterior medial (light green round shape), location of BML region of interest was determined using MRI coordinates. C) Coronal view of AM subregions from control, OA-no BML and OA-BML. Subchondral plate (yellow) was manually selected to obtain plate thickness.

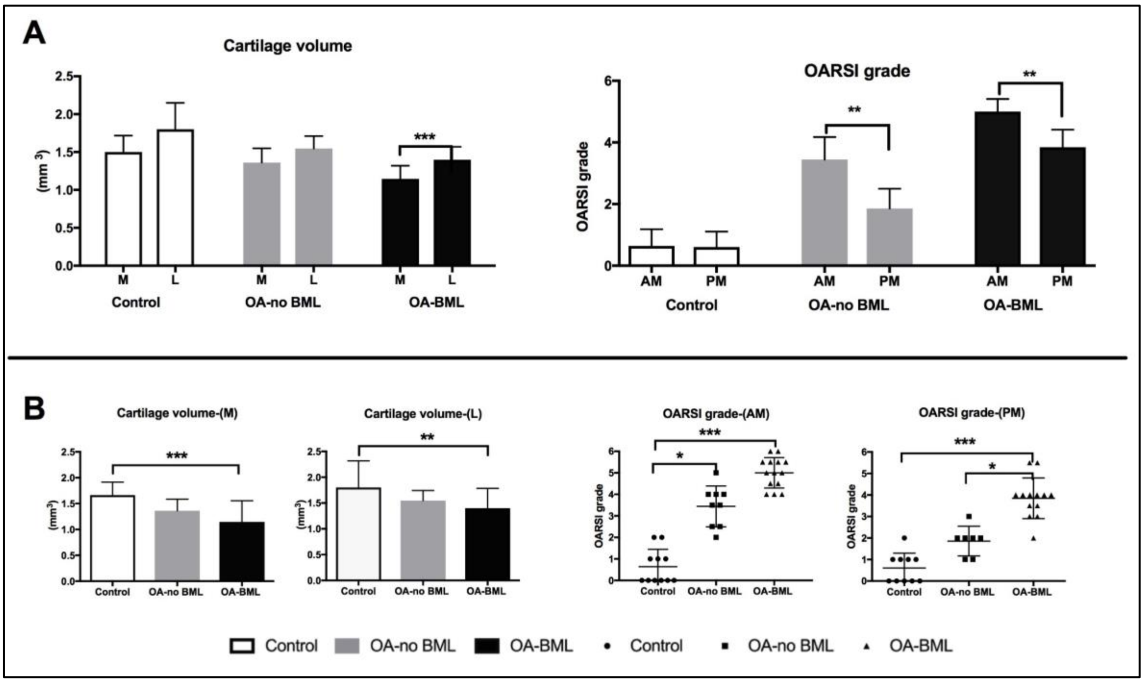

Figure 5-2 A). Cartilage volume and OARSI grade (Intragroup variability; B). Cartilage volume and OARSI grade between groups.

***p<0.05, **p<0.005, ***p<0.0005, **** p<0.0001**

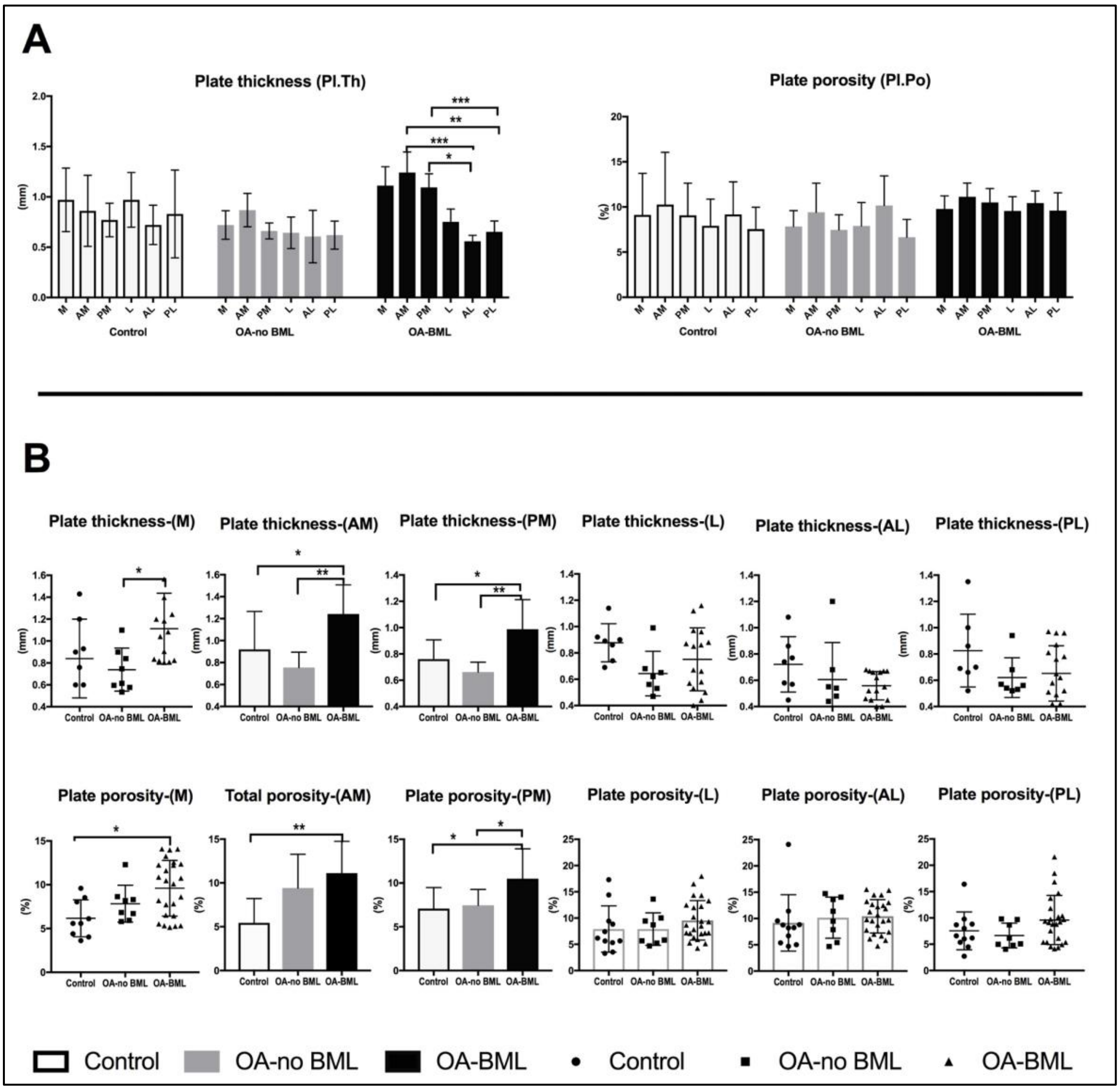

Figure 5-3 A). Intragroup variability; B). Subchondral bone plate microstructure between groups.

***p<0.05, **p<0.005, ***p<0.0005, **** p<0.0001.**

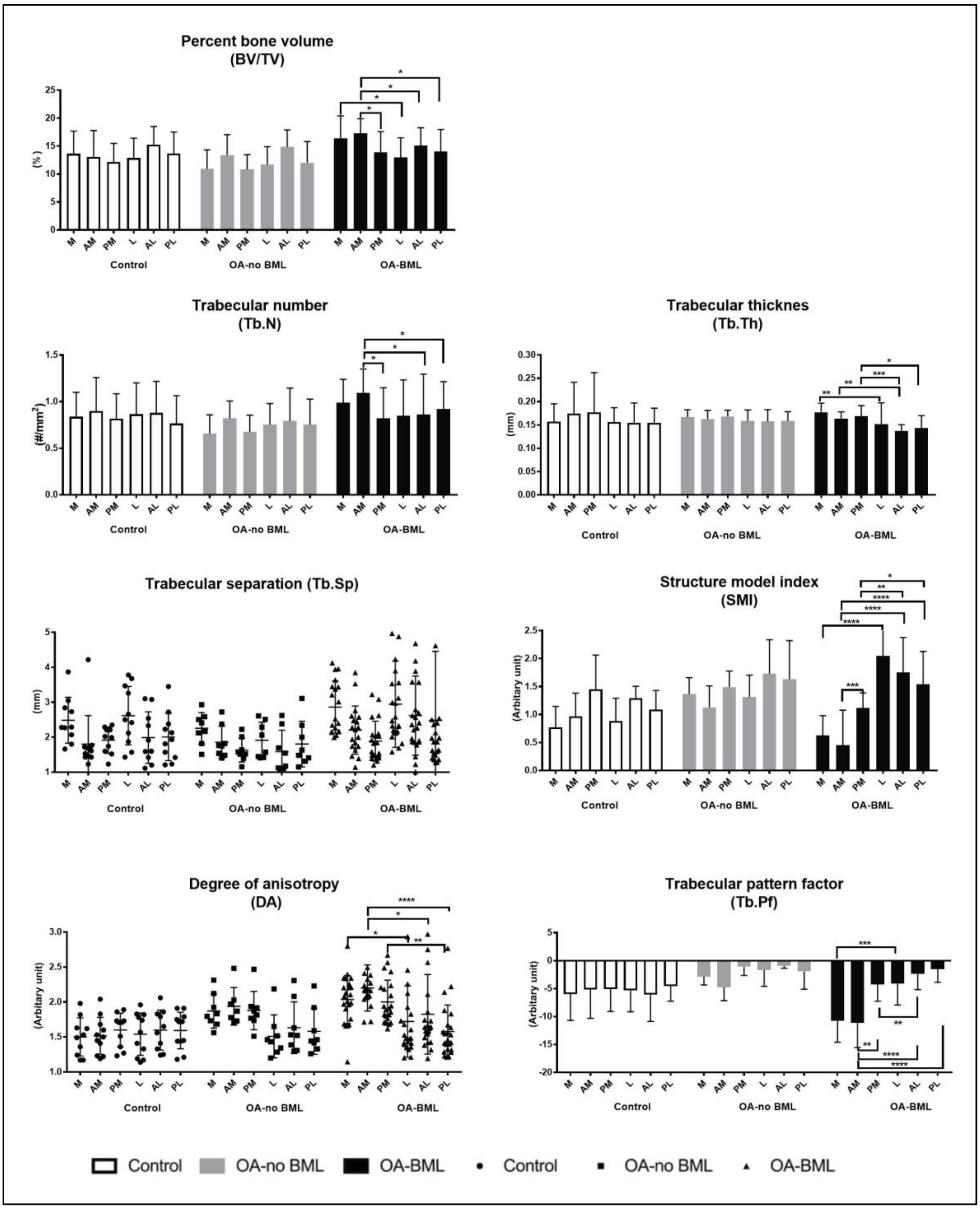

Figure 5-4 Parameters describing trabecular bone microstructure of medial and lateral compartments and its anterior and posterior subregions in Controls, OA-no BML and OA-BML groups.

***p<0.05, **p<0.005, ***p<0.0005, **** p<0.0001.**

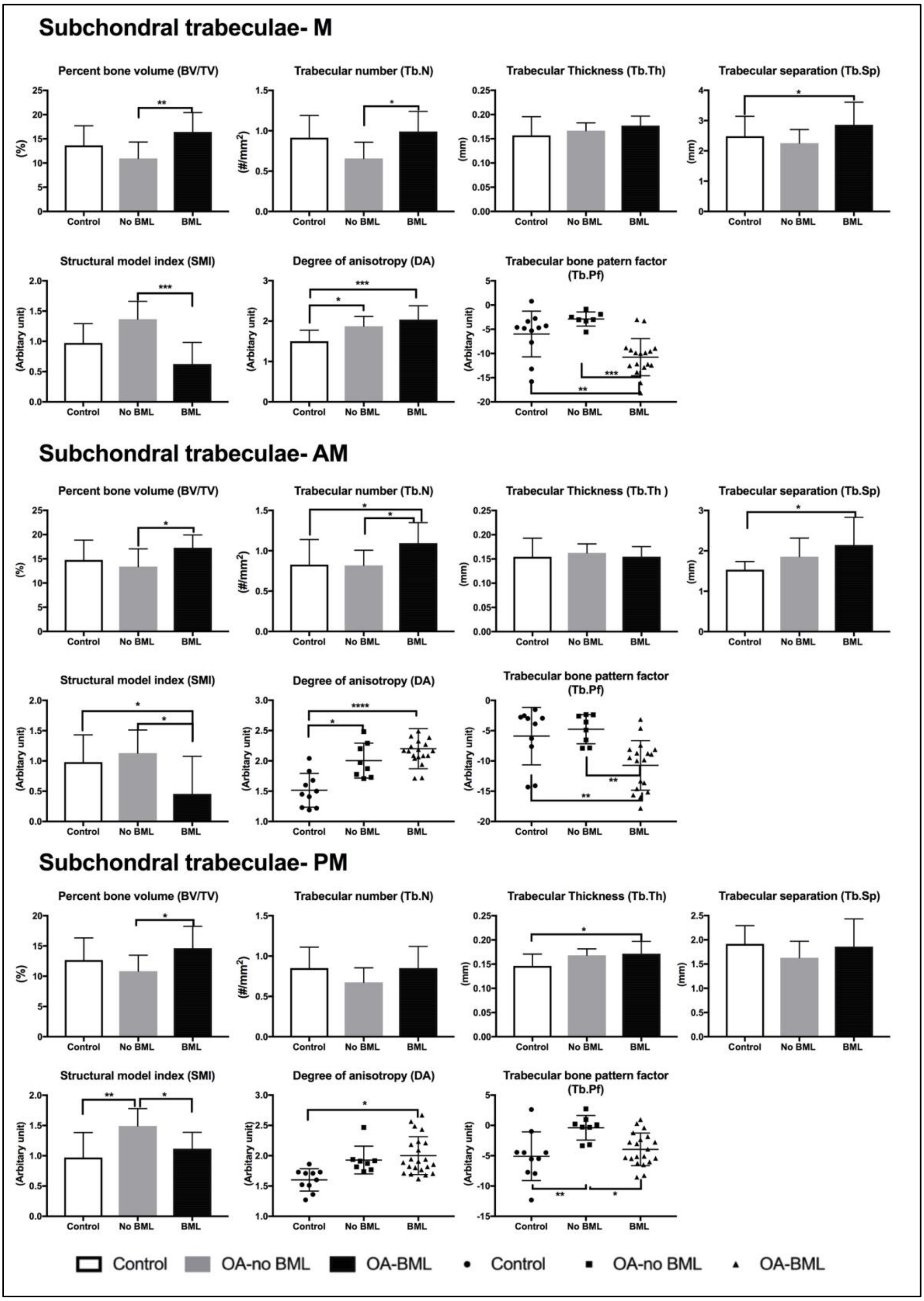

Figure 5-5 Subchondral trabecular bone microstructure between groups in medial compartment, anterior medial and posterior medial subregion.

.*p<0.05, **p<0.005, ***p<0.0005, **** p<0.0001.

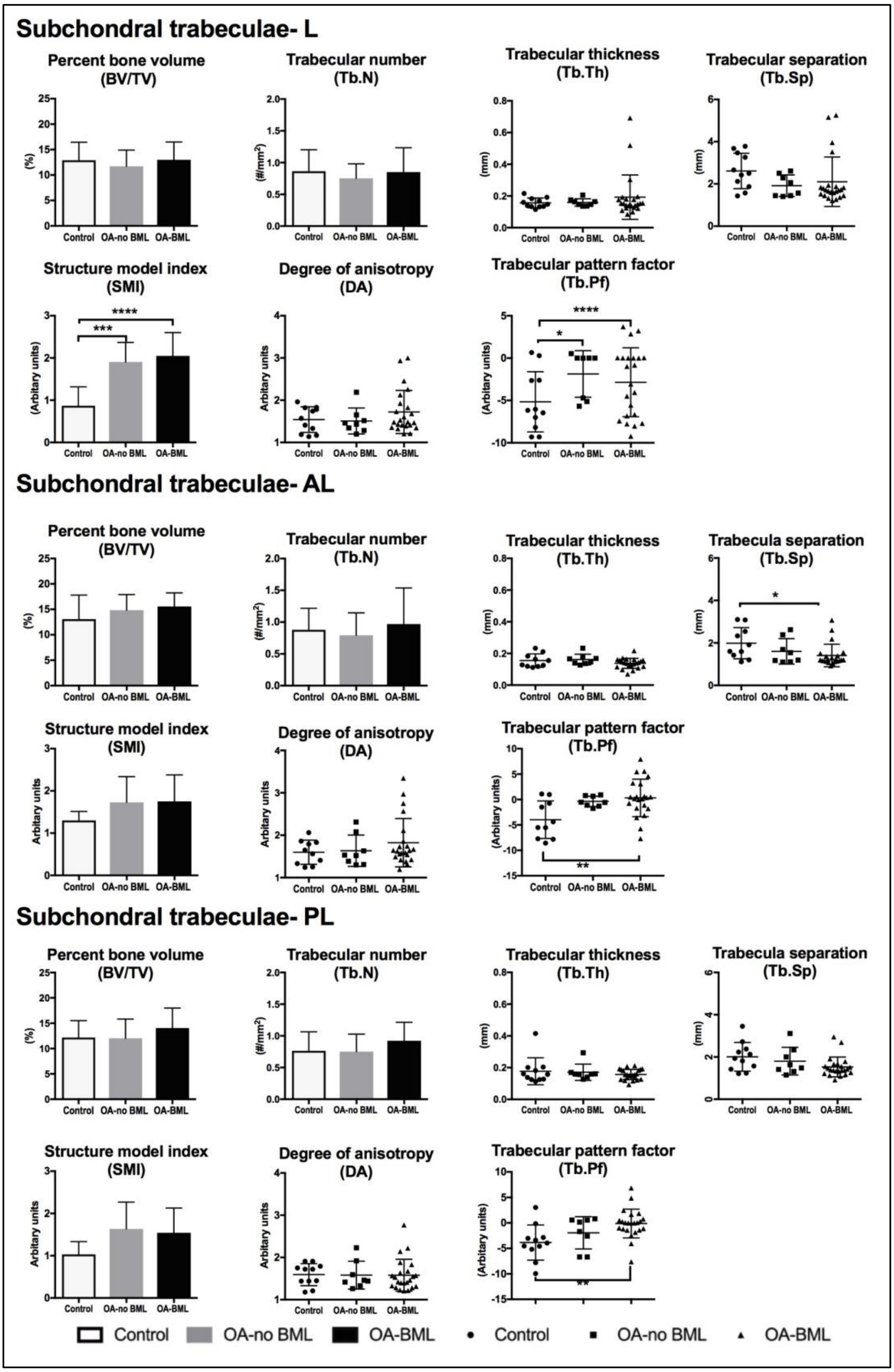

Figure 5-6 Subchondral trabecular bone microstructure between groups in lateral compartment, anterior lateral and posterior latera.

***p<0.05, **p<0.005, ***p<0.0005, **** p<0.0001.**

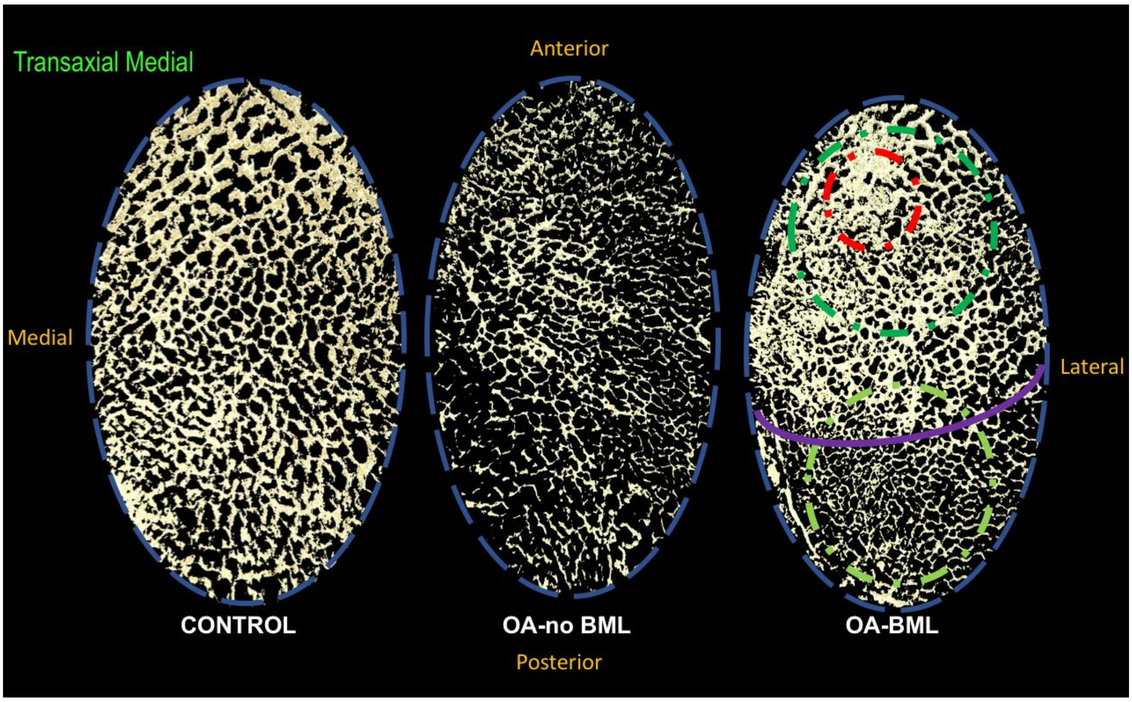

Figure 5-7 Representative image of subchondral trabeculae in the medial compartment (transaxial view) of control, OA-no BML and BML groups. In OA-BML, approximate location of BML is shown by a red circular shape, AM-anterior medial (dark green round shape), PM-posterior medial (light green round shape). Purple solid line showing extent of sclerotic appearance of trabecular bone.

Chapter 6

Summary and Future Directions

6.1 General discussion

Osteoarthritis (OA) is a slow multifactorial disease affecting the whole joint, with the most prominent degenerative changes occurring within the osteochondral unit (OCU). Despite the great endeavour of the OA research society to discover the early initiating events in OA, the pathogenesis of OA remains as an enigma. One of the main reasons for this is that human OA is mostly diagnosed at an advanced stage, when significant loss of cartilage volume has already taken place. With the evolution of high resolution imaging modalities, especially MRI, there is increasing ability to observe longitudinal structural changes in OA, such as cartilage damage and loss of cartilage volume, narrowing of joint space and pathological changes in subchondral bone.

Bone marrow lesions (BMLs), which are uniquely identified by MRI as signal changes of subchondral bone, became features of OA research interest when significant association between BML presence and loss of cartilage and clinical symptoms was found [1-6]. Since then, several large clinical studies have established the close relationship between BMLs and initiation, progression and potential outcome in human knee osteoarthritis (KOA), [7-9]. However, what MRI-identified BMLs represent at the tissue level, and what are the mechanisms behind the appearance of BMLs in subchondral bone tissue, remains unknown. The tissue level studies in this thesis were designed to address these questions and to test the hypothesis that the presence of BMLs in human proximal tibial OCU is indicative of the progression of OA disease.

6.2 Overview of study findings

In the first study described in the thesis (Chapter 2), a multi-modal tissue level analysis of the entire OCU- cartilage, subchondral bone (subchondral plate and trabeculae) and bone marrow- revealed that an OCU containing a detectable BML was characterised by more degenerative changes, such as lower volume of the cartilage, higher OARSI histological grade, thicker subchondral bone plate, increased trabecular bone volume, increased plate-like and decreased rod-like trabecular structures, increased osteoid volume, and increased bone marrow oedema, fibrosis fibrovascular cysts and fat tissue necrosis, compared to OCU without BML. Furthermore, the extent of structural changes in a tibial plateau containing a BML was different dependent on the subtype of BML detected by particular MRI sequences. BMLs detected by both PDFS and T1 sequences (BML 2) were characterised as lesions having the most advanced degenerative changes throughout the whole OCU, compared with BMLs detected only by PDFS sequences (BML 1). These data suggest that assessment of BMLs using specific MRI sequences might help to further differentiate the degree of tissue degeneration in the OCU. Although these two sequences are most commonly used to assess bone and cartilage changes in KOA, the relationship of the specific sequences to the extent of these OCU changes has not previously been appreciated. Concurrent with this study, a clinical study reported that BML 2 was associated with greater cartilage volume loss and pain than BML1 [10], results consistent with and broadly supportive of the findings described in Chapter 2. Importantly, the data from this study indicate that BML 1 may identify OA that has retained the ability to respond to treatment.

After characterising BMLs at the tissue level, the thesis next explored the potential mechanisms, by which BMLs may develop in the tissue. Previously, it has been suggested that the potential mechanism behind BML appearance in tissue might involve mechanical, metabolic and vascular factors. Thus, in Chapter 3, tissue-level evidence of mechanical and vascular influence in BML development was sought.

This study found an increased burden of microdamage to the bone matrix, and increased osteocyte density, in both the subchondral bone plate and subchondral trabeculae of BML areas. These findings provide tissue level evidence of the involvement of biomechanical factors, in particular increased mechanical loading, underlying the formation of BMLs. Furthermore, altered vascular characteristics were observed, i.e. increased arteriolar wall thickness and wall:lumen ratio, in regions within BMLs compared to no BML regions, which was in addition to the findings described in Chapter 2 of increased thick-walled arteriolar density and number of small fibrovascular cystic formations. Together, these data provide significant evidence for a vascular contribution to BML formation.

The changes in vascular wall parameters provoked further interest to explore the potential relationship between metabolic influences, such as hypertension, and the presence of BMLs. Components of the metabolic syndrome (MetS) have previously been linked the development and/or progression of KOA, making it reasonable to investigate their possible role in BML formation. In the work of Chapter 4, an increased prevalence of MetS, defined as a cluster of three or more metabolic disorders [11], was found in OA subjects with BMLs compared to OA subjects without a BML. It was also found that high total cholesterol and high BMI showed significant association with higher radiographic score (higher KL grade and loss of cartilage volume), which may indicate that metabolic factors could link to the progression of KOA. Further, high fasting glucose and triglyceride levels were significantly associated with larger BML volume size and could be factors that directly associate with BML aetiology. Taken together, these results suggest that metabolic factors may have a possible contributing role in the development and/or progression of BMLs in KOA.

Finally, in Chapter 5 a comprehensive investigation of the regional changes in subchondral bone microarchitecture of whole tibial plateau was undertaken with the aim of elucidating how the presence of a BML might affect microstructural changes across the whole tibial plateau. This study revealed that in OA subjects with no BML, bone microstructure of the subchondral plate and trabeculae did not vary significantly between subregions of the tibial plateau, while in OA subjects with BML, significant differences in microstructure between tibial subregions were evident. Microstructural changes in the subchondral bone were also closely correlated to the extent of cartilage degradation. The data suggest that areas of BML subchondral bone, previously described as focal sclerotic bone, might actually represent an area of the bone where microstructural changes start and then expand beyond the BML signal margins seen on MRI. These observations again linked the presence of a BML to OA severity.

6.3 Strengths and limitations

The strength of these studies is that the sample size use to describe the characteristics of BMLs at the tissue level was the largest compared to those previously published. These investigations are also the first to use two specific clinically approved and commonly used MRI sequences to detect BMLs in human tibial plateau tissue and (a) to explore how the presence of a BML relates to the changes in each component of the OCU (cartilage, subchondral bone and bone marrow) and (b) how the two BML subtypes can differentiate the extent of tissue degeneration. This work has made an important contribution to a better understanding of the role of subchondral bone in the progression of OA.

A limitation of the studies is that all samples obtained are by definition at 'end-stage' disease (joint replacement surgery) and the data collected are cross-sectional, rather than longitudinal. As such, it was not possible to establish definitively the relationship between findings and proposed mechanisms. In order to definitively establish the novel relationships suggested from this thesis, further studies using larger numbers across different age groups *and longitudinal in nature* should be undertaken. Examination of larger cohorts in the future will allow confirmation of the categorisation of the BML and/or OA into identifiable subtypes, suggested by the current findings. This in turn then might allow more individualised approaches to treatment and management of OA patients.

A second limitation is that only knee OA was studied and findings might differ for other skeletal joints. For example, do BMLs in different joints represent the same pathological changes at the tissue level as in the knee? Therefore, skeletal sites other than the widely-studied knee (eg. hip, hand, spine etc.) are important for further investigation.

Commonly, human joint tissue is available only upon joint replacement and therefore represents end stage disease and usually older individuals. Thus, in order to discover the potential usefulness of BMLs more dynamically and their involvement in OA progression over time, additional approaches are needed. These might include animal models or even biopsies taken from joint tissue before any sign of OA and during the course of OA development. Recently, a rabbit model has been developed to explore the direct relationship between mechanical loading and the presence of BMLs [12]. However, this study included a small sample number (n=3) and did not explore any other potential mechanisms (vascular or metabolic) or influences on the initiation or progression of BMLs. This type of preclinical study might be useful in more comprehensive exploration of BMLs in OA.

6.4 Areas for further research

In this thesis BML signals detected by MRI have been found to strongly associate with progressive structural changes in the whole OCU. Unfortunately, it has not been possible to directly correlate the signal with specific tissue pathological change. However, the data are consistent with the notion that signals originate from the bone marrow. But, to gain more knowledge about BMLs as therapeutic targets there is need to precisely define the origin of the BML-MRI signal (bone marrow, subchondral bone or combination of both). A next step to confirming this might be to remove the marrow from bone containing a BML and subject it again to MRI. In addition, very little is known about changes in BML regions at the cellular level and what molecules regulate those changes. Thus, one next step in BML research will be to investigate and define the specific molecular signature of BMLs.

Recently in a pilot project (see Appendix), we used a powerful spatial proteomic technology named matrix-assisted laser desorption/ionisation imaging mass spectrometry (MALDI-IMS) that allowed us to collect a large amount of molecular information directly from bone tissue sections [13]. Interestingly, we found that BML regions of tibial plateau had a prominent N-linked glycan signal. Protein glycosylation is one of the important processes in many regulatory mechanisms and its alteration has been found to be in close association with ischemia, vascular dysfunction and cellular oxidative stress mechanisms that have previously been indirectly associated with the presence of BMLs in the tissue [14]. Thus, further exploration and application of this method has high potential to reveal the molecular signature of BMLs and to provide unique insight into molecular regulation and aetiology of BMLs. Furthermore, this technique may directly aid in identifying differences in molecular profiles between BMLs detected by specific MRI sequences (BML1, BML 2).

The studies presented in this thesis support the growing concept that changes in the subchondral bone may be a key feature in the progression of the OA. Therefore, therapies targeting bone quality might be beneficial. Recently, the technique named Raman spectroscopy has been used to detect the overall biochemical signature of the bone, and clear differences were found between OA and non OA subchondral bone. Likewise, at the protein level, it was found that the ratio of $\alpha1{:}\alpha2$ chains of Type 1 collagen was significantly changed in OA subchondral bone compared to non-OA bone of the knee [15]. Similar changes were found in the hip [16]. However, to this date there is no study exploring these bone matrix changes in BML. It would be of considerable interest to investigate changes of bone matrix between OA bone with and without BML as the findings may help to facilitate the identification of disease processes at early/late stage and/or to identify changes that are specific for OA subtypes (OA-BML, OA-No BML).

6.5 Conclusions

The comprehensive tissue level analyses described in this thesis highlight that the changes in the whole OCU are important for the assessment of OA progression. BMLs are valuable MRI biomarkers with large potential to follow the progression of OA disease and changes in the whole OCU. Furthermore, BML are indicative of an active tissue response to OA disease and could assist in future identification of specific subtypes in human OA.

Thus, BMLs have the potential to be used as tools for monitoring the efficiency of new therapies and the development of more individual approaches of, and for the treatment at different stages of the progression of OA disease.

6.6 References

1. Felson DT, Chaisson CE, Hill CL, Totterman SM, Gale ME, Skinner KM, et al. The association of bone marrow lesions with pain in knee osteoarthritis. Ann Intern Med 2001; 134: 541-549.

2. Dore D, Quinn S, Ding C, Winzenberg T, Zhai G, Cicuttini F, et al. Natural history and clinical significance of MRI-detected bone marrow lesions at the knee: a prospective study in community dwelling older adults. Arthritis Res Ther 2010; 12: R223.

3. Felson DT, Niu J, Guermazi A, Roemer F, Aliabadi P, Clancy M, et al. Correlation of the development of knee pain with enlarging bone marrow lesions on magnetic resonance imaging. Arthritis Rheum 2007; 56: 2986-2992.

4. Kornaat PR, Bloem JL, Ceulemans RY, Riyazi N, Rosendaal FR, Nelissen RG, et al. Osteoarthritis of the knee: association between clinical features and MR imaging findings. Radiology 2006; 239: 811-817.

5. Lo GH, McAlindon TE, Niu J, Zhang Y, Beals C, Dabrowski C, et al. Bone marrow lesions and joint effusion are strongly and independently associated with weight-bearing pain in knee osteoarthritis: data from the osteoarthritis initiative. Osteoarthritis Cartilage 2009; 17: 1562-1569.

6. Raynauld JP, Martel-Pelletier J, Berthiaume MJ, Abram F, Choquette D, Haraoui B, et al. Correlation between bone lesion changes and cartilage volume loss in patients with osteoarthritis of the knee as assessed by

quantitative magnetic resonance imaging over a 24-month period. Ann Rheum Dis 2008; 67: 683-688.

7. Wluka AE, Hanna F, Davies-Tuck M, Wang Y, Bell RJ, Davis SR, et al. Bone marrow lesions predict increase in knee cartilage defects and loss of cartilage volume in middle-aged women without knee pain over 2 years. Ann Rheum Dis 2009; 68: 850-855.

8. Sharma L, Chmiel JS, Almagor O, Dunlop D, Guermazi A, Bathon JM, et al. Significance of preradiographic magnetic resonance imaging lesions in persons at increased risk of knee osteoarthritis. Arthritis Rheumatol 2014; 66: 1811-1819.

9. Roemer FW, Neogi T, Nevitt MC, Felson DT, Zhu Y, Zhang Y, et al. Subchondral bone marrow lesions are highly associated with, and predict subchondral bone attrition longitudinally: the MOST study. Osteoarthritis Cartilage 2010; 18: 47-53.

10. Wluka AE, Teichtahl AJ, Maulana R, Liu BM, Wang Y, Giles GG, et al. Bone marrow lesions can be subtyped into groups with different clinical outcomes using two magnetic resonance imaging (MRI) sequences. Arthritis Res Ther 2015; 17: 270.

11. World Health Organization: Geneva SLaoJ. Definition, diagnosis and classification of diabetes mellitus and its complications: 2011.

12. Matheny JB, Goff MG, Pownder SL, Koff MF, Hayashi K, Yang X, et al. An in vivo model of a mechanically-induced bone marrow lesion. J Biomech 2017; 64: 258-261.

13. Briggs MT, Kuliwaba JS, Muratovic D, Everest-Dass AV, Packer NH, Findlay DM, et al. MALDI mass spectrometry imaging of N-glycans on tibial cartilage and subchondral bone proteins in knee osteoarthritis. Proteomics 2016; 16: 1736-1741.

14. Findlay DM. Vascular pathology and osteoarthritis. Rheumatology (Oxford) 2007; 46: 1763-1768.

15. Kerns JG, Gikas PD, Buckley K, Shepperd A, Birch HL, McCarthy I, et al. Evidence from Raman spectroscopy of a putative link between inherent bone matrix chemistry and degenerative joint disease. Arthritis Rheumatol 2014; 66: 1237-1246.

16. Buchwald T, Niciejewski K, Kozielski M, Szybowicz M, Siatkowski M, Krauss H. Identifying compositional and structural changes in spongy and subchondral bone from the hip joints of patients with osteoarthritis using Raman spectroscopy. J Biomed Opt 2012; 17: 017007.

Chapter 7 APPENDIX

MALDI Mass Spectrometry Imaging of *N*-Glycans on Tibial Cartilage and Subchondral Bone Proteins in Knee Osteoarthritis

(Manuscript published during candidature, but external to thesis material)

DOI 10.1002/pmic.201500461

TECHNICAL BRIEF

MALDI mass spectrometry imaging of *N*-glycans on tibial cartilage and subchondral bone proteins in knee osteoarthritis

Matthew T. Briggs[1,2], *Julia S. Kuliwaba*[3,4], *Dzenita Muratovic*[3,4], *Arun V. Everest-Dass*[5,6], *Nicolle H. Packer*[5,6], *David M. Findlay*[3] *and Peter Hoffmann*[1,2]

[1] Adelaide Proteomics Centre, School of Biological Sciences, University of Adelaide, Adelaide, South Australia, Australia
[2] Institute of Photonics and Advanced Sensing (IPAS), University of Adelaide, Adelaide, South Australia, Australia
[3] Discipline of Orthopaedics and Trauma, School of Medicine, University of Adelaide, Adelaide, South Australia, Australia
[4] Bone and Joint Research Laboratory, SA Pathology, Adelaide, South Australia, Australia
[5] Biomolecular Frontiers Research Centre, Faculty of Science, Macquarie University, Sydney, New South Wales, Australia
[6] Centre of Excellence for Nanoscale BioPhotonics (CNBP), Macquarie University, Sydney, New South Wales, Australia

Magnetic resonance imaging (MRI) is a non-invasive technique routinely used to investigate pathological changes in knee osteoarthritis (OA) patients. MRI uniquely reveals zones of the most severe change in the subchondral bone (SCB) in OA, called bone marrow lesions (BMLs). BMLs have diagnostic and prognostic significance in OA, but MRI does not provide a molecular understanding of BMLs. Multiple *N*-glycan structures have been observed to play a pivotal role in the OA disease process. We applied matrix-assisted laser desorption/ionization (MALDI) mass spectrometry imaging (MSI) of *N*-glycans to formalin-fixed paraffin-embedded (FFPE) SCB tissue sections from patients with knee OA, and liquid chromatography-electrospray ionization-tandem mass spectrometry (LC-ESI-MS/MS) was conducted on consecutive sections to structurally characterize and correlate with the *N*-glycans seen by MALDI-MSI. The application of this novel MALDI-MSI protocol has enabled the first steps to spatially investigate the *N*-glycome in the SCB of knee OA patients.

Received: November 18, 2015
Revised: February 15, 2016
Accepted: March 11, 2016

Keywords:
Bone marrow lesion / Glycans / Glycoproteomics / Maldi imaging / Mass spectrometry / Osteoarthritis

Additional supporting information may be found in the online version of this article at the publisher's web-site

Human osteoarthritis (OA) is an increasingly prevalent age-related joint disease with a high burden of personal and economic cost. The disease is characterized by articular cartilage degeneration, with the addition of both generalized and focal changes of the subchondral bone [1, 2]. Bone marrow lesions (BMLs) are features that have been identified in both early asymptomatic and severe late-stage OA patients and their presence associates with loss of overlying cartilage [3, 4]. Classically, BMLs are identified using magnetic resonance

Correspondence: Professor Peter Hoffmann, Adelaide Proteomics Centre, School of Molecular and Biomedical Science, University of Adelaide, Adelaide, South Australia
E-mail: peter.hoffmann@adelaide.edu.au
Fax: +61 (08) 0 8313 4362

Abbreviations: **BML**, bone marrow lesion; **CAAR**, citric acid antigen retrieval; **ECM**, extracellular matrix; **FFPE**, formalin-fixed paraffin-embedded; **ITO**, indium tin oxide; **MRI**, magnetic resonance imaging; **OA**, osteoarthritis; **PDFS**, proton density-weighted

Colour Online: See the article online to view Figs. 1 and 2 in colour.

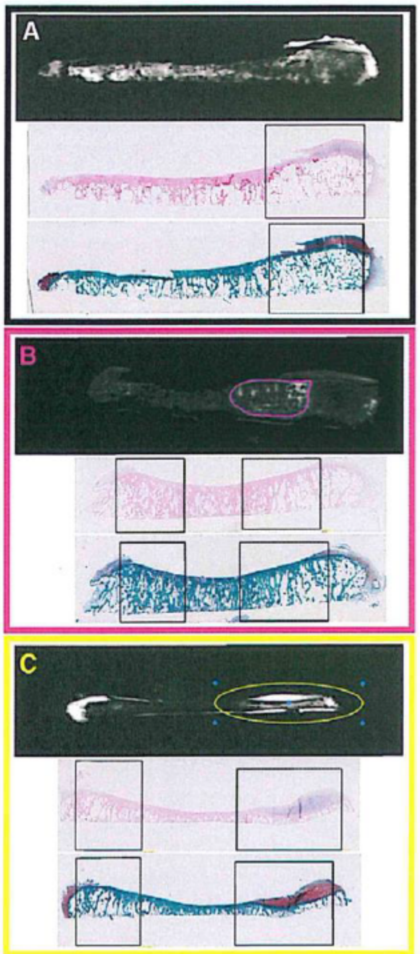

Figure 1. Knee osteoarthritis (OA) patients (A) without bone marrow lesions (No BML), (B) with BML stage 1 (BML 1), and (C) with BML stage 2 (BML 2). Each panel includes (from top to bottom) a PDFS-weighted MRI of the tibial plateau (BML stage 1 and 2 are annotated in pink and green, respectively), a haematoxylin and eosin (H&E) stain, and a Safranin-O/Fast Green stain of consecutive FFPE tissue sections. Regions of interest are annotated in black.

imaging (MRI) by either fat-suppressed and/or proton dense T2 weighted scans. The difference between T1 and T2 weighted scans is that BML areas appear hypointense (i.e. low signal) for T1 and hyperintense (i.e. high signal) for T2 [5, 6]. Therefore, T2 weighted scans depict BMLs to their full extent, while T1 weighted scans usually assess cartilage. A combination of these sequences provides diagnostic and prognostic information regarding OA disease progression [7, 8]. However, MRI does not provide a molecular understanding of BML formation and OA disease progression.

Adjacent to BMLs in the SCB is overlying cartilage composed of extracellular matrix (ECM) glycoproteins [9, 10]. Besides proteoglycans, there are glycosylated cell surface proteins, such as CD44 and integrins, which play an important role in mediating chondrocyte and ECM interactions [11, 12]. Glycans attached to these cartilage ECM glycoproteins are classified into mainly two groups: (i) *N*-linked glycans that are attached to asparagine residues and (ii) *O*-linked glycans that are attached to serine/threonine residues [13]. *N*-glycans are the most common glycan, with well-established methods for analysis from tissue [14, 15]. Multiple *N*-glycan structures have been observed to play a pivotal role in OA disease progression. Recently, using HPLC-MS, it has been shown that high-mannose type *N*-glycans are significantly decreased on proteins from both murine and human OA cartilage tissue [16]. In 2013, glycophenotyping of OA cartilage was carried out using several techniques, such as RT-PCR, MS and immunohistochemistry. Liquid chromatography-electrospray ionization-tandem mass spectrometry (LC-ESI-MS/MS) separation and structural identification of the released glycans confirmed 21 *N*-glycans on the human OA chondrocyte proteins isolated from femoral condyle articular cartilage [17]. The *N*-glycome of bone marrow from OA patients has not yet been characterized.

MALDI mass spectrometry imaging (MALDI-MSI) has previously been applied to the proteomic analysis of fresh frozen human OA knee cartilage and synovial tissue. Deep and superficial knee cartilage from human healthy and OA patients were sectioned and analysed by MALDI-MSI of the tryptic peptides [18]. Fibronectin and cartilage oligomeric matrix protein (COMP) were 2 glycoproteins identified in the OA patients, but not in the healthy controls. Moreover, the glycoprotein fibronectin was identified in the synovial membranes from OA patients, but not in healthy controls. In summary, glycoproteins have been observed to play an important role in OA changes of human knee cartilage and synovial tissue.

The measurement of *N*-glycans by MALDI-MSI on fresh frozen mouse brain tissue and various formalin-fixed paraffin-embedded (FFPE) tissues has been established previously [19, 20], with regions of interest, such as tumour and non-tumour, differentiated based on the pattern of *N*-glycans released. The limitation of MALDI analysis is that *N*-glycan masses can identify the glycan compositions but cannot identify the sequence and branching of the glycan structures. This has recently been overcome with a new workflow combining *N*-glycan analysis by MALDI-MSI and LC-ESI-MS/MS [21].

Here we investigate the *N*-glycome of FFPE cartilage and bone marrow tissue. Human knee SCB, from OA patients with BMLs (stage 1 and 2) or without BMLs were analysed to investigate *N*-glycosylation patterns.

Tibial plateaus were obtained from three patients (one male aged 52 years, two females aged 68 and 74 years) undergoing knee arthroplasty surgery for radiographic and severe symptomatic OA. Tibial plateau specimens were scanned ex vivo, using an MR scanner with an 8-channel wrist coil (3T MRI Siemens TRIO), at two specific sequences; fat

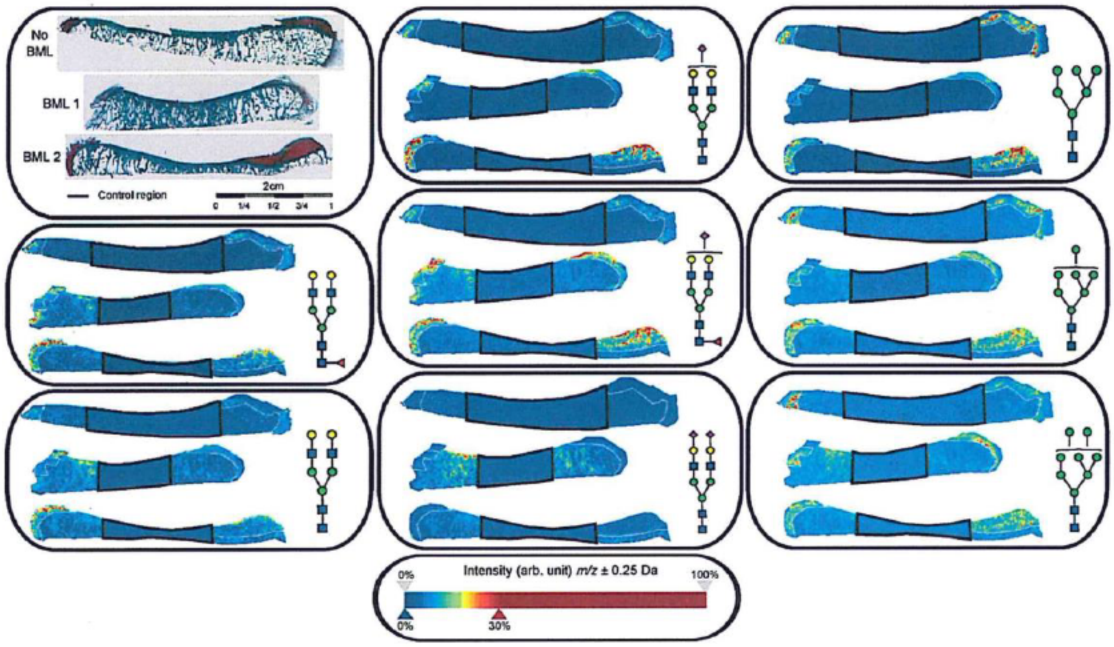

Figure 3. Safranin-O stained images and ion intensity maps of complex/hybrid, sialylated and high-mannose *N*-glycans observed in patients without bone marrow lesions (No BML), with BML stage 1 (BML 1) and with BML stage 2 (BML 2). *N*-glycans were released in situ on FFPE tissue sections using PNGase F and analysed by MALDI-TOF/TOF-MS. *m/z* values were selected and visualized in SCiLS lab software (V2015a, Bruker Daltonics, Bremen, Germany). Ion intensity maps were co-registered with safranin-O stained images to identify the distribution of the selected *N*-glycans. There was no distinct pattern between the same families (i.e. complex/hybrid, sialylated and high-mannose) of N-glycans. Control and calibrant regions (i.e. regions not treated with PNGase F) are annotated in black.

suppressed (FS) fast spin-echo proton density-weighted (PDFS) and T1 weighted spin echo in sagittal and coronal plane. Sagittal slice thickness was 1.6 mm with distance factor of 25%. Coronal slice thickness was 3.0 mm with 10% distance factor. Ex vivo MR imaging was confirmed to correspond to pre-operative imaging, by comparing pre- and post-operative MR data. BMLs were defined as changes of the MRI signal intensity in the bone marrow, located beneath cartilage and visible at least on two consecutive slices. BMLs detected on the PDFS sequence only (no signal on T1) are classified as BML stage 1 and correspond to mild-to-moderate osteochondral OA pathology; BMLs detected on both PDFS and T1 sequences are classified as BML stage 2 and represent severe OA osteochondral pathology [22]. Using precise mapping of BMLs (OsiriX software, Pixmeo-SARL, Switzerland), a sagittal slice of cartilage-subchondral bone (width 5 mm x depth 5 to 12 mm) containing the BML area (Fig. 1) was dissected using a low speed diamond wheel saw (Model 660, South Bay Technology, Inc.). Sagittal blocks of tissue were fixed in 4% (w/v) paraformaldehyde and slowly decalcified in 15% (w/v) ethylenediaminetetra acetic acid (EDTA). Following complete decalcification as determined by X-ray, samples were processed, embedded in paraffin and cut on a rotary microtome (Leica RM 2235 Nussloch, Germany) into 5μm thick sections.

FFPE human OA tissue sections on indium tin oxide (ITO) or polyethylene naphthalate (PEN) slides were rehydrated using a modified procedure of citric acid antigen retrieval (CAAR) at 70° for 3 h instead of 98° for 30 min and printing 15 nL of PNGase F instead of 30 nL [21]. Mass spectra were acquired using an ultrafleXtreme MALDI-TOF/TOF mass spectrometer or LC-iontrap ESI-MS/MS analysis as described previously [21, 23].

BMLs were identified using PDFS and T1 weighted scans in MRI of the tibial plateaus. As depicted in Fig. 1 Panel A, there was no BML detected in this patient, while in Fig. 1 Panels B and C, BML stage 1 and 2, respectively, were detected. These BMLs are annotated in pink and green, as indicated on the MRI. Below each MRI, staining of FFPE tissue sections are shown. Haematoxylin and eosin (H&E) staining provides histological information and Safranin-O highlights the cartilage in red. Following acquisition of the MRI, the image was overlaid with the stained FFPE tissue sections and regions of interest were annotated in black. Although the identification of these BMLs using MRI is useful, it does not provide molecular information. Therefore, we performed MALDI-MSI of

[5] Loeuille, D., Chary-Valckenaere, I., MRI in OA: from cartilage to bone marrow lesion. *Osteoporos. Int.* 2012, *23 Suppl 8*, S867–S869.

[6] Dore, D., Martens, A., Quinn, S., Ding, C. et al., Bone marrow lesions predict site-specific cartilage defect development and volume loss: a prospective study in older adults. *Arthritis Res. Ther.* 2010, *12*, R222.

[7] Driban, J. B., Tassinari, A., Lo, G. H., Price, L. L. et al., Bone marrow lesions are associated with altered trabecular morphometry. *Osteoarthritis Cartilage* 2012, *20*, 1519–1526.

[8] Hayashi, D., Guermazi, A., Kwoh, C. K., Hannon, M. J. et al., Semiquantitative assessment of subchondral bone marrow edema-like lesions and subchondral cysts of the knee at 3T MRI: a comparison between intermediate-weighted fat-suppressed spin echo and Dual Echo Steady State sequences. *BMC Musculoskelet. Disord.* 2011, *12*, 198.

[9] Toegel, S., Pabst, M., Wu, S. Q., Grass, J. et al., Phenotype-related differential alpha-2,6- or alpha-2,3-sialylation of glycoprotein N-glycans in human chondrocytes. *Osteoarthritis Cartilage* 2010, *18*, 240–248.

[10] Ishihara, T., Kakiya, K., Takahashi, K., Miwa, H. et al., Discovery of novel differentiation markers in the early stage of chondrogenesis by glycoform-focused reverse proteomics and genomics. *Biochim. Biophys. Acta* 2014, *1840*, 645–655.

[11] Knudson, C. B., Knudson, W., Cartilage proteoglycans. *Semin. Cell Dev. Biol.* 2001, *12*, 69–78.

[12] Nicoll, S. B., Barak, O., Csoka, A. B., Bhatnagar, R. S., Stern, R., Hyaluronidases and CD44 undergo differential modulation during chondrogenesis. *Biochem. Biophys. Res. Commun.* 2002, *292*, 819–825.

[13] Kobata, A., Structures and functions of the sugar chains of glycoproteins. *Eur. J.Biochem.* 1992, *209*, 483–501.

[14] Tian, Y., Gurley, K., Meany, D. L., Kemp, C. J., Zhang, H., N-linked glycoproteomic analysis of formalin-fixed and paraffin-embedded tissues. *J. Proteome Res.* 2009, *8*, 1657–1662.

[15] Hu, Y., Zhou, S., Khalil, S. I., Renteria, C. L., Mechref, Y., Glycomic profiling of tissue sections by LC-MS. *Anal. Chem.* 2013, *85*, 4074–4079.

[16] Urita, A., Matsuhashi, T., Onodera, T., Nakagawa, H. et al., Alterations of high-mannose type N-glycosylation in human and mouse osteoarthritis cartilage. *Arthritis Rheum.* 2011, *63*, 3428–3438.

[17] Toegel, S., Bieder, D., Andre, S., Altmann, F. et al., Glycophenotyping of osteoarthritic cartilage and chondrocytes by RT-qPCR, mass spectrometry, histochemistry with plant/human lectins and lectin localization with a glycoprotein. *Arthritis Res. Ther.* 2013, *15*, R147.

[18] Cillero-Pastor, B., Eijkel, G. B., Kiss, A., Blanco, F. J., Heeren, R. M., Matrix-assisted laser desorption ionization-imaging mass spectrometry: a new methodology to study human osteoarthritic cartilage. *Arthritis Rheum.* 2013, *65*, 710–720.

[19] Powers, T. W., Jones, E. E., Betesh, L. R., Romano, P. R. et al., Matrix assisted laser desorption ionization imaging mass spectrometry workflow for spatial profiling analysis of N-linked glycan expression in tissues. *Anal. Chem.* 2013, *85*, 9799–9806.

[20] Powers, T. W., Neely, B. A., Shao, Y., Tang, H. et al., MALDI imaging mass spectrometry profiling of N-glycans in formalin-fixed paraffin embedded clinical tissue blocks and tissue microarrays. *PloS one* 2014, *9*, e106255.

[21] Gustafsson, O. J., Briggs, M. T., Condina, M. R., Winderbaum, L. J. et al., MALDI imaging mass spectrometry of N-linked glycans on formalin-fixed paraffin-embedded murine kidney. *Anal. Bioanal. Chem.* 2015, *407*, 2127–2139.

[22] Muratovic, D., Cicuttini, F. M. Wluka, A. E., Wang, Y., Findlay, D. M. et al., Bone marrow lesions detected by different magnetic resonance sequences as potential biomarkers for knee osteoarthritis: comprehensive tissue level analysis. *Osteoarthritis Cartilage* 2015, *23*, A303–A305.

[23] Jensen, P. H., Karlsson, N. G., Kolarich, D., Packer, N. H., Structural analysis of N- and O-glycans released from glycoproteins. *Nat. Protoc.* 2012, *7*, 1299–1310.

[24] Gustafsson, J. O., Oehler, M. K., McColl, S. R., Hoffmann, P., Citric acid antigen retrieval (CAAR) for tryptic peptide imaging directly on archived formalin-fixed paraffin-embedded tissue. *J. Proteome Res.* 2010, *9*, 4315–4328.

